Unclassified

SECURITY CLASSIFICATION OF THIS PAGE

Dist: A

REPORT DOCUMENTATION PAGE

1a. REPORT SECURITY CLASSIFICATION: Unclassified	1b. RESTRICTIVE MARKINGS: -
2a. SECURITY CLASSIFICATION AUTHORITY: -	3. DISTRIBUTION/AVAILABILITY OF REPORT: Approved for public release distribution unlimited A
2b. DECLASSIFICATION/DOWNGRADING SCHEDULE: -	
4. PERFORMING ORGANIZATION REPORT NUMBER(S): Department of Anatomy and Neurobiology University of Tennessee, Memphis	5. MONITORING ORGANIZATION REPORT NUMBER(S): AFOSR-TR- 94 0733
6a. NAME OF PERFORMING ORGANIZATION: University of Tennessee, Memphis; 6b. OFFICE SYMBOL (*If applicable*): -	7a. NAME OF MONITORING ORGANIZATION: Air Force Office of Scientific Research/NL
6c. ADDRESS (*City, State and ZIP Code*): University of Tennessee, Memphis 875 Monroe Avenue, Memphis Tennessee 38163	7b. ADDRESS (*City, State and Zip Code*): 110 Duncan Ave, Suite B115 Building 410 Bolling AFB, D. C. 20332-0001
8a. NAME OF FUNDING/SPONSORING ORGANIZATION: AFOSR; 8b. OFFICE SYMBOL (*If applicable*): NL	9. PROCUREMENT INSTRUMENT IDENTIFICATION NUMBER: USAF GR AFOSR 91-0333
8c. ADDRESS (*City, State and ZIP Code*): Building 410 Bolling AFB, D. C. 20332-6448	10. SOURCE OF FUNDING NOS.

PROGRAM ELEMENT NO.	PROJECT NO.	TASK NO.	WORK UNIT NO.
61102F	2312	BS	

11. TITLE (*Include Security Classification*)

12. PERSONAL AUTHOR(S): Randall J. Nelson, Ph. D.

13a. TYPE OF REPORT	13b. TIME COVERED	14. DATE OF REPORT (*Yr., Mo., Day*)	15. PAGE COUNT
Annual Technical	FROM 7/1/93 TO 6/30/94	94, 11, 21	12

16. SUPPLEMENTARY NOTATION: Two enclosures per copy included (20pp and 45pp, respectively).

17. COSATI CODES			18. SUBJECT TERMS (*Continue on reverse if necessary and identify by block number*)
FIELD	GROUP	SUB. GR.	Changes in sensory responsiveness; Response gating; Reaction times; Cortical neuronal responses; visual and vibratory cues; Monkeys; Humans

19. ABSTRACT (*Continue on reverse if necessary and identify by block number*)

Three research goals were accomplished during this third year. 1) Analysis of data indicated that the responsiveness of primary somatosensory (SI) cortical neurons is "unattenuated" if when behavioral conditions become unpredictable. This observation fits with the hypothesis that during stereotyped behavior, neuronal responsiveness is gated so that the CNS may partially engage in other activities. 2) SI cortical neurons that respond to vibratory go-cues for wrist movement with the greatest fidelity have their activity modulated just prior to movement onset. This observation fits with the hypothesis that prior to active movement, sensory inputs that are no longer behaviorally relevant are gated so as not to interfere with monitoring movement parameters by the primate CNS. 3) SI cortical neurons that may bind together other SI neurons with their rhythmic activity have this activity disrupted at go-cue onset and just prior to movement onset. This observation fits with the hypothesis that prior to behaviorally significant events, the activity of these neurons that may tonically gate other SI neurons is suppressed to allow the monitoring sensory events and the initiation of movements.

20. DISTRIBUTION/AVAILABILITY OF ABSTRACT	21. ABSTRACT SECURITY CLASSIFICATION
UNCLASSIFIED/UNLIMITED ☒ SAME AS RPT. ☐ DTIC USERS ☐	Unclassified
22a. NAME OF RESPONSIBLE INDIVIDUAL: Genevieve Haddad, Ph. D.	22b. TELEPHONE NUMB (*Include Area Code*): 202-767-502

DD FORM 1473, 83 APR — EDITION OF 1 JAN 73 IS OBSOLETE.

RESEARCH OBJECTIVES

General goals of these continuing studies were a) to understand the influence of behavioral unpredictability and knowledge of results upon sensorimotor cortical activity, b) to understand the special role that these neurons play in sensorimotor integration during the initiation and execution of movements and c) to determine, eventually, if human subjects perform the behavioral tasks in a way that strengthens the contention that neurophysiological events in the primate brain reflect what occurs in homologous regions of the human CNS while performing under the same behavioral conditions.

Three research goals were accomplished during this third year. 1) Analysis of data indicated that the responsiveness of primary somatosensory (SI) cortical neurons is "unattenuated" if when behavioral conditions become unpredictable. This observation fits with the hypothesis that during stereotyped behavior, neuronal responsiveness is gated so that the CNS may partially engage in other activities. 2) SI cortical neurons that respond to vibratory go-cues for wrist movement with the greatest fidelity have their activity modulated just prior to movement onset. This observation fits with the hypothesis that prior to active movement, sensory inputs that are no longer behaviorally relevant are gated so as not to interfere with monitoring movement parameters by the primate CNS. 3) SI cortical neurons that may bind together other SI neurons with their rhythmic activity have this activity disrupted at go-cue onset and just prior to movement onset. This observation fits with the hypothesis that prior to behaviorally significant events, the activity of these neurons that may tonically gate other SI neurons is suppressed to allow the monitoring sensory events and the initiation of movements.

Each study will be described following a general outline of the Background which lead to the design of the studies described below. Some of the work has either been published or has been submitted for publication and is undergoing review. Manuscripts have been enclosed.

Background

Active movement involves stimulus detection and classification, as well as response programming, selection and production. Moreover, proper motor control also involves the use of information about external environmental conditions and the current "internal state" of the parts of the body that will be moved. The availability and utilization of sensory information about both the internal and external behavioral and environmental states are subject to alteration by the attentional system, which, by Posner and Petersens's definition, is responsible for "...a) orienting to sensory events; b) detecting signals for focal (conscious) processing, and c) maintaining a vigilant or alert state". In addition to attentional factors, it seems important to add intention to move and emotional constituents (e.g., expectation of successful behavioral outcome) to the list of factors influencing motor performance. Finally, the internal representations of current behavioral circumstances, as they relate to impending actions, must be updated efficiently to account for any changes in conditions that could affect movements waiting to be planned or executed if previously programmed. Each concept is based upon the knowledge, available through introspection, but difficult to prove scientifically, that "much information is continuously transmitted by sensory receptors from the environment to the brain, but only a fraction of this information is consciously perceived at any one time".

Previous studies have demonstrated several basic principles regarding the influences of behavioral context upon sensory responsiveness and ultimately upon sensorimotor integration. We based our studies on these principles. First, it is usually presumed that there is a behavioral "steady state" achieved during performance of necessarily overtrained and stereotypic behaviors. Changes in sensory responsiveness and motor performance are referenced to this baseline. Second, regions of the CNS involved in sensorimotor integration are more responsive to inputs when animals or subjects are actively engaged in the task. Responses to inputs presented passively are diminished in comparison. Third, more complex behavioral requirements, such as discrimination rather than mere detection of inputs, engage the sensorimotor integration system even more. This results not only in changes in signal-to-noise ratio during the initial phases of a behavioral trial, but may also result in responsiveness modulation prior to response onset to "readjust" certain parts of the system for their participation in response programming, selection and production. Fourth, nearly identical behavioral responses can be made over a number of behavioral trials and these responses can be elicited by several types of go-cues provided that these cues are selected carefully and the animals or subjects adequately taught to make proper responses. Thus, subtle effects of continuous stimulus presentation and possible effects

of stimulus interference with response programming, selection and production can be determined. Finally, while the source of the central influences which maintain response integrity and regulate sensory inputs is not known, these influences are probably mediated through the motor cortices.

As our working hypothesis, we suggested that corollary discharge from motor cortical areas is the intermediate source of the inputs that result in sensory responsiveness modulation in SI. Recent studies have shown that motor intracortical microstimulation can alter SI evoked responses and suggest that neuronal sensory responsiveness is altered by the same mechanism. In addition, neurons in motor, premotor and parietal cortices, recorded during behavioral tasks similar to ours, are activated at times (>100ms before movement) that could account for our observations regarding premovement activity (PMA) onset. These cortical regions have preparatory neurons that encode the goal or target and the intended direction of movement independent of their movement-related discharge. Changes in somatosensory inputs to MI are said to be sufficient to reorganize MI outputs thus emphasizing the importance of sensory inputs for maintaining the organization of the motor system, which, in turn, may regulate sensory responsiveness. However, premotor and MI cortices may have different capacities for response plasticity since the proportion of cue-related responses in premotor cortex increases with extended learning while it does not in MI. It is not known if these effects form the substrate for SI modulation or may result from changes in SI responsiveness. It is certainly not known if these same neurons show trial-by trial modulation when a learned task becomes suddenly unpredictable. Since it is difficult to follow sensorimotor cortical neurons during learning, we decided instead to examine SI neurons of monkeys when the security of the associations between cues and movements are unpredictably altered. Finally, many neurons in motor and premotor cortices have characteristics that fit suggested components of a model we developed to account for PMA and sensory responsiveness modulation in SI. We wish to gain data from SI cortical neurons to determine if the timing of activity changes adds to the validity of the model or suggest changes in it.

STATUS OF CURRENT RESEARCH

Statement of Work

We derived experiments to test the hypothesis that SI neuronal activity, related to stimulus detection, and movement initiation and execution, changes markedly when animals are uncertain about conditions that influence their behavior. This hypothesis is based upon a slight modification of the second and third of Matthews' tenets regarding corollary discharge, that is, the assumption that this discharge is generated only if necessary and then at a time, of a polarity and of a magnitude to gate potentially interfering peripheral inputs resulting from ongoing palmar vibration. Finally, it is based upon the assumption that requiring the use of peripheral sensory information in motor behavior will increase the selective attention directed toward inputs carrying that information. It assumes comparable behavioral responses will be made under different sensory cueing conditions. Thus, motor-set was not altered significantly in the experiments that will be described. Our goal has been to record from area 3a, 3b and 1 neurons initially and to then record from neurons in areas 2,4,5 and 6 as time permitted. The rationale for recording in anterior and central SI is that these cortical areas are known to respond well to the stimuli that will be used for the go cue. The rationale for recording from the latter cortical areas is essentially the same as listed above.

Preliminary Results

Three studies, either recently completed or currently underway were conducted during the reporting period. We report the 1) Preliminary results from the recordings from 327 task related sensorimotor cortical neurons that indicate that when behavioral conditions become suddenly unpredictable, responsiveness to peripheral sensory and centrally-generated inputs is increased. This is tentatively being viewed as a release from the tonic attenuation that probably occurs during the performance of stereotypic behaviors. 2) Analyses of data that indicated that primary somatosensory (SI) cortical neurons that respond to vibratory go-cues for wrist movement with the greatest fidelity have their activity modulated just prior to movement onset. This observation fits with the hypothesis that, prior to active movement, sensory inputs that are no longer behaviorally relevant are gated so as not to interfere with monitoring movement parameters by the primate CNS. 3) SI neurons that discharge rhythmically as monkeys hold a steady position commonly have this consistent firing pattern disrupted at behaviorally salient points in time (e.g, go-cue onset and/or prior to movement onset when the decision to move has been reached). These neurophysiological

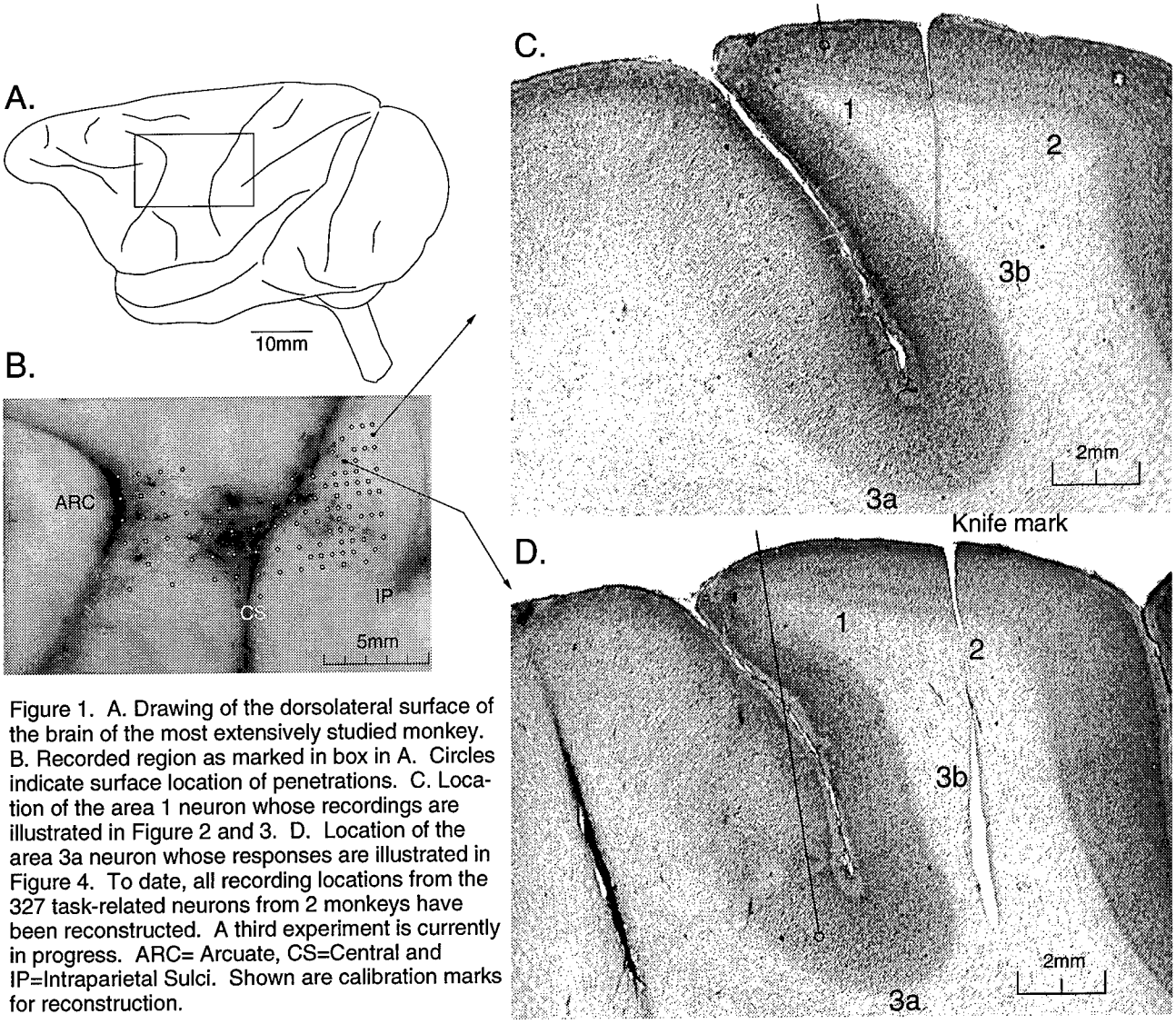

Figure 1. A. Drawing of the dorsolateral surface of the brain of the most extensively studied monkey. B. Recorded region as marked in box in A. Circles indicate surface location of penetrations. C. Location of the area 1 neuron whose recordings are illustrated in Figure 2 and 3. D. Location of the area 3a neuron whose responses are illustrated in Figure 4. To date, all recording locations from the 327 task-related neurons from 2 monkeys have been reconstructed. A third experiment is currently in progress. ARC= Arcuate, CS=Central and IP=Intraparietal Sulci. Shown are calibration marks for reconstruction.

experiments suggest that the responsiveness of SI neurons is profoundly influenced by behavioral conditions.

1) Sensory Cortical Neuron Responsiveness During The "Unpredictable Task".

Goals of the Study-

We are currently conducting experiments that test the hypothesis that variations in expectation alter SI neuronal sensory responsiveness and premovement activity. The basic paradigm used is described in detail in Enclosure #1. Using an unpredictable reward schedule for correct task performance, we have created a condition under which monkeys sometimes are not reinforced for seemingly appropriate movements. Several results are thought to be possible. In trials immediately following correct but unrewarded performance ("after trials"), both sensory responsiveness and premovement activity may be either enhanced or suppressed. We have described these changes quantitatively and qualitatively.

Brief Description of Methods-

Three monkeys were trained to make wrist flexion and extension movements in response to vibratory and/or visual go-cues. We are currently recording from the third of these. Each monkey first held a centered wrist position and awaited the trial's go-cues. Upon receipt of that cue, he made ballistic wrist flexion or extension movements, in blocks of ten. Using a pseudo-random reward schedule, we created a condition in which behavioral outcome could not be reliably predicted. About 75% of the trials in which the monkey performed correctly were rewarded. The other 25% were not. The activity patterns of 327 task-related neurons have been studied in detail. A total of 68/327 were vibratory responsive. Vibratory responsive neurons exhibited sustained or transient changes in neuronal activity associated with stimulus presentation. Of these, 14 had Deep and 38 had Cutaneous receptive fields (RFs). Fourteen

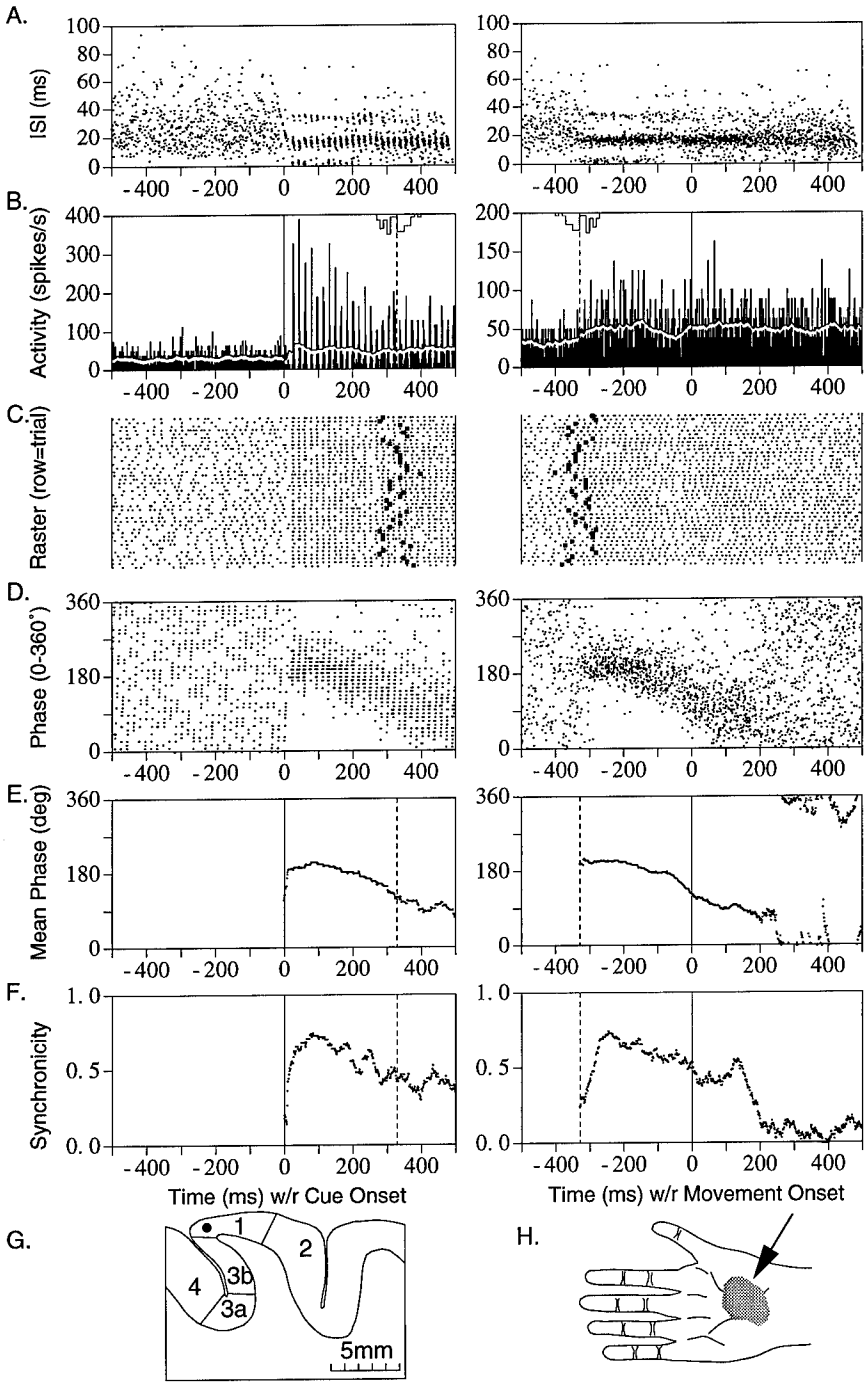

A.' B.' C.' D.' E.' F.'

Figure 2. Displays of the parameters, as a function of "behavioral time", centered on vibration onset (left; regular) or movement onset (right; prime). All records are from trials that followed a rewarded trial (regular trials). A. Interspike intervals (ISI) constructed by plotting the ISI of the nth spike in behavioral time. Rhythmic firing appears as horizontal bands. B. Histograms showing instantaneous and mean firing rates. Entrainment may occur without significant increases in mean firing rate. C. Rasters in which each dot represents a spike and each row represents a single trial. (conventions as in figure 4). D. Phase plots which preserve the temporal relationship of spikes to the vibratory stimulus period when trials are "re-aligned" on movement onset. E. Mean phase for the spikes occurring after stimulus onset. F. Synchronicity, a measure of how well the firing pattern is entrained to the frequency of the peripheral vibratory stimulus, scaled from zero (random firing) to 1.0 (perfectly entrained). This Area 1 neuron (G. and Fig. 1C) had a cutaneous receptive field (H.) on the thenar pad extending to the hypothenar eminence.

of these neurons were lost before an RF could be determined and for two, no RF was found. A total of 314/327 exhibited premovement activity. From these, 300 were selected for reasons described below. Of these, 40 showed reciprocal, 67 exhibited unidirectional and 193 had nondirectional premovement activity patterns. Locations of penetrations in the most extensively studied monkey are shown in Figure 1.

Results-

Neuronal activity during rewarded trials (Figure 2) was compared with that for after trials (Figure 3) when monkeys made similar wrist movements. Often, qualitative differences in the activity patterns of these SI cortical neurons during "regular" (rewarded) and after trials were readily noticeable. For example, compare the activity occurring ~100ms before movement onset in Figure 2&3. In initial quantitative examinations, we calculated the premovement activity (PMA) magnitudes and onsets of magnitude changes for all neurons. Using a modified version of the Cumulative Sum Method (CUSUM) and paired t-tests to determine significant differences measurements for neurons within each cortical region studied, we analyzed 300/327 neurons which 1) had significant changes in PMA magnitude prior to movement in at least one direction that 2) occurred between 20-250ms before movement onset. Figure 5G shows results that indicate that PMA magnitude and onset for the regular and the after trials appear to be distributed in two statistically different populations. In panels A-E of this figure, the distribution of the enhancement indices (EIs; after trials PMA magnitude / regular trial PMA magnitude) are presented. This figure also shows the

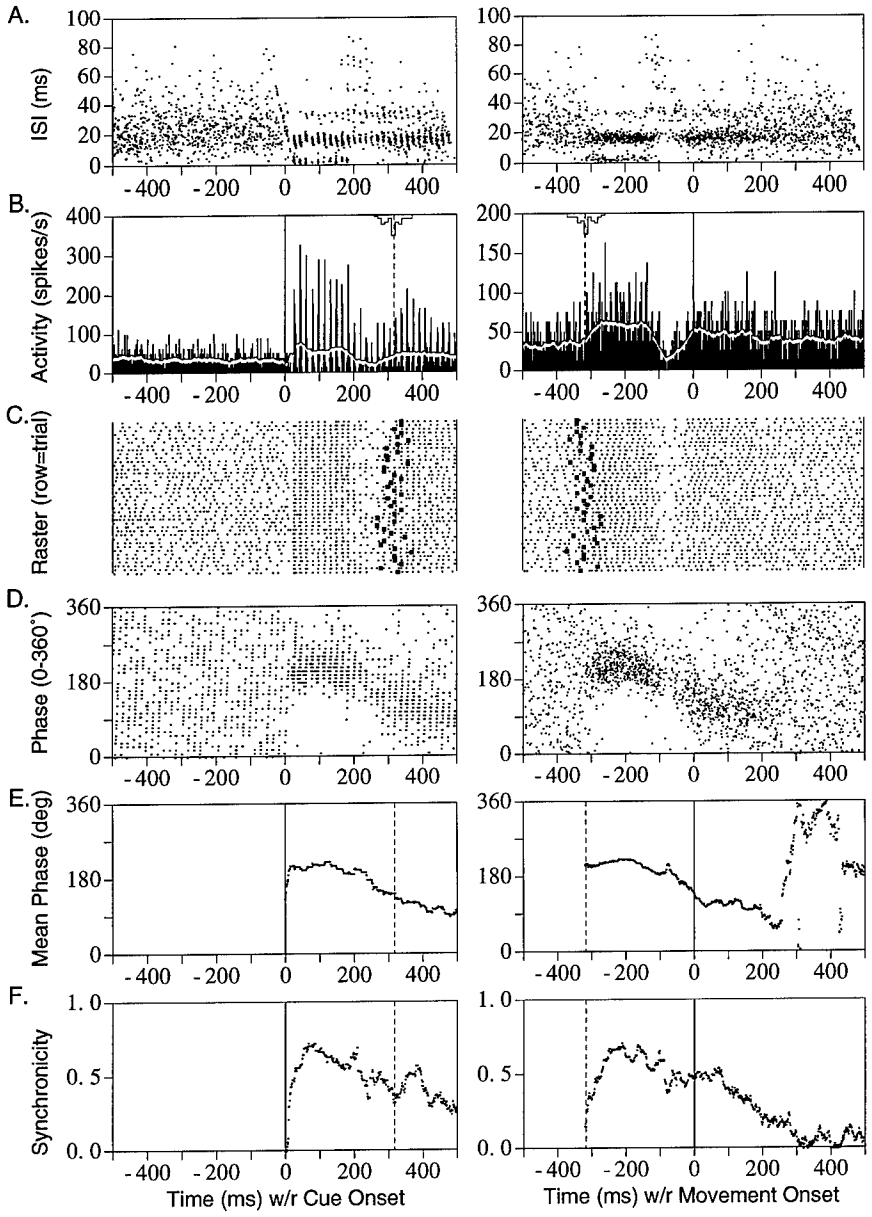

Figure 3. Conventions as in figure 2. Activity of the same neuron except that records show firing associated with trials that immediately followed withholding of reward for correct behavior (after trials). This and the previous figure were constructed from peri-event records associated with vibratory-cued wrist extension movements.

distribution of recorded neurons by cortical location and RF type.

From these initial PMA analyses, we have developed working hypotheses to guide subsequent experiments. First, and in general, in trials triggered by vibratory but not as consistently by visual cues, PMA onsets occurred earlier in regular as compared with after trials (Figure 5G). Thus, PMA changes occur nearer movement onset when the behavioral conditions are less predictable. Second, PMA magnitudes are greater during after trials than during regular trials. The mean EIs are often greater than unity and indicate that statistically significant changes in PMA may be, on average, 12-48% greater in after trials. The broad distribution of these EIs may be explicable once we have additional data so that we can conduct a detailed analysis of EIs for each RF type for each cortical area. In addition, more data is crucial for our ability to make statements regarding changes in activity in more posterior somatosensory cortical areas (areas 2 and 5) during this paradigm.

We have analyzed, in detail, the activity patterns of 68 vibratory-responsive neurons (see Figure 4). Our findings indicate that these sensorimotor cortical neurons tend to be more responsive to peripheral stimuli in after trials as compared with regular trials (Figure 5G). The statistically significant increase in mean firing rate (MFR) in after trials may be due to general increases in excitability as indicated by increases in background activity. When MFRs are normalized by subtracting background activity (Figure 5G ΔPMA) these differences lose statistical significance. We also observed that RTs in after trials were shorter and less variable than in regular trials. These final observations are consistent with hypotheses made previously about what might occur if addition selective attention were directed toward the task.

We are now conducting a similar analysis on over 50 vibratory responsive and other task-related neurons from which we have recently recorded. Observations stated above will be confirmed by these additional data.

Conclusions and Comments-

When the behavioral outcome is predictable (i.e., when the monkey has previously been rewarded for performing correctly) both sensory responsiveness and PMA in SI neurons are at some baseline level. In trials which follow

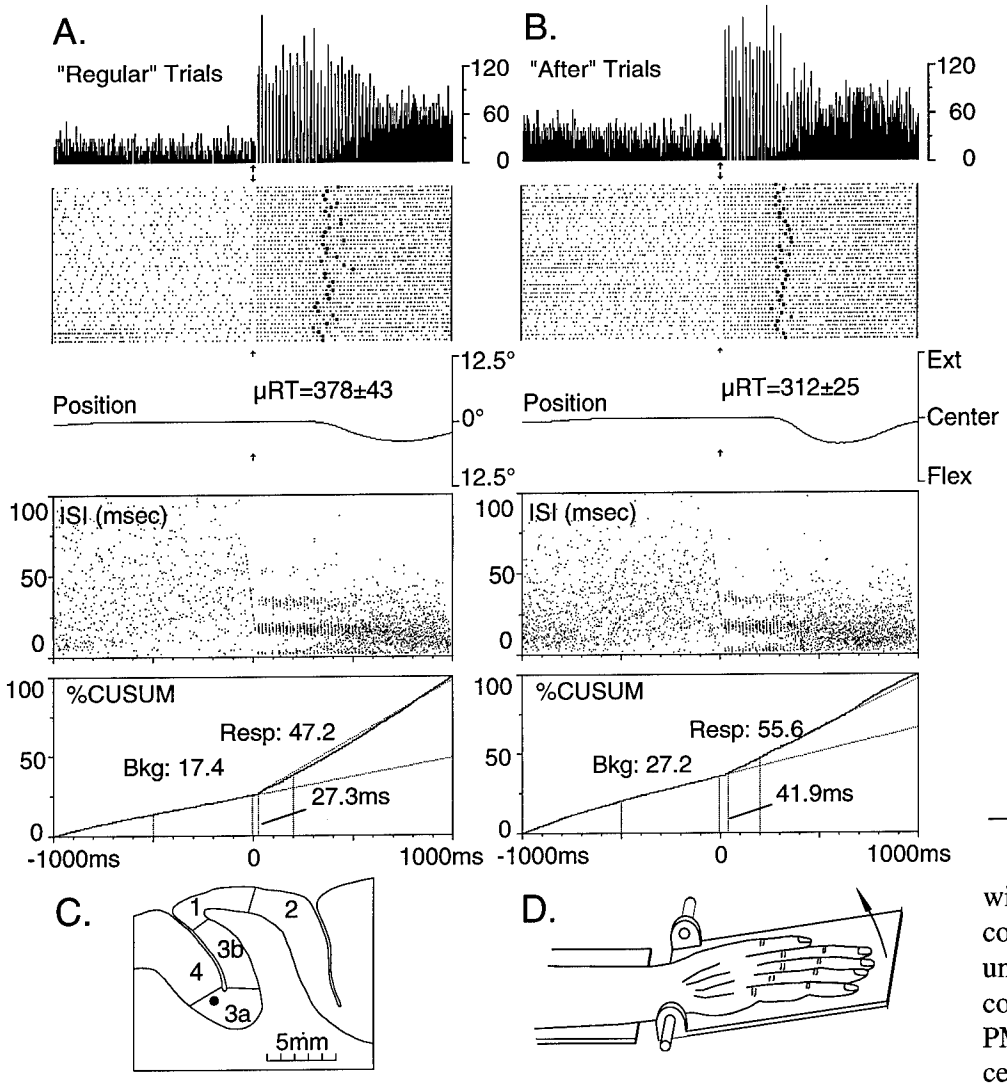

Figure 4. The vibratory responses of an Area 3a somatosensory cortical neuron (C and Fig. 1D) recorded during the performance of regular (A) and after trials (B). Measurements of the mean firing rate during the 500ms of active holding against the load (Bkg; background activity) are given below, to the left of the arrow, which indicates vibration onset, in each of the panels. Values above the arrow the lower panel indicate the mean firing rate during the first 150ms following the onset of the 57 Hz vibratory stimulus which served as the go cue for flexion or extension (not shown) movements. Each was calculated using the CUSUM method whereby the slope of the CUSUM is the mean firing rate. Also listed are mean reaction times (RT) ±SD (upper panels). In general, background activity was greater in after trials than in the regular trials. Vibratory response during the first 150ms after stimulus onset was often greater than in the regular trials. RTs where faster and more consistent in after trials. Mean values for these parameters are listed in the following figure. The neuron was recorded at a depth of 7.8mm from the cortical surface. It responded to passive wrist extension (D) and palpation of the flexor carpi ulnaris. It showed similar entrainment at 27Hz, but responded only transiently to 127Hz vibration.

withholding of the reward for correct performance, outcome is unpredictable. When behavioral conditions become unpredictable, PMA (which may reflect either central or peripheral inputs, depending upon when it occurs), and sensory responsiveness appear to be enhanced. However, decreased predictability is associated with later PMA onset, perhaps because of behavioral uncertainty.

These data are open to at least two types of interpretations. We have previously argued that PMA may gate the response of other SI neurons that do not play an important part in the upcoming movement. We have also argued that PMA may reflect a corollary discharge from primary motor cortex (MI) since neurons in SI areas receiving direct MI projections tend to show PMA while those in areas without direct MI projections do not. MI stimulation is known to alter SI neuronal responsiveness to cutaneous and proprioceptive inputs. Finally we have observed, for the 68 completely analyzed sensory-responsive neurons, that vibratory stimulus-related responses are greater in the after trials. This last observation indicates that during conditions of predictable behavioral outcome, the responsiveness of sensorimotor cortical neurons is attenuated. When conditions become unpredictable, this attenuation appears to be removed. The observation that PMA is, in general, greater in the after trials fits the hypothesis that a general mechanism decreases the activity of SI neurons in response to both peripheral and centrally-generated inputs. One possible role for an increase in PMA might then be to suppress or disrupt the activity of other neurons that do not convey important information about the subsequent movements. Another interpretation is that these neurons are themselves the behaviorally important ones and that increased PMA actually reflects increased information transfer, perhaps related to increased selective attention directed toward behaviorally important events. These two roles are not mutually exclusive and probably occur simultaneously.

Regardless of which interpretation is favored, it appears that sensory gating is dependent upon whether there is a reasonable expectation that attenuating some inputs and strengthening others may actually improve performance by removing potentially competitive sources of information coming from the periphery. Further experimentation will

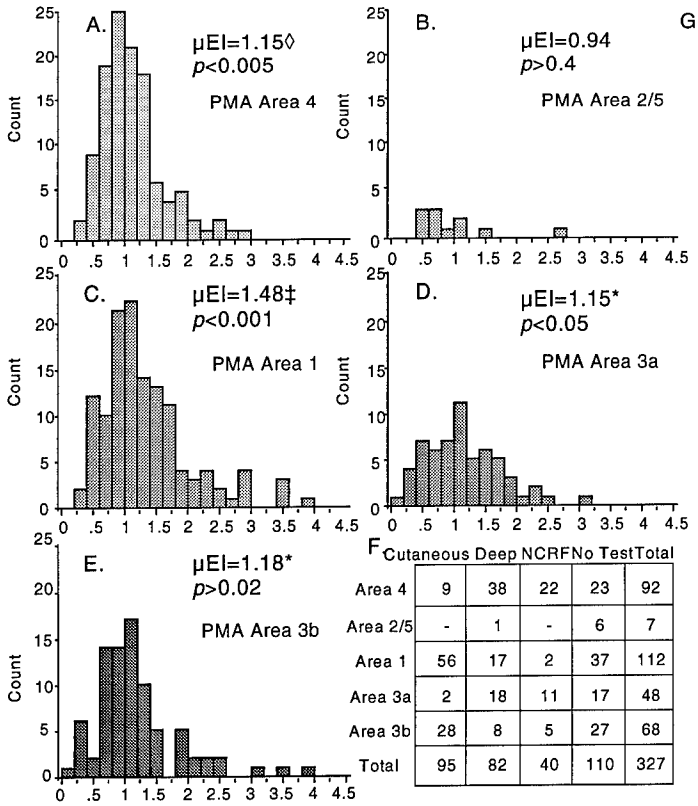

F

	Cutaneous	Deep	NCRF	No Test	Total
Area 4	9	38	22	23	92
Area 2/5	-	1	-	6	7
Area 1	56	17	2	37	112
Area 3a	2	18	11	17	48
Area 3b	28	8	5	27	68
Total	95	82	40	110	327

G. Visually -Cued Trials

Premovement Activity (PMA)

	N	Reg. Onset	After Onset	ΔBKG	ΔOnset	ΔMFR	ΔPMA
Area 4	117	169±62	159±63	1.05	1.19◊	1.08*	1.12◊
Area 2/5	-	-	-	-	-	-	-
Area 1	71	107±47	103±53	1.04	1.86	1.14*	1.27*
Area 3a	46	122±47	127±53	1.18‡	1.21	1.11◊	1.22*
Area 3b	37	86±42	85±45	1.04*	1.24	1.04	1.09

Vibratory -Cued Trials

Premovement Activity (PMA)

	N	Reg. Onset	After Onset	ΔBKG	ΔOnset	ΔMFR	ΔPMA
Area 4	116	177±56	160±60	1.37◊	1.02	1.10◊	1.15◊
Area 2/5	11	149±64	150±61	1.10	1.04	0.94	0.98
Area 1	131	137±59	129±59	1.17‡	1.21*	1.16◊	1.48‡
Area 3a	59	134±52	125±50	1.15*	1.18	1.12*	1.15*
Area 3b	82	91±44	79±46	1.03	1.10	1.04	1.18*

Cue-Related Activity

	N	ΔBKG	μOnset	ΔMFR	ΔResp.
Area 4	8	1.24◊	49±40	1.00	1.67
Area 2/5	-	-	-	-	
Area 1	53	1.21‡	41±26	1.12*	1.07
Area 3a	21	1.10*	33±21	1.07◊	1.03
Area 3b	30	1.03	37±22	1.01	0.96

Reaction Times (RTs)

	Days	Regular	After	ΔRT
Flex	110	326±43	312±33	13.9‡
Ext	110	330±57	309±45	20.7‡

N=number of cases (1 each for significant change for each movement direction for each neuron). Results different from one by one-factor ANOVA. * = $p<0.05$; ◊ = $p<0.01$; ‡ = $p<0.005$. Ratio for EIs of Onsets is regular/after value.

Figure 5. Distributions of the ratios of the magnitudes of premovement activity [PMA (MFR-BKG see below); (A-E)] in after trials compared with during regular trials (Enhancement Index; EI= after trial value/regular trial value). Significant changes in premovement activity during the after trials were ~ 12-48%. F) Table listing the number of task-related neurons analyzed as a function of receptive field (RF) type (upper) and cortical location (left). NCRF=no clear RF; NT=not tested. G) Means and SDs of onsets of activity and Reaction Times (in msec). EIs (=Δ) for background activity (BKG; during the hold phase of the paradigm), MFR (Mean Firing Rate) and PMA for the cases from those neurons having PMA. Below, Δ for the activity of vibratory-responsive neurons during the initial 150ms after vibratory go-cue presentation. RTs are for the entire 110 recording sessions. (see text)

determine if cortical location and RF type are important factors determining the effects of reward predictability upon neuronal responsiveness in SI.

2) Sensory Cortical Neuron Responsiveness Synchronized to Vibratory Stimuli.

Goals of the Study-

Primary somatosensory cortical (SI) neurons exhibit characteristic patterns of activity prior to initiation of voluntary movements. It is believed that premovement activity in SI neurons may result from centrally-generated as well as peripheral inputs. We examined premovement activity patterns for a group of SI neurons that represent somatosensory peripheral stimuli in a most faithful way. These neurons were characterized by entrainment of their activity to vibrotactile stimuli (i.e., by a very close temporal correlation between the stimuli and the neurons' responses to them). We hypothesized that, for selected neurons, activity patterns of central and peripheral origin can be distinguished. It was expected that central input, if any, might introduce a component into the vibration-entrained neuronal firing that is asynchronous with the peripheral vibratory stimulus. Thus, vibration-entrained firing might have its synchrony reduced at about the same time that other, non-entrained cortical neurons exhibit PMA (previously published observations).

Brief Description of Methods-

Monkeys made wrist flexion and extension movements in response to sinusoidal vibration (27, 57 or 127 Hz) of their palms. Vibration remained on until the animal moved at least 5° from the initial hold (center) position. The activity of 55 extracellularly recorded SI neurons (areas 3a, 3b, 1, 2 respectively: 10, 13, 28, 4) was vibration-entrained. The temporal relationship between the vibratory stimuli and neuronal firing was described by the mean phase (MP) of spikes with respect to the vibratory cycle. The degree of entrainment was quantified as synchronicity (Sync), which was derived from the standard deviation (SD) of the phase and expressed in units scaled between the SD for non-entrained firing and the SD for a constant response phase. Mean firing rate (MFR) was derived from the number of spikes per vibratory cycle. More complete descriptions of the behavioral paradigm, the electrophysiological recording procedures and methods of data analysis can be found in Enclosure #1.

Results-

Typically, during the hold phase of the paradigm preceding vibration onset, neurons with either cutaneous or deep receptive fields (RFs) exhibited background activity. The background firing rate was, on the average, larger for units with deep RFs (mean=30.2 spike/s) than for units with cutaneous RFs (mean=21.5 spike/s). After a transitory burst in response to vibration onset, the studied neurons responded to the ongoing vibration in a steady-state manner. During this period of stabilized response, which was usually about 100 ms in duration, neuronal firing was entrained to the vibratory stimulus. For some neurons, MFR of the stabilized response was not substantially different from background MFR. Thus, the characteristics of peripheral input were coded by the temporal firing pattern rather than by MFR. For neurons with deep RFs at all tested vibratory frequencies, and for neurons with cutaneous RFs at 27 and 57Hz, MFRs were not significantly different (mean=46.4 spike/s). At 127Hz, for neurons with cutaneous RFs, MFR decreased (mean=19.4 spike/s).

For the majority of cells, the pattern of stabilized response was modulated prior to movement onset. Cases of MFR increase (premovement activation) and of MFR decrease (premovement suppression) were observed. Also, two premovement changes in MFR often were observed (two-event cases). For two-event cases, early and late MFR changes could be distinguished. In many cases, premovement changes of MFR began before EMG onset, suggesting that this modulation results from centrally-generated inputs rather than from movement-associated peripheral reafference (Details provided in Enclosure #1).

Premovement activation was accompanied by shifts of mean phase towards earlier responses to the ongoing vibratory stimulus, and by a decrease of response Sync. The correlations of the onset of MFR increases with these shifts in MP and Sync were statistically significant. The desynchronization was more profound at the lower vibratory frequency (27 Hz) when compared to higher ones (57 and 127 Hz). However, MP shifts were more prominent at the higher vibratory frequencies. We suggest that, during premovement activation, an asynchronous signal is integrated with the periodic peripheral input. This asynchronous signal may make neurons more likely to discharge and to do so earlier with respect to the vibratory input. The asynchronous component may also disrupt the vibration-entrained activity pattern. Several observations lead us to suggest this working hypothesis. First, the degree to which the firing patterns of primary somatosensory cortical neurons were synchronized with on-going peripherally-delivered vibratory stimuli could be calculated and expressed as a scaled parameter. Second, the value of Sync often decreased prior to movement onset. This was in spite of the fact that the time at which these decreases occurred often preceded any detectable peripheral positional or muscular (EMG) activity changes and that the firing rate actually underwent an accompanying increase (Enclosure #1, figure 8). Third, premovement activity changes in entrained SI neurons occur at approximately that same time as activity changes in non-entrained SI neurons. These activity changes in non-entrained neurons are themselves, not in synchrony with the peripheral stimulus frequency, suggesting that in these neurons, PMA is not merely a late vibratory stimulus related activity. Finally, the activity of entrained neurons was not desynchronized at that time following vibratory stimulus onset when animals are instructed to withhold movements in response to the same stimuli that have previously served as go-cues in the movement paradigm (unpublished observations). Thus, as a working hypothesis, we continue to suggest that it may be possible to distinguish between the response to periodic peripheral stimuli and an input which does not possess the same periodicity and which, by virtue of the fact that responses to it occur prior to EMG and positional changes and are associated with impending movement, may be central in origin. Thus, differences in MP and Sync changes at different vibratory frequencies probably reflect the interaction between the temporal properties of these inputs. We are just beginning to model the possible interactions between inputs of known frequencies, such as those presented peripherally, and those that might arise centrally, such as those which may reach neurons of this type from rhythmically firing neurons in cortical or subcortical structures (see below). What seems clear is that additional inputs to these neurons would tend to make them fire earlier with respect to external stimuli, but also desynchronize their responses to on-going peripheral periodic stimuli.

Premovement suppression was not associated with consistent shifts of MP and Sync. The cases of premovement suppression commonly had larger MFRs during stabilized responses than the cases of premovement activation (e.g., at the vibratory frequency of 57Hz, for one-event patterns, mean value of MFR during stabilized responses for cases of suppression was 56.2 spike/s, and for activation it was 32.0 spike/s).

The onset times of premovement changes in MFR, MP and Sync were compared with RTs for each animal. For animals with longer RTs, premovement events occurred earlier relative to movement onset. Such a relationship is unlikely for peripherally-induced events. The dependence of premovement modulation onset upon RT was more prominent for earlier than later activity changes.

The variability of the firing characteristics associated with the direction of subsequent movement was estimated. This was done for the activity during the stabilized response period and the later premovement period by examining the flexion-extension activity differences. For the stabilized response period, these difference values (for MFR, MP, but not for Sync) were significantly larger for neurons with cutaneous RFs. For the premovement period, modulation patterns substantially varied depending on movement direction. These premovement patterns were classified as reciprocal or symmetrical with respect to movement direction. For two-event cases, early events were more often symmetrical than late events (Please see Enclosure #1 for details).

Conclusions and Comments-

We conclude that the activity patterns of SI neurons that most faithfully represent the sensory periphery are modulated prior to voluntary movements. We suggest that inputs of central origin contribute to this premovement modulation. Presumably, the role of the central inputs may be to prepare the sensory cortical areas for changes in activity (reafference) that result from voluntary movement.

3) Sensory Cortical Neurons Which Fire Rhythmically During Active Holding.

Goals of the Study-

Much attention has recently been devoted to examining rhythmic activity in the mammalian neocortex and thalamus. This is due in part to theories regarding the possible functional role of these rhythms in the gating of the thalamocortical transmission of information and/or in switching between different behavioral states. In earlier studies, we had observed single sensorimotor cortical neurons that fired rhythmically, most notably during the period in which monkeys held a handle steadily, against a load, and awaited a vibratory go-cue that triggered stereotypic wrist flexion and extension movements. Our goal was to determine if these neurons showed profound changes in firing rate during this task and, if so, did these changes occur in relation to specific behavioral events or the transitions between different parts of the task.

Brief Description of Methods-

The analyzed data were taken from neurons recorded, but not described, in previous studies. Interspike interval, expectation density and renewal density histograms were constructed to determine the frequency of the rhythmic discharge during the time that the animals held a steady wrist position against a load for at least 500msec, the stationarity of the rhythmic firing and the presence or lack of serial dependence. The onset of changes in mean firing rate, relative to behavioral events such as vibratory go-cue onset and movement onset were determined using cumulative sum (CUSUM) plots in which these onset were detected as changes in the inclination of the CUSUM of more than 3 SDs for at least 40msec consecutively.

Results-

A total of 105 SI neurons (23, 36, 34 and 12 from areas 3a, 3b, 1 and 2) were selected because expectation density (autocorrelation) histograms of their firing patterns during the hold period had peaks at multiples of the mean interspike interval (ISI). An example of one such neuron and the types of analyses normally conducted are shown in Figure 6. Changes in firing patterns from background levels (MFR 33.5±5.8 spike/s) occurred often, following vibration onset for these (49/105) SI neurons. SI activity changes at vibration onset were typically brief firing rate suppressions (44/49). Movement-associated suppressions or facilitations occurred for each of these SI neurons (n=105), but usually didn't vary as a function of subsequent movement direction (70/105 symmetrical; 35/105 directional). For these SI neurons, facilitatory and suppressive influences disrupted rhythmical firing patterns rather than modulating mean ISIs. The mean onset of changes in rhythmic activity that preceded movement onset was 57.5±43.5. ISIs for these SI neurons, and thus their firing patterns, were regularly and narrowly distributed. Of those neurons with confirmed RFs (n=58), the majority (40/58) had deep RFs while only 18/58 had cutaneous RFs. The similarity of the Expectation Density and the Renewal Density plots (i.e., multiple peaks at regular intervals of approximately the same height) indicates that the source of the rhythmic driving of this neuron is relatively secure in its frequency.

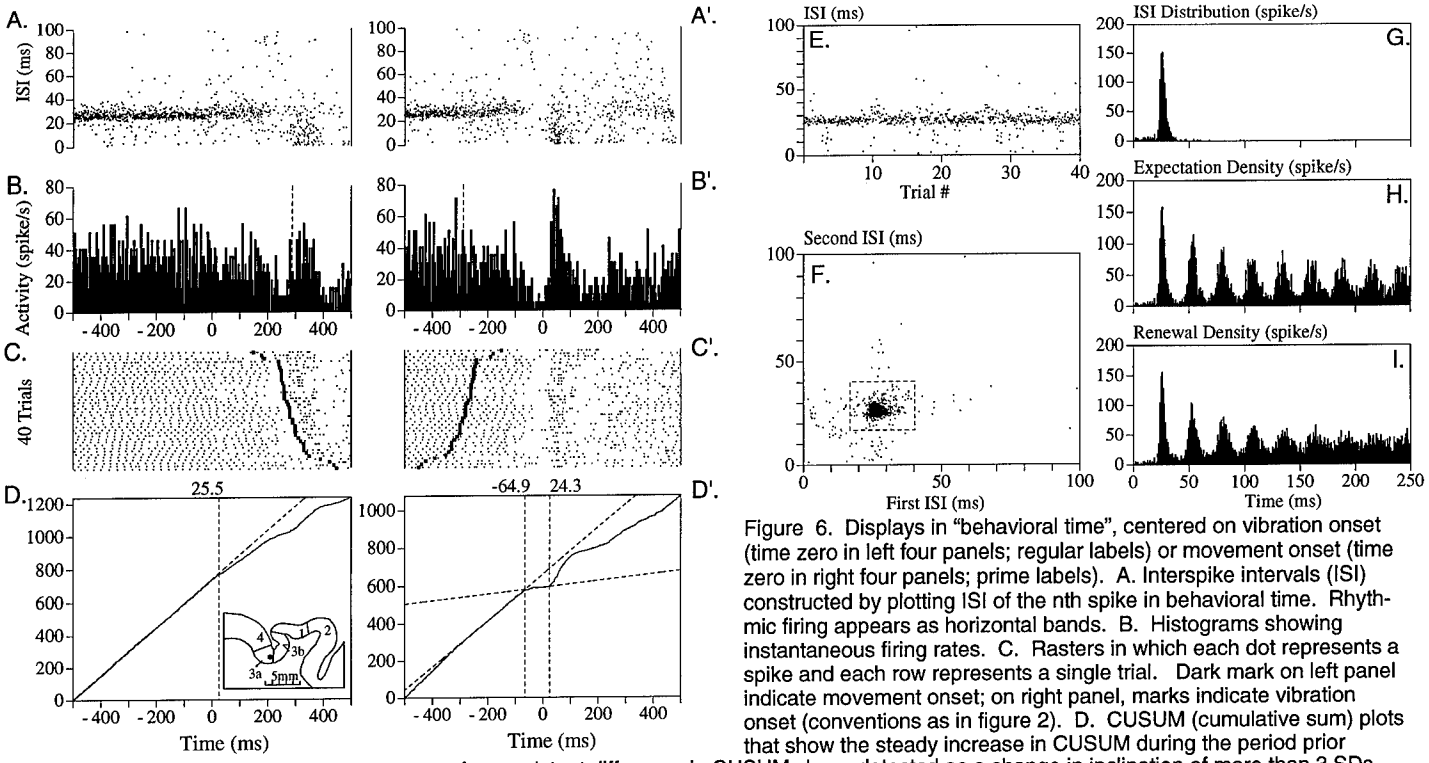

Figure 6. Displays in "behavioral time", centered on vibration onset (time zero in left four panels; regular labels) or movement onset (time zero in right four panels; prime labels). A. Interspike intervals (ISI) constructed by plotting ISI of the nth spike in behavioral time. Rhythmic firing appears as horizontal bands. B. Histograms showing instantaneous firing rates. C. Rasters in which each dot represents a spike and each row represents a single trial. Dark mark on left panel indicate movement onset; on right panel, marks indicate vibration onset (conventions as in figure 2). D. CUSUM (cumulative sum) plots that show the steady increase in CUSUM during the period prior to vibration onset and the first occurrence of a consistent difference in CUSUM slope, detected as a change in inclination of more than 3 SDs for at least 40ms. A small decrease in firing rate occurred at 25.5ms after vibration onset. Inset; Recording location. D'. Onsets of two changes in firing rate occurring at 64.9ms before movement onset and 24.3 after movement onset. E. Plot of all ISIs during the last 500ms of the hold period (left half Panel C.) as a function of trial number. This plot indicates that the rhythmic firing of this neuron during active holding against a load did not change systematically over the recording period. F. Plot of the nth vs. the nth+1 ISI for all spikes showing only small variations in the ISI. G. Distribution of ISI for spikes occurring during the hold period. H. Expectation Density plot of hold period firing. This is, in essence, an autocorrelation plot over a short interval. I. A Renewal Density plot in which the ISIs are randomly shuffled and then plotted is a manner similar to that for the Expectation Density plot. The similarity of the Expectation Density and the Renewal Density plots (i.e., multiple peaks at regular intervals of approximately the same height indicates that the source of the rhythmic driving of this neuron is relatively secure in its frequency although it does not uneqivocally indicate whether this neuron is an intrinsic oscillator or is driven by a synaptically secure source.

However, it does not unequivocally indicate whether this neuron is an intrinsic oscillator or is driven by a synaptically secure source.

Conclusions and Comments-

Some investigators have suggested that rhythmic neuronal firing may be due to intrinsic oscillatory properties while others consider secure external driving to be necessary. However, the precise role of rhythmic activity in sensorimotor integration is not known. Observations have lead authors to seemingly mutually exclusive conclusions regarding its function. It has been stated that oscillatory activity and/or rhythmic firing 1) is encountered more frequently in MI, than SI, 2) is encountered more often in sensory, than non-sensory regions, 3) is often reduced by tactile stimulation or self-initiated movements, and 4) may facilitate interactions between neurons during movements in which selective attention to sensory motor integration is needed. Clearly, more investigation of the behavioral conditions under which rhythmic activity occurs and the events resulting in its disruption is necessary. Regardless of what causes rhythmic firing, SI neurons change activity at times consistent with the hypothesis that they are involved in switching between behavioral modes.

Summary

Each of the experiments described above has yielded data that will be compared with previously obtained data from sensorimotor cortical neurons, recorded while monkeys perform the similar tasks. The specific goals of these continuing studies are a) to understand the influence of behavioral unpredictability and knowledge of results upon sensorimotor cortical activity, b) to understand the special role that these neurons play in sensorimotor integration during the initiation and execution of cutaneous and proprioceptively guided movements and c) to determine eventually if human subjects perform the behavioral tasks in a way that strengthens the contention that neurophysiological

events in the primate brain reflect what occurs in homologous regions of the human CNS while performing under the same behavioral conditions. The long-term goal of our work is to better understand the role the sensorimotor cortices play in motor control during stimulus detection and classification, response programming and selection (initiation) and response production (execution). Through an understanding of the normal sensorimotor integrative functions during complex behaviors, new insights can be gained regarding what occurs during sensorimotor dysfunction as well as manual control of sophisticated devices.

LIST OF PUBLICATIONS

M.A. Lebedev, J.M. Denton and R.J. Nelson. Vibration-entrained and premovement activity in monkey primary somatosensory cortex. *J. Neurophysiol.* 72(4): 1654-1673, 1994

M.A. Lebedev and R.J. Nelson. Rhythmically firing (20-50Hz) neurons in monkey primary somatosensory cortex: Activity patterns during initiation of vibratory-cued hand movements. (Submitted; *J. Computational Neurosci.*)

R.J. Nelson, E.D. Thomas and J.M. Denton. Reaction times and movement times for visually-cued and combined vibratory- and visually-cued hand movements. (In preparation for *J. Motor Behavior*)

M.A. Lebedev and R.J. Nelson. Two types of Pacinian-Like neurons in monkey primary somatosensory cortex (SI) studied during active hand movements. *Neuroscience Abst.* 20:1388, 1994

R.J. Nelson, J.M. Denton and M.A. Lebedev. Activity of monkey sensorimotor (SMC) and neostriatal (NS) neurons during hand movements made under unpredictable conditions. *Neuroscience Abst.* 20:983, 1994

ASSOCIATED PERSONNEL

John M. Denton continues to be employed as a Research Assistant. He has, over the four years, proved to be important in the studies conducted under this grant. He now has expertise in data analysis and behavioral training of monkeys. Beginning July 1, 1994, he ceased to receive any support from this grant.

Michael A. Lebedev joined the laboratory this three years ago as a graduate student following his arrival from Moscow, Russia. He brought to the laboratory an extensive background in mathematics and physics. He is largely responsible for the analyses of the vibratory responsive neurons described herein and presented one of the abstracts listed above at this year's Annual Meeting of the Society for Neuroscience. He is truly a remarkable individual and an asset to the laboratory. Beginning July 1, 1993, he received 50% of his support for funds of AFOSR 91-0333. The other 50% of his support comes from an award by the Center of Excellence in Neuroscience at the University of Tennessee, Memphis. Beginning July 1, 1994, he ceased to receive any support from this grant.

INTERACTIONS

Invited Presentations:

"Set and the Single Simian Somatosensory Cell." University of Montreal December 1993.

"Modulation of sensory responsiveness in somatosensory cortex: possibly by basal ganglia." Montreal Neurological Institute December 1993

Meetings:

1994 Society for Neuroscience Annual Meeting, Miami Beach, FL Nov. 12-17.

NEW DISCOVERIES

none

JOURNAL OF NEUROPHYSIOLOGY
Vol. 72, No. 4, October 1994. *Printed in U.S.A.*

Vibration-Entrained and Premovement Activity in Monkey Primary Somatosensory Cortex

MICHAEL A. LEBEDEV, JOHN M. DENTON, AND RANDALL J. NELSON
Department of Anatomy and Neurobiology, University of Tennessee, College of Medicine, Memphis, Tennessee 38163

SUMMARY AND CONCLUSIONS

1. Primary somatosensory cortical (SI) neurons exhibit characteristic activity before the initiation of movements. This premovement activity (PMA) may result from centrally generated as well as from peripheral inputs. We examined PMA for 55 SI neurons (10, 13, 28, and 4 in areas 3a, 3b, 1, and 2, respectively) with activity that was entrained to vibrotactile stimulation (i.e., was temporally correlated with the stimulus). We sought to determine whether the temporal characteristics of vibration-entrained discharges would change throughout the reaction time period, and, if they did, whether these changes might be accounted for by central inputs.

2. Monkeys made wrist flexions and extensions in response to sinusoidal vibration (27, 57, or 127 Hz) of their palms. Vibration remained on until the animal moved at least 5° from the initial hold position. Mean firing rate (MFR), a measure of the level of activity, was derived from the number of spikes per vibratory cycle. The correlation between the vibration and the neuronal firing was described by the mean phase (MP) of the vibratory cycle at which spikes occurred. The degree of entrainment was quantified as synchronicity (Synch), a statistical parameter that could change from 0 for no entrainment to 1 for responses at a constant phase.

3. Premovement MFR increases (activation) and decreases (suppression) were observed. Moreover, two changes in MFR often were observed for the same neuron (2-event PMA). Many MFR shifts, especially the first in the two-event PMA, preceded electromyographic (EMG) onset. The pre-EMG MFR shifts more often had the same sign both for flexion and extension movements rather than having opposite signs. However, with equal frequency, post-EMG PMA events had the same or opposite sign for different movement directions. We suggest that the pre-EMG PMA has an origin different from movement-related peripheral reafference.

4. Premovement activation was accompanied by shifts of MP corresponding to earlier responses to the ongoing vibratory stimulus and by decreases of response Synch. Premovement suppression was not associated with consistent shifts of MP and Synch. We suggest that during premovement activation, asynchronous (uncorrelated with vibration) signals are integrated with the vibratory input. These asynchronous signals may make neurons more likely to discharge and to do so earlier with respect to the vibratory stimulus. The asynchronous component may also disrupt the vibration-entrained activity pattern.

5. From these data we conclude that the activity of SI neurons that most faithfully represent the sensory periphery is modulated before voluntary movements. We suggest that inputs of central origin may contribute to this premovement modulation. Presumably, the role of the central inputs may be to prepare SI for changes in sensory activity that result from voluntary movement. Premovement asynchronous signals, both of central and peripheral origin, disrupt the fidelity of coding of the vibratory stimulus by SI neurons. This deterioration of the quality of representation of sensory inputs by SI neurons may be related to the phenomena of premovement elevation of the tactile threshold of perception and of premovement decrease of somatosensory-evoked potentials.

INTRODUCTION

Extracellular recordings from the primary somatosensory cortex (SI) of behaving monkeys have demonstrated that many neurons exhibit characteristic activity associated with voluntary movements of the forelimb made either in response to go-cues (Bioulac and Lamarre 1979; Evarts 1972; Fromm and Evarts 1982; Lamarre et al. 1983; Nelson 1984, 1987, 1988; Nelson and Douglas 1989; Nelson et al. 1991) or during self-paced tasks (Soso and Fetz 1980). Interestingly, the firing patterns of some SI neurons are modified before muscle activation [electromyographic (EMG)]. It has been suggested (Jiang et al. 1991; Nelson 1987, 1988; Nelson and Douglas 1989; Nelson et al. 1991; Soso and Fetz 1980) that for these early firing SI neurons, premovement activity (PMA) may result from centrally generated preparatory signals. These central signals, presumably coming from motor centers, have been referred to as corollary discharge (Evarts 1971; von Holst 1954). Since the time of von Helmhotz, it has been thought that sensation can be modulated by central influences (von Helmholtz 1962; see Miles and Evarts 1979 for review). However, the functional significance and neuronal mechanisms of such modulatory influences are still not completely understood (Matthews 1988).

The presumed interaction between peripheral inputs to SI neurons and those of central origin can be studied with the use of an experimental paradigm in which monkeys make wrist movements in response to vibrotactile stimuli applied to the working hand (Nelson 1984, 1987, 1988). Several types of SI activity under these conditions have been found. It has been reported that some SI neurons exhibit quickly adapting phasic responses associated with vibratory stimulation (Nelson et al. 1991). Moreover, these same neurons resume firing before movement onset. In many cases, this reactivation of neuronal firing occurs before EMG onset, suggesting the involvement of a centrally generated activity component. Analyzing the responsiveness of these neurons to the vibrotactile stimuli and the magnitude of their PMA showed that their PMA includes a stimulus-related component. The relative contribution of peripheral and central premovement inputs was also ana-

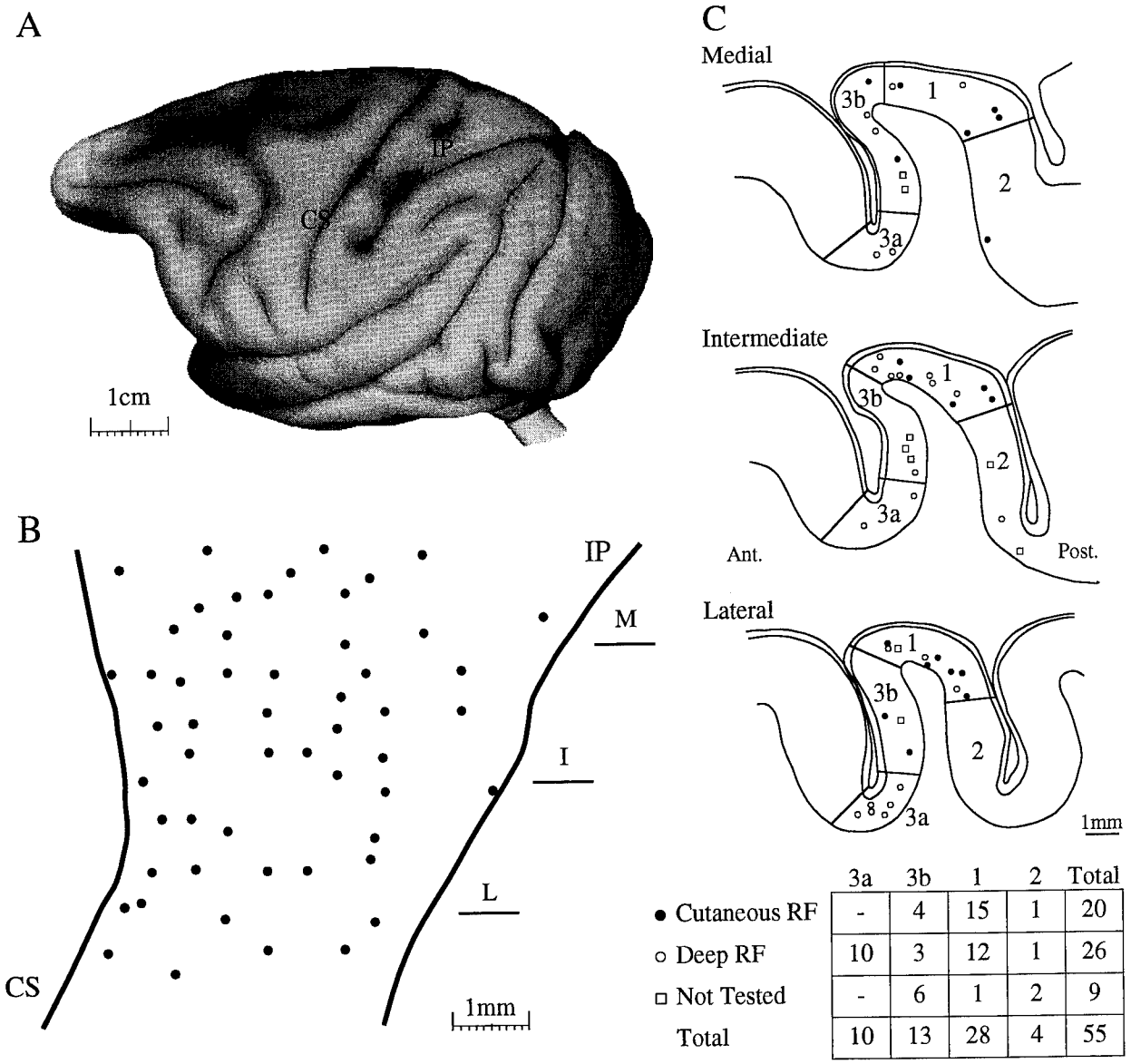

	3a	3b	1	2	Total
● Cutaneous RF	-	4	15	1	20
○ Deep RF	10	3	12	1	26
□ Not Tested	-	6	1	2	9
Total	10	13	28	4	55

FIG. 1. *A*: digitized view of the dorsolateral surface of the brain (*monkey H*). The brain has been tilted 30° in the coronal and sagittal planes. Central sulcus (CS) and intraparietal sulcus (IP) are marked. *B*: composite showing the relative location of recording sites. Fifty-four surface locations are shown. The activity of 2 neurons, located in area 1, was recorded simultaneously. Locations of penetrations for *monkeys C, F,* and *G* were transposed into the surface map of the most extensively studied monkey (*H*). Representative parasagittal sections, indicating the location of neurons at 3 levels [lateral (L), intermediate (I), and medial (M)] are shown in *C*.

lyzed by comparing activity patterns exhibited by SI neurons during movements in response to vibratory and to visual go-cues (Nelson and Douglas 1989; Nelson et al. 1991).

In the present study we examined the activity during initiation of vibratory-cued movements in a special class of SI neurons characterized by the faithful way in which they represented the sensory periphery. They responded to ongoing vibratory stimuli by sustained, entrained discharges. The entrainment of neuronal activity to periodic somatosensory stimuli (i.e., close temporal correlation between the stimuli and responses) is a well-known phenomenon. Entrainment has been demonstrated for cutaneous and deep afferents (Bianconi and van der Meulen 1963; Burke et al. 1976a,b; Johansson et al. 1982; Morley and Goodwin 1987; Ribot-Ciscar et al. 1989; Roll and Vedel 1982; Talbot et al. 1968; Wall and Cronly-Dilon 1960), motoneurons (Burke and Schiller 1976; Desmedt and Godaux 1980; Homma 1976; Lebedev and Polyakov 1991, 1992; Person and Kozhina 1992), spinal interneurons (Honda et al. 1986), as well as for neurons in somatosensory cortical areas (Burton and Sinclair 1991; Ferrington and Rowe 1980; Mountcastle et al. 1969, 1990; Nelson 1988). The entrainment of neuronal activity to the temporal characteristics of peripheral stimuli is believed to be an important coding mechanism (Morley and Goodwin 1987; Mountcastle et al. 1969, 1990; Nelson 1988; Talbot et al. 1968).

We hypothesized that, for SI neurons that faithfully fol-

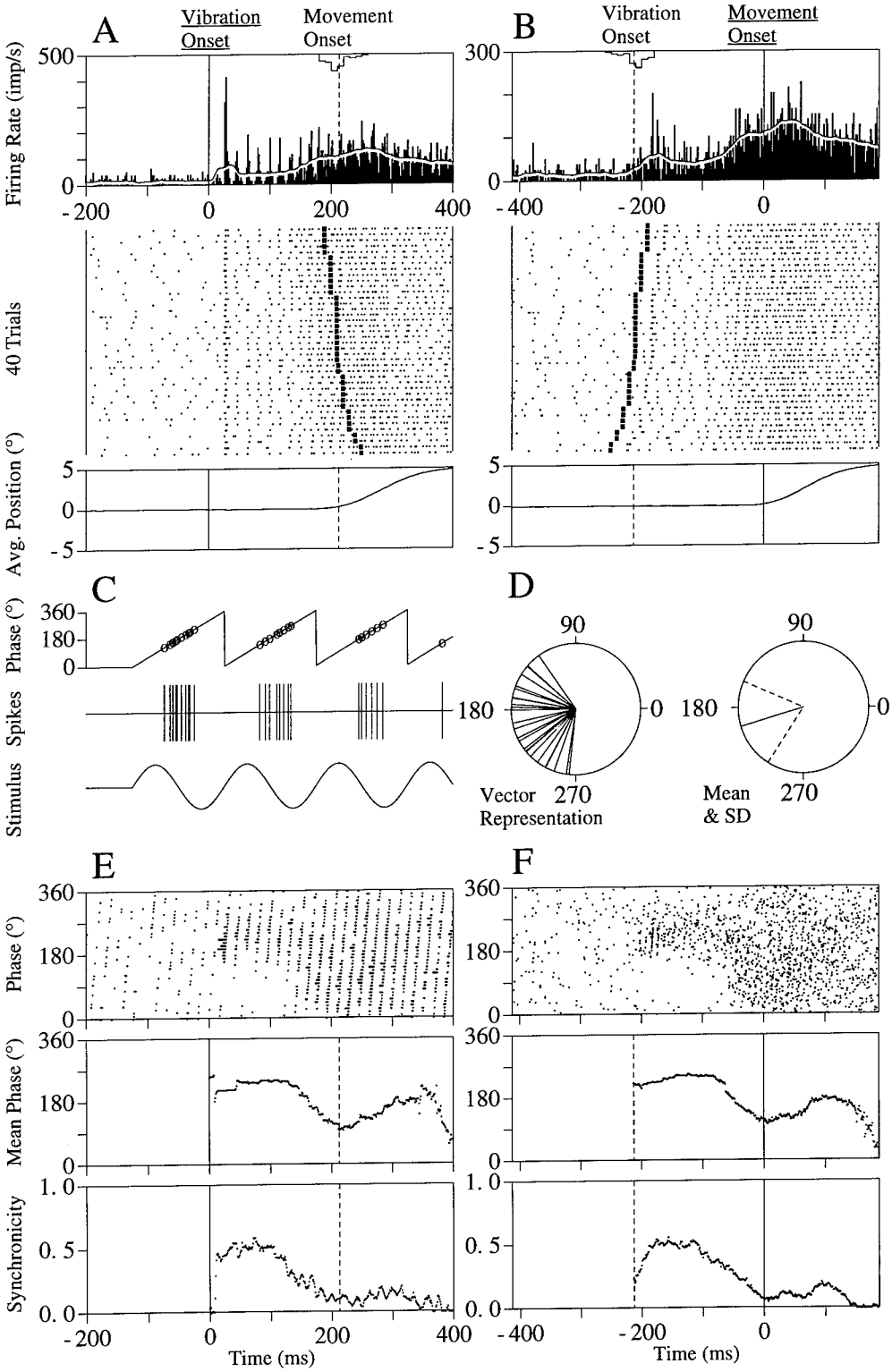

FIG. 2. Example of analyses of vibration-entrained firing for an area 1 neuron (*monkey H*). This neuron was activated by passive wrist extension. Activity pattern exhibited during active extensions in response to 57-Hz vibration is illustrated. *A* and *B*: histograms (binwidth = 2 ms) of activity and raster displays aligned on vibration onset (*A*) and on movement onset (*B*). Mean firing rate traces are superimposed on the histograms. In rasters, movement onset (*A*) and vibration onset (*B*), respectively, are shown by darker marks. Distribution histograms for these onsets are displayed in the top of the panels. The periodic pattern of the vibration-entrained activity is visible in *A*. However, this pattern is not evident in the movement-aligned display (*B*). Mean firing rate increased 80 ms before movement onset (*B*). *C*: representations of the phase of the vibration-entrained responses. *D*: vector representation of the phase. Expression of mean phase and of standard deviation of phase using this representation. *E* and *F*: raster displays of phase and traces of mean phase and synchronicity aligned on vibration onset (*E*) and movement onset (*F*). In *E*, for better visibility, individual dots were rearranged into minihistograms over the vibratory cycle. Onsets of mean phase shift and of synchronicity decreases were 75 and 100 ms before movement onset, respectively (*F*).

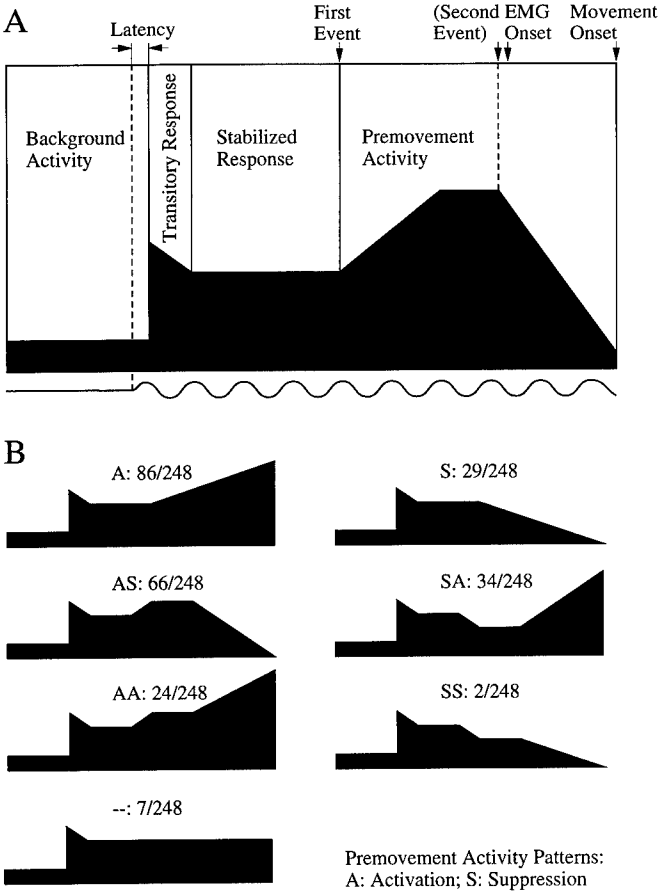

FIG. 3. *A*: different epochs of neuronal activity in this reaction time paradigm. Background firing preceded vibratory stimulus onset. After a transitory response to the stimulus, a stabilized response was observed. Premovement activity then occurred (1 or 2 events of mean firing rate change). The onsets of 2nd events, if present, usually were close to electromyographic (EMG) onset. *B*: different types of premovement activity and the number of cases for which they were observed.

low vibratory stimuli, activity patterns associated with vibrotactile stimulation can be distinguished from the activity induced by other inputs. We assumed that peripheral vibration would induce responses that were temporally correlated with the stimuli, whereas inputs from other sources would introduce an activity component in these neurons that was temporally uncorrelated with the stimuli (asynchronous component). Thus the degree of correlation of neuronal activity with vibratory stimuli can indicate the relative influence of peripheral vibratory inputs versus asynchronous signals. Asynchronous inputs that affect SI activity during movement initiation may be associated with peripheral reafference, or they may have a central origin. If PMA of SI neurons occurs early with respect to EMG onset, it is probably centrally generated. On the basis of these assumptions, we analyzed entrained neuronal activity in terms of parameters characterizing the temporal relationships between the vibratory stimuli and the neuronal discharges (phase) and the degree of entrainment (synchronicity). Firing rates were analyzed as well. Some of the data have been presented previously in preliminary form (Lebedev and Nelson 1992).

METHODS

Experimental set-up and behavioral paradigm

Four adult male rhesus monkeys (*Macaca mulatta; C, F, G,* and *H*) were taught to make wrist flexion and extension movements after a vibratory stimulus to the palm (Nelson et al. 1991). The monkeys were cared for in accordance with the National Institutes of Health Guide for Care and Use of Laboratory Animals, revised 1985. Each monkey sat in an acrylic monkey chair with his right forearm on an armrest and his right palm on a plate attached, at the end nearest to the wrist, to the axle of a brushless DC torque motor (Colburn and Evarts 1978). A load of 0.07 Nm was applied to the plate, which assisted extension and opposed flexion movements. The monkeys exerted a flexion force to maintain a centered wrist position. Animals viewed a visual display, located 35 cm in front of them at eye level. The display, consisting of 31 light-emitting diodes (LEDs), provided visual feedback of the current wrist position. A central, red LED indicated a centered wrist position. Each smaller, yellow LED above or below the central LED indicated a deviation of wrist position of 1° .

Each monkey made self-paced wrist flexions or extensions in response to vibratory go-cues (Nelson et al. 1991). Trials began when the monkey centered the plate. A movement direction instruction was given by the presence or lack of illumination of a red LED located in the upper left corner of the visual display. If this LED was illuminated, extension was the appropriate movement. Otherwise, the monkey was to flex. The monkey was required to maintain the centered (hold) position for 0.5, 1.0, or 1.5 s (pseudorandomized). Movements of >0.5° from center during the hold period cancelled the trial. If the animal held the center position, a 27-, 57-, or 127-Hz low-amplitude stimulus (sine wave <0.06° angular deflection) vibrated the plate. Vibratory stimuli, which served as the go-cues, remained on until the monkey moved at least 5° from the held position. If he made the requested movement, the monkey received a fruit juice reward. A new trial began when the monkey once again held a steady position.

Electrophysiological recordings and histology

Once animals reached a steady daily performance level, stainless steel recording chambers were surgically implanted, and extracellular recordings were made of SI neurons by using platinum-iridium microelectrodes. Transdural penetrations were made daily into the somatosensory cortex, and the activity of single units was amplified, discriminated, and stored in a computer by conventional means (Evarts 1966; Lemon 1984; Nelson 1988; Nelson et al. 1991). At regular intervals, EMG recordings of the forearm muscles acting across the wrist were made. With the use of sterile 25-gauge needle electrodes as guides, intramuscular EMG wires (stranded stainless steel, Teflon insulated; Bergen Wire Rope) were temporarily implanted in muscles. The recorded EMG activity was converted into pulse data with a window discriminator (Vaadia et al. 1988) and stored in a computer in the same form as the neuronal data.

On the last recording day, electrolytic lesions were made in cortical locations of interest by passing 10 μA of current for 10–20 s. The animals were then deeply anesthetized with pentobarbital sodium and transcardially perfused with 10% buffered formol-saline. Histological sections of the cortex were prepared, and electrode tracks were reconstructed based on the depth of each recording site from the point where the cortical activity was first encountered and the location of the marking lesions (Nelson 1988; Nelson et al. 1991). Only those neurons from recording sites that could be clearly identified as to their cortical location were included in this analysis. The location of each recording site was subsequently transferred to schematic reconstructions of the

TABLE 1. *Characteristics of background activity and vibratory responses*

Group of Neurons	Cutaneous RFs	Deep RFs	Not Tested for RF	All
Background firing rate, spikes/s	21.5 ± 11.0 (20)[a,b]	30.2 ± 13.5 (26)[a,b]	37.5 ± 12.6 (9)	28.2 ± 13.6 (55)
Latency of vibratory response, ms				
27 Hz	26.1 ± 7.3 (16)	27.0 ± 9.2 (17)	28.8 ± 14.9 (4)	28.8 ± 8.9 (37)[a,c]
57 Hz	23.5 ± 7.5 (20)	21.8 ± 8.6 (26)	24.0 ± 6.3 (9)	22.8 ± 7.8 (55)
127 Hz	24.6 ± 10.0 (14)	21.3 ± 7.6 (16)	14.0 ± 1.4 (2)	22.3 ± 8.8 (32)
Stabilized MFR, spikes/s				
27 Hz	51.8 ± 18.3 (16)	44.3 ± 13.9 (17)	46.3 ± 20.0 (4)	47.8 ± 16.5 (37)
57 Hz	45.7 ± 26.1 (20)	48.6 ± 22.3 (26)	54.3 ± 25.9 (9)	48.5 ± 24.1 (55)
127 Hz	19.4 ± 11.4 (14)[d,e]	40.7 ± 18.2 (16)	30.0 ± 31.6 (2)	30.7 ± 18.9 (32)
Stabilized Synch				
27 Hz	0.39 ± 0.18 (12)	0.39 ± 0.16 (16)	0.29 ± 0.11 (4)	0.38 ± 0.17 (32)
57 Hz	0.39 ± 0.18 (17)	0.38 ± 0.15 (24)	0.32 ± 0.16 (9)	0.37 ± 0.16 (50)
127 Hz	0.22 ± 0.17 (10)[a,c]	0.26 ± 0.14 (14)[a,c]	0.20 ± 0.10 (2)	0.24 ± 0.15 (26)[c,d]

Values represent means ± SD; number of neurons is in parentheses. Significance level for both 1-factor analysis of variance with the Scheffé comparison test and Mann-Whitney U test are shown. The sample for calculating Synch is less than that for other parameters because cases with bimodal phase distribution were excluded. RF, receptive field; MFR, mean firing rate; Synch, synchronicity. [a] $P < 0.05$. [d] $P < 0.01$. [b] Different from other RF type in the row. [c] Different from other vibratory frequencies in the column; [e] Different from all other combinations of RF type and vibratory frequency.

recording area after appropriate scaling and alignment of sections from individual animals based on the location of the central and intraparietal sulci (Fig. 1).

Analyses of entrained responses

SI neurons with activity entrained to vibratory stimuli were selected for analysis by visual inspection of raster displays and histograms. Entrained vibratory responses were characterized by a periodical pattern in the rasters and histograms when these were centered on vibration onset (Fig. 2*A*). In displays aligned on movement onset, the periodical pattern usually was obscured (Fig. 2*B*). The analyses of response phase were conducted to describe the dynamic changes in the pattern of entrainment quantitatively. The time of occurrence of each spike was related to the instantaneous phase of the vibratory stimulus (Fig. 2*C*). The phase of the vibratory stimulus at which spikes occur is a correlate of response latency. We defined the latency as the time from the beginning of a given vibratory cycle to the resultant spike. Variations of the phase, $\Delta\varphi$, and of the latency, ΔL, are linearly related

$$\Delta\varphi = 2\pi f \Delta L \qquad (1)$$

where f is the frequency of vibration.

The phase at which spikes occur in response to external stimuli was defined as a statistical value depending on time. Floating mean phase (MP; Fig. 2, *E* and *F*) and the standard deviation of phase were calculated. From the standard deviation, a synchronicity (Synch) parameter was derived that characterized the degree of vibratory entrainment on a 0 to 1 scale (Fig. 2, *E* and *F*). To calculate the floating mean parameters, circular statistics were used (Batschelet 1981; Zar 1974). The phase of the stimulus was represented as the angle of a unit vector in a circular diagram (Fig. 2*D*). Because a vibratory stimulus is a harmonic function of time, the unit vector can be thought of as rotating at a constant angular velocity corresponding to the frequency of vibration. With the use of complex values, this rotating unit vector, $\boldsymbol{e}(t)$, can be expressed as

$$\boldsymbol{e}(t) = \exp(i2\pi ft) \qquad (2)$$

where t is the time from vibration onset and i is an imaginary unit [$i = (-1)^{1/2}$].

Floating mean parameters were calculated as average values in a time window having a width equal to one vibratory period at 27 Hz (37.0 ms), two periods at 57 Hz (35.1 ms), and four periods at 127 Hz (31.5 ms). The width of the time window was chosen to be equal to multiples of the vibratory period to provide average values over at least one vibratory cycle, and to smooth the "bursty" pattern of vibration-entrained activity. The number of spikes, $N(t)$, in the time window was used to calculate the mean firing rate (MFR), $F(t)$

$$F(t) = N(t)/(nT) \qquad (3)$$

where T is the time window width and n is the number of trials averaged.

Mean vector, $\boldsymbol{m}(t)$, was calculated as an average of unit vectors corresponding to individual response phases

$$\boldsymbol{m}(t) = 1/N(t) \sum_{k=1}^{N(t)} \boldsymbol{e}(t_k) \quad t - T/2 < t_k \leq t + T/2 \qquad (4)$$

where t_k is the time of the kth spike's occurrence. MP, represented as $\vartheta(t)$, was calculated as the angle of the mean vector

$$\vartheta(t) = \text{angle}[\boldsymbol{m}(t)] \qquad (5)$$

The floating standard deviation of the response phase, $\sigma(t)$, was calculated by averaging the squared angular deviations of individual unit vectors with respect to the mean vector

$$\sigma(t) = \{1/[N(t) - 1] \sum_{k=1}^{N(t)} \text{angle}^2[\boldsymbol{m}(t), \boldsymbol{e}(t_k)]\}^{1/2}$$
$$t - T/2 < t_k \leq t + T/2 \qquad (6)$$

In *Eq. 6* the angle is defined as ranging between $-\pi$ and π radians (-180 and 180°).

Standard deviations calculated for small samples tend to be underestimates (Gurland and Tripathi 1971). To correct for this tendency, resulting from *Eqs. 4–6*, we used a numerical model. On the basis of this model, a correction factor was calculated in the form of a second-order polynomial of the number of samples. Standard deviation, $\sigma(t)$, was multiplied by this correction factor. For most cases, the number of samples was sufficiently large, so that the correction was small (<5% for $N_{\text{sample}} > 10$).

The Synch parameter was derived from the standard deviation. Synch served to compare the experimentally derived distribution

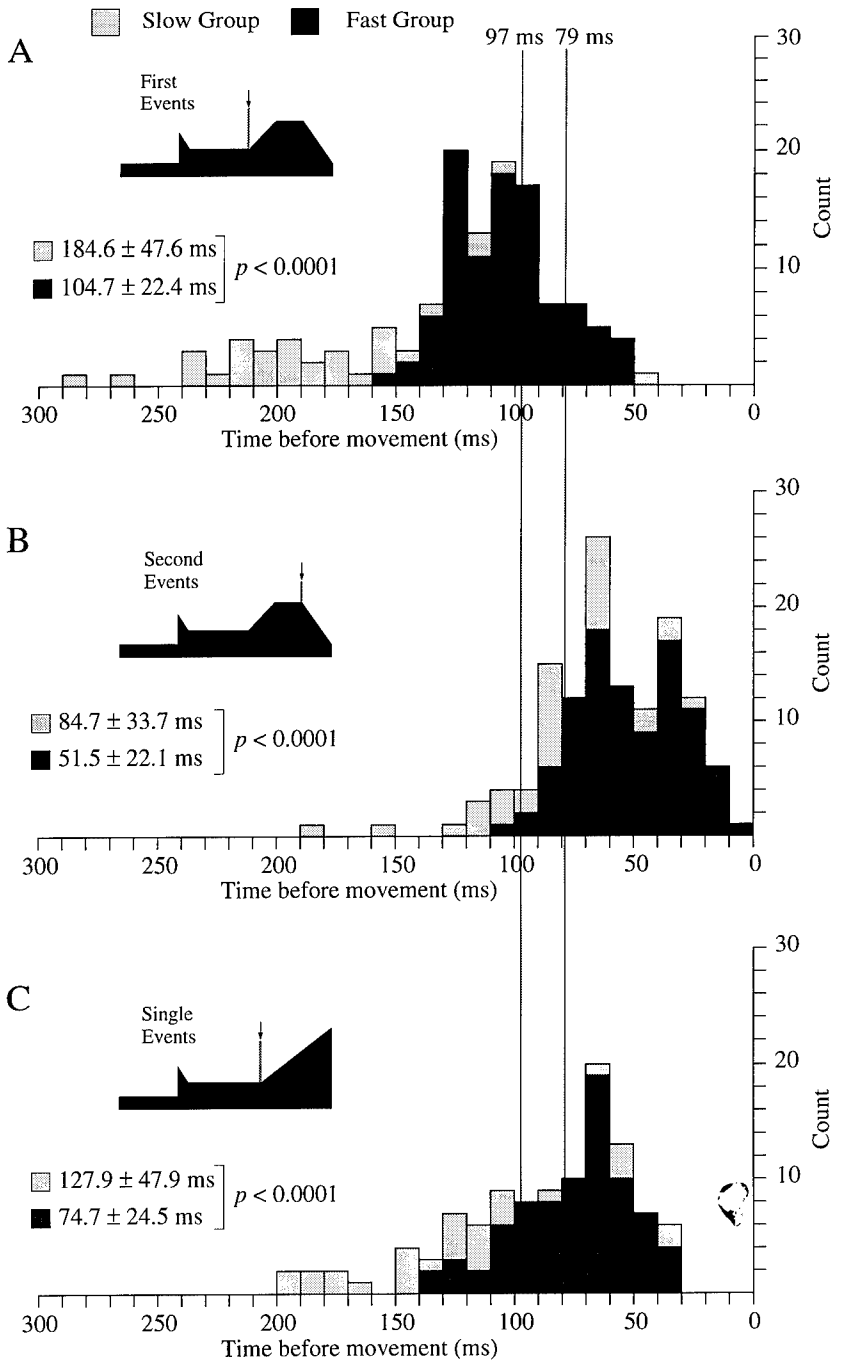

FIG. 4. Onsets of mean firing rate changes during premovement activity with statistical analyses of differences. Significance level for both unpaired t test, and Mann-Witney comparison is shown. A: onsets for 1st events in the 2-event premovement activity cases. B: onsets for the 2nd events. C: onsets for the single-event cases. The results from individual monkeys were split into 2 groups: those with fast reaction times (RTs) and those with slow RTs. For slow monkeys, premovement activity occurred, on average, earlier than for fast monkeys. The onset of changes related to peripheral reafference (EMG onset) was estimated to be 79 ms before movement onset. The line at 97 ms before movement onset accounts for possible calculation errors (see text). The majority of the 1st events occurred earlier than 97 ms before movement onset (A). Most of the 2nd events occurred later than 97 ms before movement onset (B). Approximately an equal number of the single events occurred before and after the 97-ms boundary (C). The difference in activity onsets between slow and fast monkeys was greater for the 1st events (A).

with a uniform (completely random) distribution over the vibratory cycle. The standard deviation of a uniform distribution, σ_{unif}, is equal to $3^{-1/2}\pi$ radians (103.923°). Synch, $\sigma(t)$, was calculated as

$$s(t) = [\sigma_{unif} - \sigma(t)]/\sigma_{unif} \quad (7)$$

Synch could vary from 0 to 1, where 0 corresponds to the absence of entrainment (uniform distribution), and 1 corresponds to a neuron responding at a constant phase.

The analyses of response phase routinely revealed additional information. Figure 2, E and F, illustrates the results of applying these analyses to the same data more conventionally presented in Fig. 2, A and B. Raster displays also show the phase for the time preceding the vibratory stimulation onset. For this period, individual phases (automatically calculated by the computer) were scattered randomly within the graph limits. After stimulation onset, individual phases clustered around a particular phase value (i.e., MP). MP shifted at approximately the same time that the unit was activated before movement onset (~80 ms). This change of MP corresponded to an earlier response to the ongoing vibratory stimuli (see *Eq. 1*). In addition, Synch decreased with respect to the early poststimulus onset level.

Onset of EMG and PMA

EMG onsets were determined with the use of the cumulative sum methods (CUSUM) (Ellaway 1977; Jiang et al. 1991). A linear least-square interpolation curve was calculated for the CU-

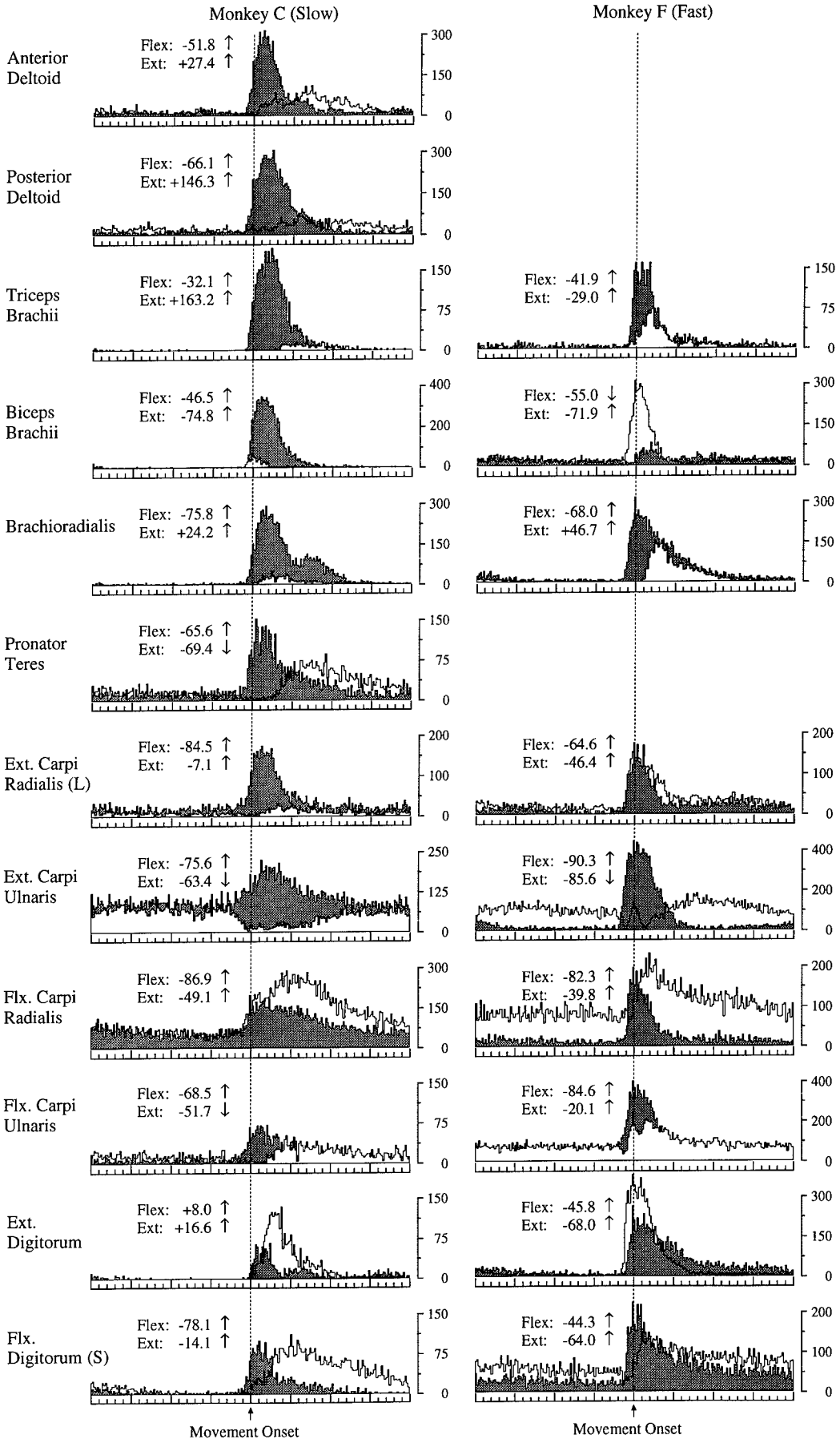
Monkey C (Slow)
Monkey F (Fast)
Anterior Deltoid
Flex: -51.8 ↑
Ext: +27.4 ↑
Flex: -41.9 ↑
Ext: -29.0 ↑
Posterior Deltoid
Flex: -66.1 ↑
Ext: +146.3 ↑
Triceps Brachii
Flex: -32.1 ↑
Ext: +163.2 ↑
Biceps Brachii
Flex: -46.5 ↑
Ext: -74.8 ↑
Flex: -55.0 ↓
Ext: -71.9 ↑
Brachioradialis
Flex: -75.8 ↑
Ext: +24.2 ↑
Flex: -68.0 ↑
Ext: +46.7 ↑
Pronator Teres
Flex: -65.6 ↑
Ext: -69.4 ↓
Ext. Carpi Radialis (L)
Flex: -84.5 ↑
Ext: -7.1 ↑
Flex: -64.6 ↑
Ext: -46.4 ↑
Ext. Carpi Ulnaris
Flex: -75.6 ↑
Ext: -63.4 ↓
Flex: -90.3 ↑
Ext: -85.6 ↓
Flx. Carpi Radialis
Flex: -86.9 ↑
Ext: -49.1 ↑
Flex: -82.3 ↑
Ext: -39.8 ↑
Flx. Carpi Ulnaris
Flex: -68.5 ↑
Ext: -51.7 ↓
Flex: -84.6 ↑
Ext: -20.1 ↑
Ext. Digitorum
Flex: +8.0 ↑
Ext: +16.6 ↑
Flex: -45.8 ↑
Ext: -68.0 ↑
Flx. Digitorum (S)
Flex: -78.1 ↑
Ext: -14.1 ↑
Flex: -44.3 ↑
Ext: -64.0 ↑
Movement Onset
Movement Onset

SUM trace of EMG pulses recorded during the epoch of steady holding against the load. Then the computer program searched forward in time to find the first deviation from the interpolated curve of more than three standard deviations for at least 40 ms. This time was designated as the EMG onset. The latency of the initial vibratory response of SI neurons was determined in a similar way. Because of the bursty character of vibration-entrained firing, an estimate of PMA onset could not be made accurately with the use of the CUSUM methods. Average parameters were analyzed instead. A stable piece of the respective trace was labeled by visual inspection. Means and standard deviations of MFR, MP, and Synch were calculated for this epoch. Then the computer program searched forward in time to find the first change of more than three standard deviations for at least 40 ms. It should be stressed that the precision of estimation of this time was principally limited. The procedure for calculating floating mean parameters was analogous to low-pass filtering. It tended to broaden sharp edges (compare in Fig. 2*A* the 2-ms binned histogram with mean firing rate trace). The maximum error in determining the occurrence of change resulting from this broadening is equal to $T/2$ ($\sim$18 ms).

Statistical analyses

To analyze factors determining the characteristics of activity patterns in different neurons, factorial analysis of variance (ANOVA; including Scheffé's post hoc test) was used. Multifactorial ANOVA served to detect with which independent factors (i.e., cortical area, receptive field type, frequency of vibration, direction of movement, etc.) MFR, MP, and Synch covaried. If some factors were not statistically significant in their covariance, averaging was performed on the set of these factors. The data were grouped to isolate combinations of significant factors. The parametric t test and the more robust nonparametric Mann-Whitney U test were used to test the significance of differences between groups. In cases when correlations between certain parameters were suspected, parametric F-statistics for the linear regression and the nonparametric Spearman rank correlation analyses were conducted.

RESULTS

Database

From the recordings for 410 vibratory responsive SI neurons, 55 units (13%) were selected as entrained to the frequency of the vibratory stimulus. These vibration-entrained units represented a subpopulation of the group of neurons activated by the vibratory stimulus (60% of the vibratory responsive cells) (Nelson 1988). *Monkeys C, F, G,* and *H* contributed 10, 6, 12, and 27 units, respectively. The best entrainment for the selected units was observed at stimulus frequencies of 27 and 57 Hz, whereas the entrainment was less at the higher frequency (127 Hz). We did not include Pacinian-like neurons (Mountcastle et al. 1969) because of their qualitatively different activity patterns. Their best responsiveness was at the higher vibratory frequency of 127 Hz. (Pacinian-like neurons will be considered separately in following studies). Determinination of cortical location was based on previously published criteria (Nelson et al. 1991). Figure 1 presents the distribution of surface locations of the recordings (*B*), their location in representative sagittal sections (*C*), and the respective number of neurons (*D*). No clear distribution patterns were evident, either within or across cortical areas. However, there was a tendency for the studied neurons to be located in the granular or infragranular cortical layers.

General activity patterns

We use the term "case" to indicate a set of activity recordings for a particular neuron at a single vibratory frequency for one direction of movement (Nelson et al. 1991). A total of 248 cases were analyzed. For 30 cases (from 10 neurons), response phases formed 2 bands rather than being grouped around a particular phase value. Probably this activity profile represented responses to both the application and withdrawal of the mechanical stimuli from the neuron's receptive field (RF). These cases were excluded from the analyses of MP and Synch. Figure 3*A* shows the typical epochs of neuronal activity that were observed: *1*) *background firing* preceding the stimulus onset; *2*) *initial transitory response* to stimulus onset; *3*) *stabilized response* to vibration; and *4*) one of several types of *PMA*. We observed premovement increases of firing rate (activation) as well as firing rate decreases (suppression). Moreover, in some cases, two consecutive changes of firing rate occurred (2-event PMA). The different types of PMA are schematically illustrated in Fig. 3*B*.

Background activity and vibratory response

The results of statistical analyses of the MFR during background activity, of the vibratory response latency, and of MFR and Synch for the period of stabilized response are presented in Table 1. No significant differences dependent on the cortical area were found. The background MFR was, on average, higher for neurons with deep RFs than for neurons with cutaneous RFs. The latency of the vibratory response averaged $\sim$23 ms. The latency was significantly longer at 27 Hz than at 57 and 127 Hz. The stabilized MFR was not significantly different for neurons with deep RFs at any of the studied frequencies nor for neurons with cutaneous RFs at 27 and 57 Hz. However, for neurons with cutaneous RFs, MFR was significantly less at the higher frequency (127 Hz). Stabilized MFR was, on average, higher than background MFR, except for neurons with cutaneous RFs at 127 Hz. An example of the activity of a neuron with a MFR increase during the stabilized response is presented in Fig. 8, *A* and *B*. In some instances, however, stabilized MFR remained virtually unchanged (e.g., Fig. 7, *A* and *B*) or even decreased (often for neurons with cutaneous RFs at 127 Hz). In these latter cases the sustained response to vi-

FIG. 5. Patterns of EMG activity of forearm muscles illustrated for 2 monkeys (*C* and *F*). EMG was converted into pulse data with the use of a window discriminator. Histograms of these pulse data, centered on movement onset, are shown (gray, flexion; white, extension). EMG onsets estimated with the use of the cumulative sum (CUSUM) method are shown (↓, suppression; ↑, activation; negative value, before movement onset; positive value, after movement onset; Flx, flexor; Ext, extensor). The earliest EMG onset was 90 ms before movement onset (*monkey F*).

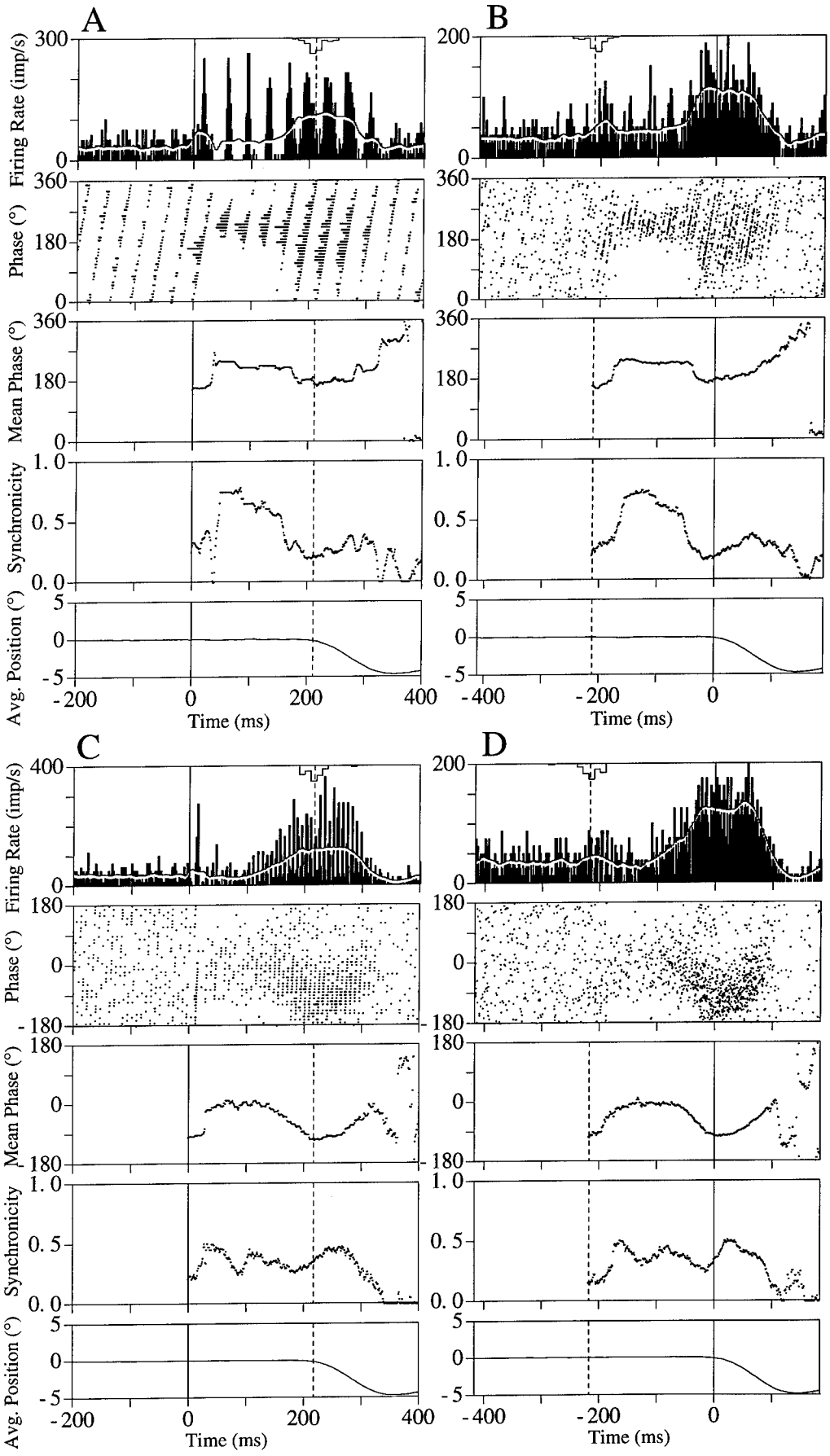
A
B
C
D
Firing Rate (imp/s)
Phase (°)
Mean Phase (°)
Synchronicity
Avg. Position (°)
Time (ms)
300
200
400
360
180
0
1.0
0.5
0.0
5
-5
-200
-400
400

bration was characterized by groupings of spikes around a particular phase of the vibratory cycle, rather than by a firing rate increase. There were no significant differences in Synch during the stabilized response period that were dependent on the RF type. Synch was not significantly different at the vibratory frequencies of 27 and 57 Hz, but it was significantly lower at 127 Hz.

Onset of PMA and EMG

The onsets of PMA and EMG were determined relative to movement onset. PMA onset differed between individual monkeys with different reaction times (RTs). For two monkeys with longer RTs (*monkeys C* and *G* with mean RTs of 330 and 360 ms, respectively), PMA onset (but not EMG onset), on average, was earlier than for two monkeys with shorter RTs (*monkeys F* and *H;* mean RTs 200 and 220 ms). Therefore we combined the data obtained from two monkeys with fast RTs into one group and the data from two monkeys with slow RTs into another. The differences in PMA onset related to RF type, cortical area, vibratory stimulus frequency, and sign of MFR shift (activation or suppression) were not significant. The onsets were analyzed separately for three groups of PMA: *1*) first events for the two-event PMAs (Fig. 4*A*); *2*) second events for the two-event PMAs (Fig. 4*B*); and *3*) single-event PMAs (Fig. 4*C*). The difference in PMA onsets between slow and fast monkeys was greater for first events than for second and single PMA events.

PMA onset was compared with the EMG onset. Figure 5 illustrates the EMG patterns of different forearm muscles for two animals, one slow (*monkey C*) and one fast (*monkey F*). The earliest EMG onset was 90 ms before movement onset (*monkey F*). The minimum conduction time necessary for peripheral signals to arrive at SI has been estimated to be 11 ms (Wiesendanger and Miles 1982). We suggest, therefore, that the peripheral reafference associated with EMG onset does not reach SI earlier than 79 ms before movement onset. In the present analyses a time-averaging procedure was used to calculate MFR, MP, and Synch. Because this procedure depends on time-window measurements, a maximal error of one-half the time window width (18 ms) was possible in estimating PMA onset. Therefore we suggest that the earliest peripherally induced changes in SI activity occur no earlier than 97 ms before movement onset. The majority of the first events occurred earlier than 97 ms before movement onset. The PMA onsets for the slow group were especially early. Most of the second events, however, began <97 ms before movement onset. Approximately an equal number of the single events ocurred before and after the 97-ms boundary.

PMA patterns

Premovement changes in MFR were accompanied by changes in MP and Synch. For a given neuron and a given movement direction, the general pattern of changes in MFR, MP, and Synch usually was consistent at different vibratory frequencies (e.g., Fig. 6). The magnitude of these changes differed depending on the vibratory frequency. During *premovement activation* an increase of MFR was typically accompanied by a shift of the MP toward earlier responses to vibratory stimuli and a decrease in Synch (e.g., Fig. 2). Usually, the decrease of Synch was greater at lower vibratory frequencies (e.g., 27 Hz in Fig. 6, *A* and *B*) than at higher frequencies (e.g., 127 Hz in Fig. 6, *C* and *D*). However, greater phase shifts were characteristic at the higher frequencies of vibration (Fig. 6, *C* and *D*). The magnitude of the change in MFR was not necessarily correlated with the magnitude of accompanying changes in MP and Synch. For example, MFR of the unit presented in Fig. 7, *A* and *B* only slightly increased 150 ms before movement onset, whereas the MP and the Synch substantially changed before movement. Another unit (Fig. 7, *C* and *D*) exhibited a small increase in MFR occurring at 120 ms before movement. In this instance, although the shift of MP was quite pronounced, no substantial changes in Synch took place.

In general, no consistent shifts in MP and Synch were temporally correlated with *premovement suppression.* An example of a single-event premovement suppression (S pattern; Fig. 3*B*) is presented in Fig. 8, *A* and *B*. In this case the MFR decreased ~150 ms before movement onset. No substantial phase shift was observed in this instance, whereas a desynchronization occurred ~30 ms before movement onset. An example of a neuron with a two-event pattern with consecutive activation and suppression (AS pattern; Fig. 3*B*) is presented in Fig. 8, *C* and *D*. In this case MFR increased ~200 ms before movement onset. A reduction in MP and a slight decrease in Synch also took place. These events, characteristic for the premovement activation, were followed by MFR decrease, which occurred ~80 ms before movement. Although the increase in MFR subsequently reversed, the MP continued to shift toward earlier responses, and the Synch decreased.

To estimate the mean time course of changes in the characteristics of vibration-entrained firing during PMA, we averaged across cases by aligning MFR, MP, and Synch traces on the onset of the MFR shift. The average traces for the patterns of the one-event cases were similar to those

FIG. 6. Changes in mean phase and synchronicity during premovement activation at low (27 Hz; *A* and *B*) and high (127 Hz; *C* and *D*) vibratory stimulus frequencies. Activity patterns of an area 1 neuron (*monkey H*) during wrist extensions made in response to vibration. This neuron had a cutaneous receptive field located on the radial base of the 1st digit. Conventions as in Fig. 1. At 27 Hz, the neuron fired approximately twice per the vibratory cycle (*A;* see the trace of the mean firing rate). Premovement activation occurred at 50 ms before movement onset at 27 Hz. During this activation the vibration-entrained firing was desynchronized. At 127 Hz, during the the stabilized response, this neuron discharged once every 5 cycles. However, during premovement activation (at 110 ms before movement onset), a 1-to-1 following of the vibratory stimulus frequency was observed (*D*). Premovement activation was accompanied by changes of mean phase and synchronicity. The shift of mean phase was greater at 127 Hz (*D*) than at 27 Hz (*B*). The synchronicity decrease was greater at 27 Hz (*B*) than at 127 Hz (*D*).

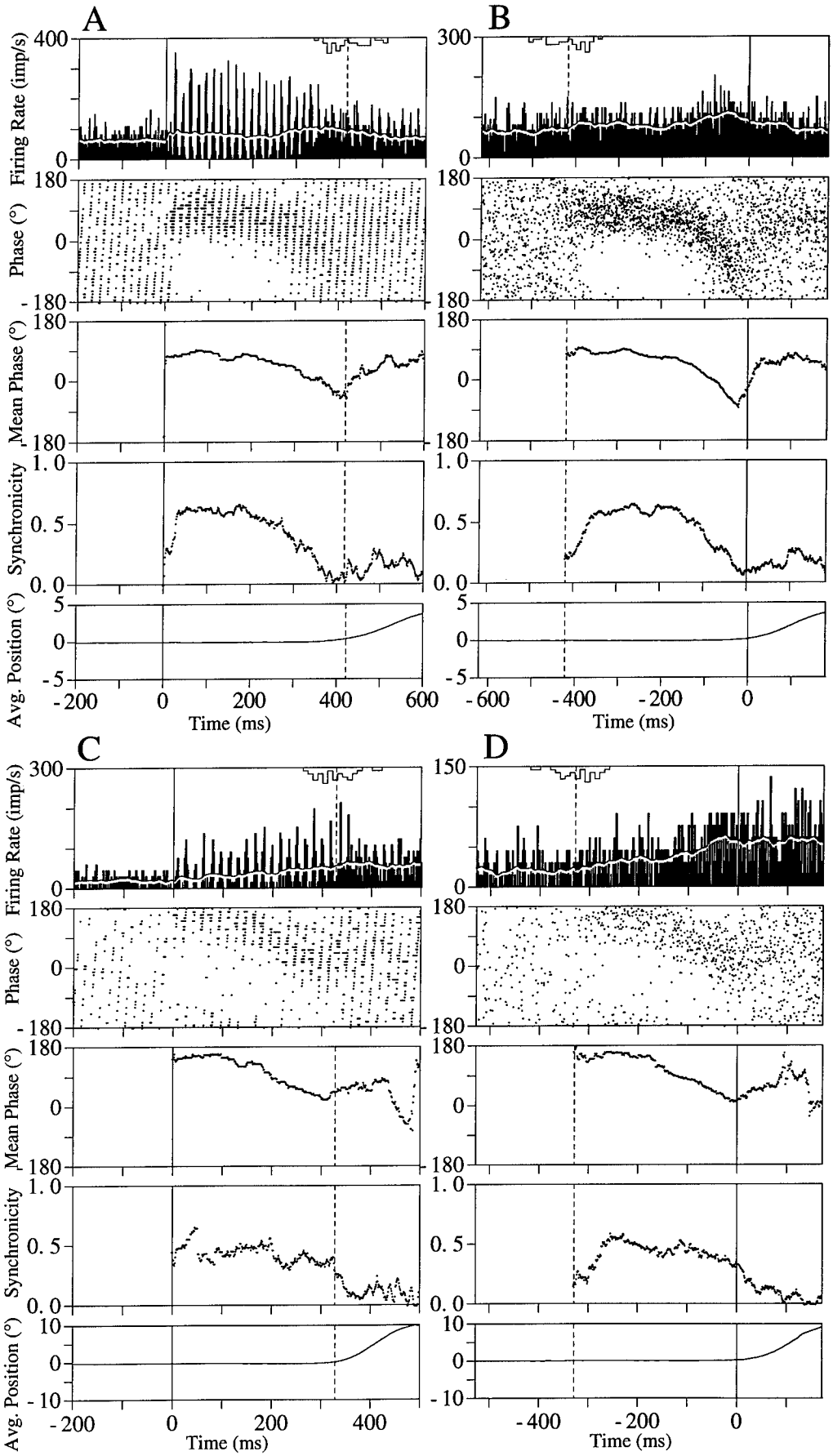
A
B
C
D
Firing Rate (imp/s)
Phase (°)
Mean Phase (°)
Synchronicity
Avg. Position (°)
Time (ms)

calculated for the shift of MFR of the same sign in the two-event cases. In Fig. 9*A*, averaged traces for premovement activation are shown (1-event and 2-event cases were not segregated). Average traces of MP and Synch revealed a phase shift toward earlier responses and a desynchronization that were correlated with the increase of MFR. The changes in MP and Synch were similar for neurons with cutaneous and deep RFs. The average MP shift was approximately the same at the two higher vibratory frequencies, 57 and 127 Hz. The phase shift was less at the lower frequency (27 Hz). However, desynchronization was greater at 27 Hz than at the higher frequencies. The onsets of both MP (Fig. 9*B*) and Synch (Fig. 9*C*) shifts were correlated with the beginning of MFR increase.

The average traces of MFR for premovement suppression (Fig 10*A*) indicated that an activation often preceded suppression. An average shift of MP toward earlier responses and a desynchronization was also evident. However, these changes of MP and Synch did not begin at the onset of MFR decrease. Rather, they occurred before suppression in many instances. Therefore changes of MP and Synch may be related to the activation that often preceded the suppression. No significant correlation was evident between the onset of MFR decrease and the shifts of MP and Synch (Fig. 10, *B* and *C*).

PMA for different directions of movement

The PMA pattern depended on the subsequent direction of movement. Figure 11 presents the records from a neuron that increased activity at ~60 ms before the onset of wrist flexions (*A* and *B*) and decreased activity at the same time before the onset of wrist extensions (*C* and *D*). This unit also showed slight increases in MFR at ~120 ms before movement onset during both extension and flexion trials (superimposed traces in Fig. 11*F*). An MP shift toward earlier responses beginning 120 ms before movement onset was also present for both directions of movement (Fig. 11*G*). During the suppression of the firing for extension trials, the MP continued to shift. In addition, a desynchronization was observed for both types of movement.

In analyzing the dependence of PMA upon movement direction, only those PMA events were selected that had onsets in extension and flexion trials separated by <30 ms. The onset of these selected PMA events was estimated as an average for different movement directions (and vibratory frequencies, if PMA satisfied the 30-ms criterion at several frequencies). PMA events were split into two groups according to the position of their onset with respect to EMG onset: those that occurred earlier than 97 ms before movement onset and those that occurred after this boundary. Most pre-EMG MFR shifts had the same sign for both flexion and extension movements (22/29). However, with equal frequency, post-EMG PMA events had the same or opposite sign for different movement directions (the same sign: 19/41; opposite signs: 22/41).

DISCUSSION

Centrally generated PMA and SI

PMA of SI neurons, often preceding the EMG onset, has been reported in a number of studies (Bioulac and Lamarre 1979; Evarts 1972; Fromm and Evarts 1982; Lamarre et al. 1983; Nelson 1984, 1987, 1988; Nelson and Douglas 1989; Nelson et al. 1991; Soso and Fetz 1980). Each study indicates that post-EMG PMA contains a substantial component associated with peripheral reafference. However, suggesting involvement of centrally generated signals in pre-EMG PMA is controversial. One argument against centrally generated PMA in SI is based on the fact that PMA occurs in SI later than in the motor cortex (Evarts 1972). However, if PMA in the SI is a corollary motor cortical discharge (Matthews 1988), then this difference in PMA onsets should be a prerequisite. Another argument is that most movement-related discharges in SI disappear after extensive deafferentation of the arm (Bioulac and Lamarre 1979). However, this result does not rule out the possibility of centrally generated PMA in SI under normal conditions. After deafferentation, the functioning of SI as a unit for somatosensory information processing may be dramatically altered. SI may no longer be capable of participating in movement control. Thus it may be excluded from the motor control loop, and therefore there might no longer be a reason to adjust SI neuronal responsiveness.

We examined PMA for a group of SI neurons that faithfully represented the somatosensory periphery. The firing of these neurons was entrained to vibrotactile stimuli. We hypothesized that, for the selected neurons, the activity patterns related to peripheral vibration can be distinguished from inputs coming from other sources. It was expected that signals that are temporally uncorrelated with vibration (asynchronous signals) would disrupt the vibration-entrained neuronal firing patterns. Asynchronous inputs may be associated with peripheral reafference, or they may have central origins. To reveal the changes in vibration-entrained neuronal activity that may be produced by asynchronous signals, we analyzed the temporal relationship between the vibratory stimuli and the neuronal responses to them in terms of the phase of the vibratory cycle

FIG. 7. Two examples of premovement activation showing that the magnitudes of the mean firing rate increase and the changes in mean phase and synchronicity were not necessarily temporally correlated. Conventions as in Fig. 1. *A* and *B*: activity patterns exhibited by an area 1 neuron (*monkey G;* receptive field not tested) recorded during extensions made in response to vibration (57 Hz). The mean firing rate increased slightly at ~150 ms before movement onset. However, changes in mean phase and synchronicity were evident. Note that the stabilized mean firing rate was not substantially different from that during background period. *C* and *D*: activity patterns of an area 1 neuron (*monkey C*) during extensions made in response to 57-Hz vibration. This neuron was activated during passive wrist flexions. A small increase of firing rate was detected 120 ms before movement onset. However, a shift of mean phase at ~170 ms before movement onset was evident. In this case, no substantial premovement changes in the synchronicity occurred.

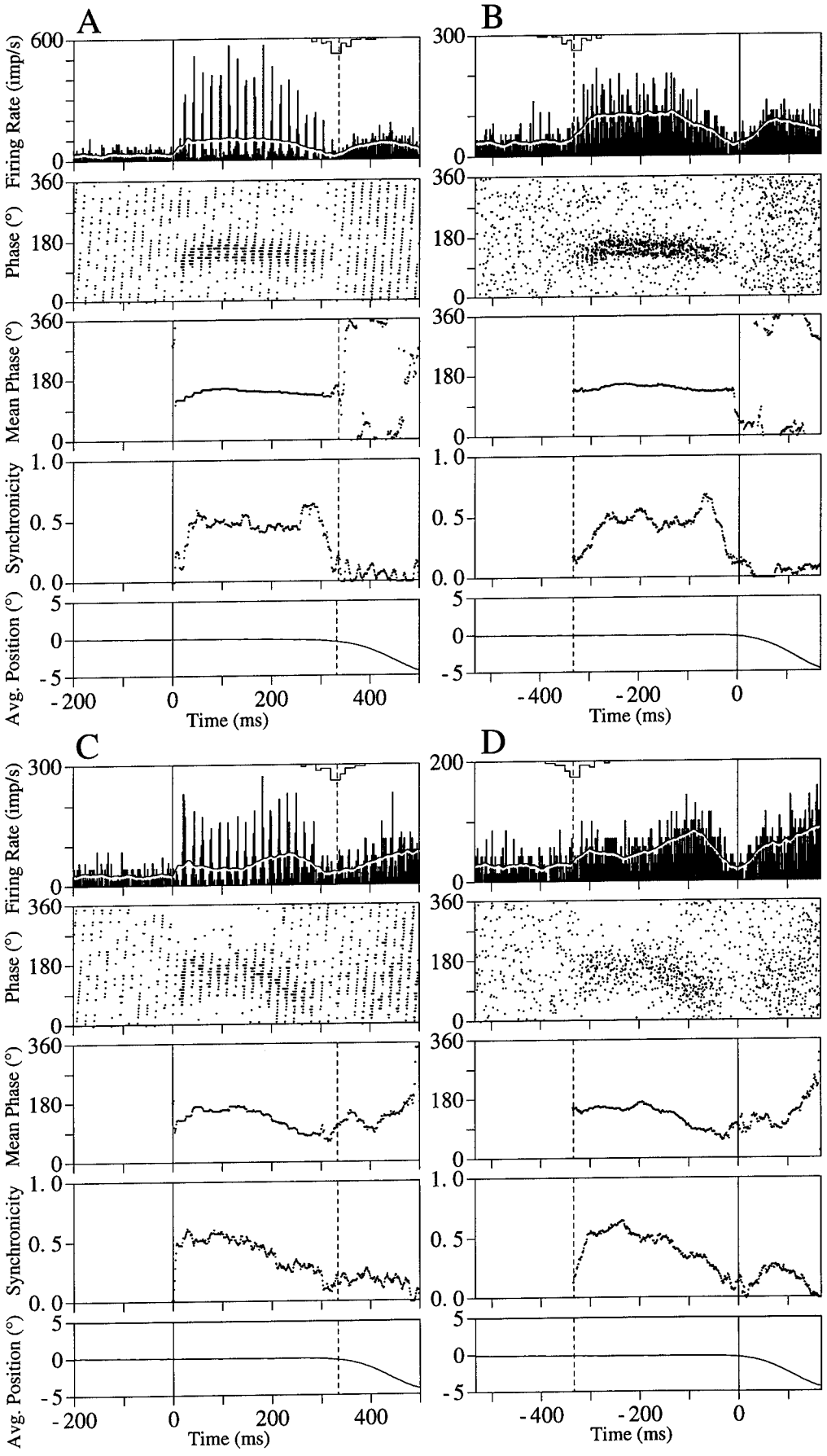
A
B
C
D
Firing Rate (imp/s)
Phase (°)
Mean Phase (°)
Synchronicity
Avg. Position (°)
600
300
200
360
180
0
1.0
0.5
0.0
5
-5
-200
400
-400
Time (ms)

at which individual spikes occurred. The phase was considered as a statistical value varying in time. This value was described with the use of floating mean parameters, MP and Synch, which characterized, respectively, the preferred phase of responses and the degree of vibratory entrainment. For the majority of the selected neurons, the pattern of responses to ongoing vibration changed before movement onset. Changes in firing rate were accompanied by changes in MP and in Synch. Typically, the vibration-entrained pattern was disrupted before movement onset. In many cases, premovement changes in activity began before EMG changes. We suggest that inputs of central origin may contribute to premovement changes in the activity of the studied SI neurons.

Background activity and responses to vibration

During the hold phase of the paradigm, most neurons typically were active with a firing rate of ~30 spikes/s. On average, neurons with deep RFs had higher background firing rates than those with cutaneous RFs. It is possible that the higher background firing of neurons with deep RFs was related to tonic muscle activity that occurred during holding of the handle against a load. Muscle spindles are activated during maintained voluntary contractions due to γ-motoneuron discharges (Hagbarth and Vallbo 1968; Vallbo 1970). The latency of vibratory responses was significantly longer for the lowest tested vibratory frequency (27 Hz) than for 57 and 127 Hz. Probably, this longer latency was related to a less steep onset of the vibratory stimulus at 27 Hz than at the higher frequencies. During the stabilized response to vibration, MFR did not vary significantly with different vibratory frequencies, with the exception of the responsiveness of neurons with cutaneous RFs at 127 Hz. Relatively constant MFRs of somatosensory cortical neurons despite changes in peripheral stimulus frequency have been reported (Burton and Sinclair 1991; Gardner et al. 1992; Mountcastle et al. 1969, 1990). It has been suggested that the characteristics of vibrotactile input are encoded by the temporal pattern of neuronal responses rather than by MFR. The decreased activity that was observed for the neurons with cutaneous RFs at 127 Hz may be due partially to reduced responsiveness of cutaneous receptors at higher stimulus frequencies (Talbot et al. 1968). However, this is probably not the only reason, because in a number of cases, pronounced entrained responses were observed before movement onset in 127-Hz trials (Fig. 6, *C* and *D*). Thus the decrease in MFR of neurons with cutaneous RFs at 127 Hz may be due to inhibitory mechanisms dependent on the stimulus frequency. The SI activity pattern characterized by rapid adaptation of neuronal responses to the vibratory stimuli, and then a reactivation of sensory responsiveness before movement onset, has been analyzed previously (Nelson et al. 1991).

PMA patterns

Several types of PMA were observed and classified according to models of MFR changes (Fig. 3*B*). For the cases when two consecutive changes in MFR occurred (2-event PMA), most of the first MFR changes occurred before EMG onset, whereas most of the second MFR changes occurred after EMG onset. Approximately an equal number of the single events began before and after EMG onset. EMG onset reflects the time when the muscle force and, consequently, the force on the receptive field may begin to change. Therefore we suggest that pre-EMG PMA is not caused by peripheral reafference, whereas post-EMG PMA probably is. It would be reasonable to expect that peripherally induced MFR shifts have opposite signs for flexion and extension movements, at least in some cases. Indeed, a considerable number of the post-EMG MFR shifts of this type were observed. However, pre-EMG MFR shifts more often had the same sign both for flexions and extensions rather than having opposite signs. This fact provides indirect evidence that these PMA events were not peripherally induced. PMA onset was earlier with respect to movement onset for monkeys with slower RTs. Probably the difference in PMA onsets between monkeys reflects the difference in sensorimotor strategies used by the animals during movement preparation. We presume that this difference would not occur if the PMA was induced exclusively by peripheral movement-related reafference, because there was no evidence of faster peripheral conduction for slow monkeys. Also, no similar differences were observed for EMG onsets. Moreover, the difference between slow and fast monkeys was greater for pre-EMG PMA events that presumably were not associated with peripheral reafference, because of their early occurrence.

Premovement activation was typically accompanied by shifts in MP toward earlier responses to stimuli and by decreases in Synch. We suggest that the decrease in Synch signifies that the activation is produced by inputs uncorrelated with the vibratory stimulus (asynchronous inputs). Adding an asynchronous component to a neuron's entrained response would induce a shift in the response phase. When two excitatory signals are superimposed, the membrane potential may be brought to threshold earlier compared with when it is activated by only one input. Desynchronization was most pronounced at the lowest vibratory frequency (27 Hz). The changes in MP, on the other hand, were greater at the higher vibratory frequencies (57

FIG. 8. Examples of single-event premovement suppression (*A* and *B*) and of suppression preceded by activation (*C* and *D*). Conventions as in Fig. 1. *A* and *B*: activity patterns of an area 3b neuron (*monkey G;* receptive field was not tested) during extensions made in response to 57-Hz vibration. The mean firing rate decreased 150 ms before movement onset. No substantial phase shift occurred. Desynchronization began 30 ms before movement onset. *C* and *D*: activity patterns of an area 3a neuron (*monkey G;* receptive field was not tested) during active flexions made in response to 57-Hz vibration. Activation began 200 ms before movement onset and was accompanied by a reduction of mean phase and a decrease of synchronicity. The mean firing rate was suppressed 80 ms before movement onset. However, the mean phase and synchronicity continued to shift in the same direction.

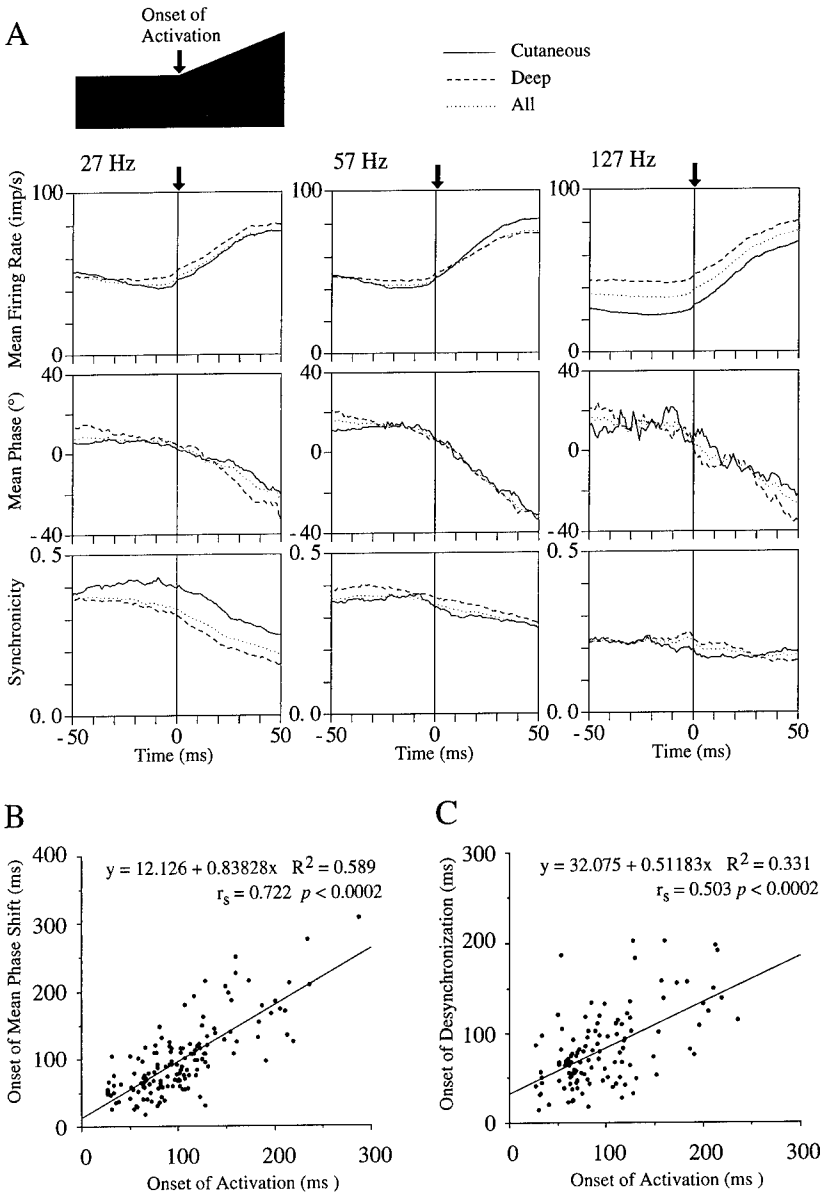

FIG. 9. Average traces of mean firing rate, mean phase, and synchronicity for premovement activation (*A*) and correlation analyses of activation onsets and onsets of mean phase (*B*) and synchronicity (*C*) changes. For averaging, the appropriate traces were centered on the onset of mean firing rate shift. Zero-phase in the displays (*B*) was chosen arbitrary. *A*: average traces indicate mean phase reduction and synchronicity decreases associated with activation. The change in mean phase was larger at the higher vibratory stimulus frequencies (57 and 127 Hz), whereas the change in synchronicity was larger at the lower frequency (27 Hz). No substantial differences in these changes, dependent on the type of receptive field (deep or cutaneous), were observed. *B* and *C*: correlation between activation onsets and the onsets of mean phase and synchronicity changes was statistically significant for both the F-statistics for linear regression and Spearman rank correlation analyses.

and 127 Hz). We suggest that the above differences, dependent on the vibratory stimulus frequency, reflect an interaction between the frequency components of the vibration-entrained input and those of asynchronous signals. It is possible that, when two excitatory components are added, the membrane potential will more often cross the threshold on the rising edge of the higher frequency signal.

Premovement suppression of MFR was sometimes accompanied by MP shifts and desynchronization. However, the decrease of MFR and the changes of MP and Synch were not related. For some two-event cases, premovement suppression may have been superimposed on an activation pattern. The first premovement event in these cases was an activation associated with changes of MP and Synch. The second event was a suppression. However, MP and Synch continued to shift in the same direction (Fig. 8, *C* and *D*). The neuronal mechanism for the interaction between premovement facilitatory and inhibitory signals cannot be resolved from the present data. It is unclear whether this mechanism is based on the convergence of different inputs onto a single neuron or on network interactions.

Possible roles of centrally generated PMA

Several sources are possible for centrally generated PMA (Nelson et al. 1991). First, PMA may result from inputs coming from motor centers (Evarts 1971; Miles and Evarts 1979; Soso and Fetz 1980; von Holst 1954). Second, PMA may originate in SI itself and provide an output signal driving or subserving the drive of movements. Third, PMA may reflect some intrinsic regulation of SI activity. It has been suggested that PMA in SI pyramidal tract neurons contributes to the motor drive (Fromm and Evarts 1982). We do not have direct evidence of what class of SI neurons, having vibration-entrained responses, were studied. However, we assume that, because these are neurons that faithfully respond to peripheral inputs, they are likely to be close to the input site for somatosensory afference. Therefore it is un-

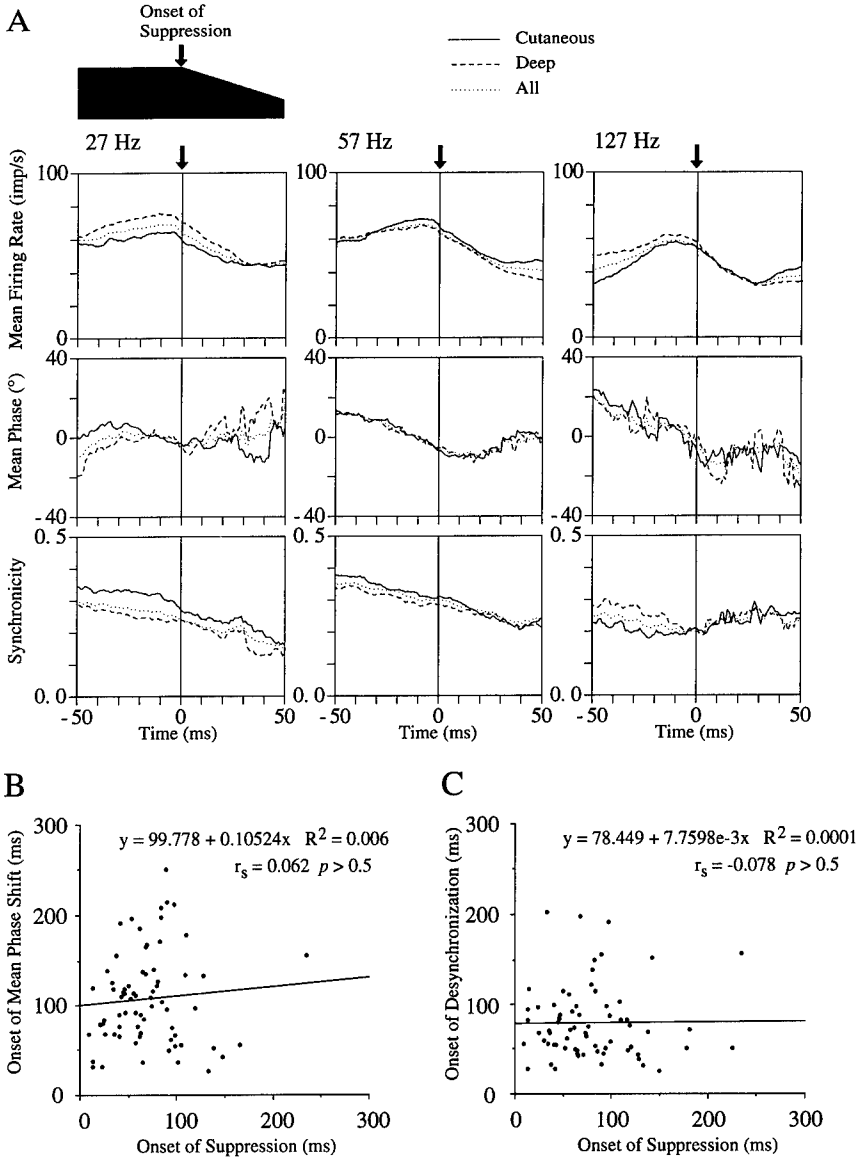

FIG. 10. Average traces for premovement suppression. Conventions as in Fig. 8. *A*: templates indicate that mean phase and synchronicity changes precede the suppression rather than begin with it. *B* and *C*: there was no statistically significant correlation between activation onsets and the onsets of mean phase and synchronicity changes.

likely that the studied neurons generate a direct motor control signal. Rather, their activity provides an input for other regions involved in sensorimotor integration. We assume that centrally generated PMA in these neurons may be induced either by inputs from motor centers or by intrinsic signals.

Signals originating in the motor cortex can influence SI activity. This was demonstrated with the use of microstimulation of area 4 during monitoring of somatosensory-evoked potentials in monkey areas 1 and 3b (Jiang et al. 1990a). However, motor cortical discharges may reach SI via indirect pathways. Besides providing direct input to SI (Jones and Porter 1980; Vogt and Pandya 1978), these discharges may interact with ascending somatosensory transmission at the level of the dorsal column nuclei and the thalamus (see Mountcastle 1984 for review). Changes of afferent transmission have been observed in the medial lemniscus and ventroposterolateral nucleus of the thalamus during arm movements in monkeys (Chapman et al. 1988) and during locomotion in rats (Shin and Chapin 1990). However, these changes were always less than those observed in the SI itself. Thus it is reasonable to assume that the strongest influence of motor cortex over SI responsiveness is at the cortical level.

Several functional roles can be suggested for centrally generated PMA. The first possibility is that centrally generated PMA is a component of the corollary discharge, or a sensory signal originating in the brain itself rather than coming from periphery (Miles and Evarts 1979; Soso and Fetz 1980). This corollary discharge may subserve kinesthetic sensation during self-initiated as opposed to passive movements (Matthews 1988). Premovement modulation of sensory activity may make the system work as a system with anticipation, which could be more effective for motor control (Prochazka 1989). Evidence supporting the theory of corollary discharge has been provided by experiments in which a sense of movement was elicited by magnetic stimulation of human motor cortex when the forearm was ischemically paralyzed (Amassian et al. 1989).

Another possibility is that PMA may reflect gating of so-

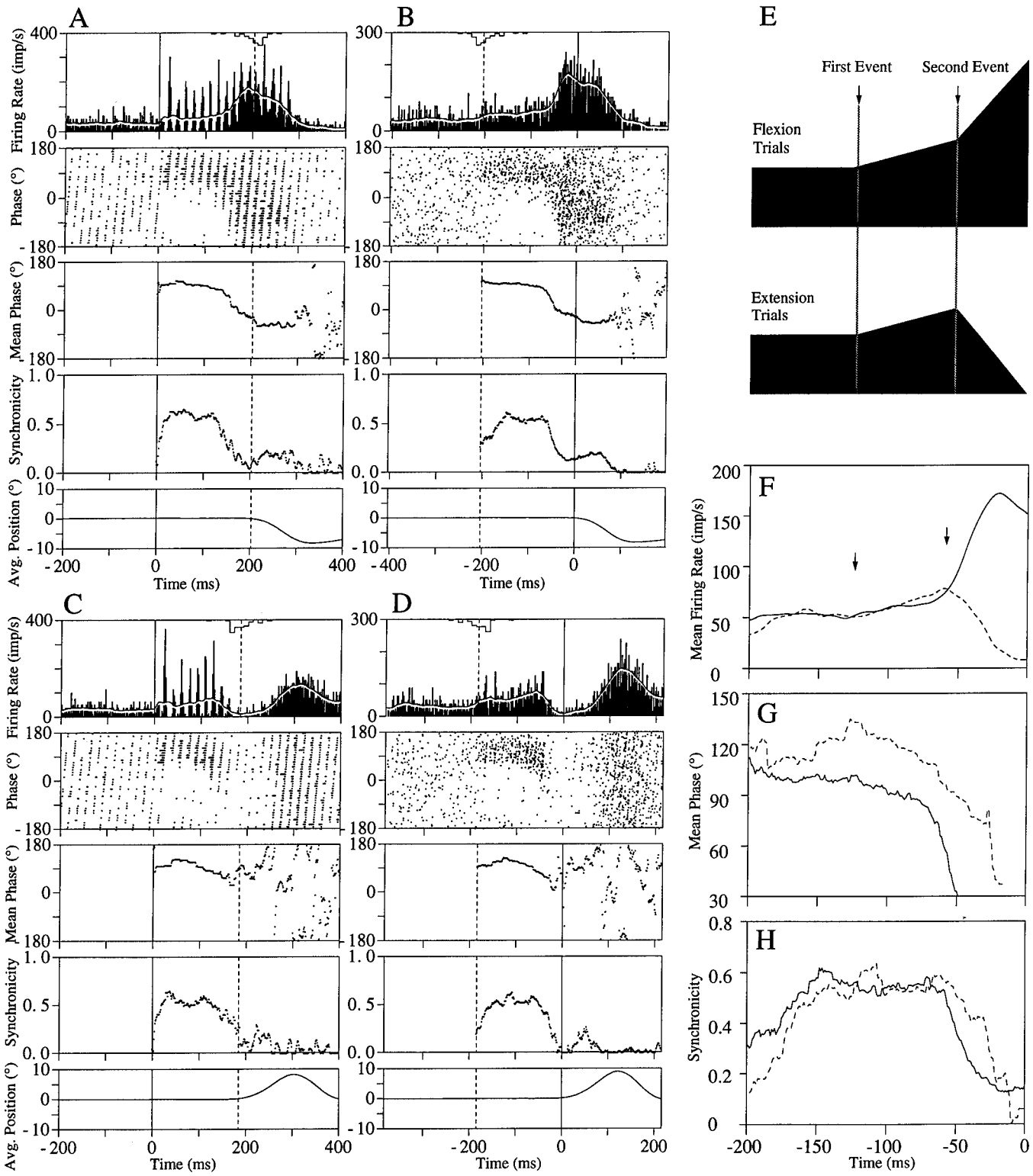

FIG. 11. Variability of premovement activity patterns with respect to movement direction (flexion or extension). The activity of an area 1 neuron (*monkey F*) during flexions (*A* and *B*) and extensions (*C* and *D*) made in response to 57-Hz vibration is illustrated. This neuron was activated during palpation of flexor carpi ulnaris and during passive flexions of the 3rd metacarpophalangeal joint. An activation-activation (AA) pattern was observed during flexions, and an activation and suppression pattern was observed during extensions (see Fig. 3*B*). Thus the activity change associated with the 1st event that occurred 120 ms before movement onset had the same sign for different movement directions. That occurring for the 2nd event (60 ms before movement onset) had the opposite signs for flexions and extensions (*E* and *F*). *F*: superimposed traces of mean firing rate. *G*: superimposed traces of mean phase. *H*: superimposed traces of synchronicity.

matosensory responsiveness that depends on the phase of a behavior. Initially, the vibrotactile stimulus in our paradigm serves as the go-cue, and its detection is obviously important. However, during movement execution, this stimulus may interfere with afferent signals providing feedback about movements (Nelson 1988; Nelson et al. 1991; Wiesendanger and Miles 1982). It has been shown that vibratory stimulation of muscle receptors during voluntary movements leads to errors in planned movement trajectories (Capaday and Cooke 1981; Cody et al. 1990; Inglis and Frank 1990). Thus it may be important to suppress the sensory responsiveness to vibration before movement onset. We indeed observed premovement suppression for a number of neurons. These observations are consistent with the results of other studies (Jiang et al. 1991; Nelson 1987, 1988).

PMA and the quality of peripheral stimulus representation

PMA often was associated with a disruption of the pattern of vibrotactile stimulus representation in SI neuronal activity. First, the quality of peripheral stimulus representation deteriorated because the firing of some neurons was suppressed. Second, during premovement activation, neuronal sensory responsiveness was also effectively suppressed because of desynchronization. We suggest that these mechanisms of masking peripheral stimuli are related to the previously demonstrated elevation of the threshold for tactile perception before and during voluntary movements (Coquery 1978; Dyhre-Poulsen 1978; Schmidt et al. 1990a,b). PMA may result in premovement decreases of somatosensory-evoked potentials (Cohen and Starr 1987; Coquery et al. 1972; Jiang et al. 1990b; Rushton et al. 1981). From our data showing premovement changes in the phase of responses to ongoing vibration, it may be predicted that similar premovement changes may occur in the latency of responses evoked by other stimuli (evoked potentials, air puff, etc.).

Conclusions

When monkeys make wrist movements in response to vibrotactile stimulation of their hands, some SI neurons exhibit sustained sensory responses that faithfully follow the vibratory stimulus frequency. However, the vibration-entrained firing pattern of these neurons changes before movement onset. Some neurons exhibit additional activation, whereas the firing of others is suppressed. Premovement changes in the phase of responses to vibration and in the fidelity of entrainment, both of which are correlated with the changes of firing rate, also occur. We suggest that the patterns of premovement activity result from the interaction between periodic vibration-related inputs and signals uncorrelated with vibration. In many cases, premovement changes precede EMG onset, indicating that they probably do not originate from movement-associated peripheral reafference. We suggest that inputs of central origin contribute to premovement activity. Presumably, the role of the central inputs is to prepare sensory cortical neurons for reafference resulting from voluntary movement, even if these neurons previously responded to peripheral stimuli with entrained activity.

We thank V. D. Douglas for technical assistance in data collection, and D. L. Armbruster for detailed comments on the manuscript.

This work was supported by United States Air Force Grant AFOSR 91-0333 to R. J. Nelson. M. A. Lebedev received a predoctoral fellowship from the Neuroscience Center of Excellence, University of Tennessee, Memphis.

Address for reprint requests: R. J. Nelson, Dept. of Anatomy and Neurobiology, University of Tennessee, 875 Monroe Ave., Memphis, TN 38163.

Received 13 January 1994; accepted in final form 27 May 1994.

REFERENCES

AMASSIAN, V. E., CRACCO, R. Q., AND MACCABEE, P. J. A sense of movement elicited in paralyzed distal arm by focal magnetic coil stimulation of human motor cortex. *Brain Res.* 479: 355–360, 1989.

BATSCHELET, E. *Circular Statistics in Biology.* New York: Academic, 1981.

BIANCONI, R. AND VAN DER MEULEN, J. P. The responses to vibration of the end-organs of mammalian muscle spindles. *J. Neurophysiol.* 26: 177–190, 1963.

BIOULAC, B. AND LAMARRE, Y. Activity of postcentral cortical neurons of the monkey during conditioned movements of a deafferented limb. *Brain Res.* 172: 427–437, 1979.

BURKE, D., HAGBARTH, K.-E., LOFSTEDT, L., AND WALLIN, B. G. The responses of human spindle endings to vibration of non-contracting muscles. *J. Physiol. Lond.* 261: 673–693, 1976a.

BURKE, D., HAGBARTH, K.-E., LOFSTEDT, L., AND WALLIN, B. G. The responses of human spindle endings to vibration during isometric contraction. *J. Physiol. Lond.* 261: 695–711, 1976b.

BURKE, D. AND SCHILLER, H. H. Discharge patterns of single motor units in the tonic vibration reflex of human triceps surae. *J. Neurol. Neurosurg. Psychiatry* 39: 729–741, 1976.

BURTON, H. AND SINCLAIR, R. J. Second somatosensory cortical area in macaque monkeys. 2. Neuronal responses to punctate vibrotactile stimulation of glabrous skin on the hand. *Brain Res.* 538: 127–135, 1991.

CAPADAY, C. AND COOKE, J. D. The effects of muscle vibration on the attainment of intended final position during voluntary human arm movements. *Exp. Brain Res.* 42: 228–230, 1981.

CHAPMAN, C. E., JIANG, W., AND LAMARRE, Y. Modulation of lemniscal input during conditioned arm movements in the monkey. *Exp. Brain Res.* 72: 316–334, 1988.

CODY, F. W. J., SCHWARTZ, M. P., AND SMIT, G. P. Proprioceptive guidance of human voluntary wrist movements studied using muscle vibration. *J. Physiol. Lond.* 427: 455–470, 1990.

COHEN, L. G. AND STARR, A. Localization, timing and specificity of gating of somatosensory evoked potentials during active movements in man. *Brain* 110: 451–467, 1987.

COLBURN, T. R. AND EVARTS, E. V. Long-loop adjustments during intended movements: use of brushless DC torque motors in studies of neuromuscular function. In: *Progress in Clinical Neurophysiology,* edited by J. E. Desmedt. New York: Karger, 1978, vol. 4, p. 153–166.

COQUERY, J.-M. Role of active movements in control of afferent input from skin in cat and man. In: *Active Touch: the Mechanisms of Object Manipulation: a Multidisciplinary Approach,* edited by G. Gordon. Oxford, UK: Pergamon, 1978, p. 161–169.

COQUERY, J.-M., COULMANCE, M., AND LERON, M.-C. Modifications des potentiels evoques corticaux somesthesiques durant des movements actifs et passifs chez l'homme. *Electroencephalogr. Clin. Neurophysiol.* 33: 269–276, 1972.

DESMEDT, J. E. AND GODAUX, E. The tonic vibration reflex and the vibration paradox in limb and jaw muscles in man. In: *Progress in Clinical Neurophysiology. Spinal and Supraspinal Mechanisms of Voluntary Motor Control and Locomotion,* edited by J. E. Desmedt. Basel: Karger, 1980, vol. 8, p. 215–247.

DYHRE-POULSEN, P. Perception of tactile stimuli before ballistic and during tracking movements. In: *Active Touch: the Mechanisms of Object Manipulation: a Multidisciplinary Approach,* edited by G. Gordon. Oxford, UK: Pergamon, 1978, p. 171–176.

ELLAWAY, P. H. An application of cumulative sum technique (cusums) to neurophysiology (Abstract). *J. Physiol. Lond.* 265: 1–2P, 1977.

EVARTS, E. V. Methods for recording activity of individual neurons in moving animals. In: *Methods in Medical Research,* edited by R. F. Rushmer. Chicago, IL: Year Book, 1966, vol. II, p. 241–250.

EVARTS, E. V. Feedback and corollary discharge: a margin of the concepts. *Neurosci. Res. Prog. Bull.* 9: 86–112, 1971.

EVARTS, E. V. Contrasts between activity of precentral and postcentral neurons of cerebral cortex during movement in the monkey. *Brain Res.* 40: 25–31, 1972.

FERRINGTON, D. G. AND ROWE, M. Differential contribution to coding of cutaneous vibratory information by cortical somatosensory areas I and II. *J. Neurophysiol.* 43: 310–331, 1980.

FROMM, C. AND EVARTS, E. V. Pyramidal tract neurons in somatosensory cortex: central and peripheral inputs during voluntary movement. *Brain Res.* 238: 186–191, 1982.

GARDNER, E. P., PALMER, C. I., HAMALAINEN, H. A., AND WARREN, S. Simulation of motion on the skin. V. Effect of stimulus temporal frequency on the representation of moving bar patterns in primary somatosensory cortex of monkeys. *J. Neurophysiol.* 67: 37–63, 1992.

GURLAND, J. AND TRIPATHI, R. C. A simple approximation for unbiased estimation of the standard deviation. *Am. Stat.* 25: 30–32, 1971.

HAGBARTH, K. E. AND VALLBO, Å. B. Discharge characteristics of human muscle afferents during muscle stretch and contraction. *Exp. Neurol.* 22: 674–694, 1968.

HOMMA, S. Frequency characteristics of the impulse decoding ratio between the spinal afferents and efferents in the stretch reflex. In: *Progress in Brain Research. Understanding the Stretch Reflex,* edited by S. Homma. Amsterdam: Elsevier, 1976, vol. 44, p. 15–30.

HONDA, C. N., SURMIER, D. J., AND WILLIS, W. D. Sensitivity of primate spinothalamic tract neurons to sinusoidal stimulation of the skin. *Soc. Neurosci. Abstr.* 12: 227, 1986.

INGLIS, J. T. AND FRANK, J. S. The effect of agonist/antagonist muscle vibration on human position sense. *Exp. Brain Res.* 81: 573–580, 1990.

JIANG, W., CHAPMAN, C. E., AND LAMARRE, Y. Modulation of somatosensory evoked responses in the primary somatosensory cortex produced by intracortical microstimulation of the motor cortex in the monkey. *Exp. Brain Res.* 80: 333–344, 1990a.

JIANG, W., CHAPMAN, C. E., AND LAMARRE, Y. Modulation of the cutaneous responsiveness of neurones in the primary somatosensory cortex during conditioned arm movements in the monkey. *Exp. Brain Res.* 84: 342–354, 1991.

JIANG, W., LAMARRE, Y., AND CHAPMAN, C. E. Modulation of cutaneous cortical evoked potentials during isometric and isotonic contractions in the monkey. *Brain Res.* 536: 69–78, 1990b.

JOHANSSON, R. S., LANDSTRÖM, U., AND LUNDSTRÖM, R. Responses of mechanoreceptive afferent units in the glabrous skin of the human hand to sinusoidal skin displacements. *Brain Res.* 244: 17–25, 1982.

JONES, E. G. AND PORTER, R. What is area 3a? *Brain Res. Rev.* 2: 1–43, 1980.

LAMARRE, Y., SPIDALIERI, G., AND CHAPMAN, C. E. A comparison of neuronal discharge recorded in the sensori-motor cortex, parietal cortex and dentate nucleus of the monkey during arm movements triggered by light, sound or somesthetic stimuli. In: *Experimental Brain Research. Neural Coding of Motor Performance,* edited by J. Massion, J. Paillard, W. Schultz, and M. Wiesendanger. Berlin: Springer-Verlag, 1983, suppl. 7, p. 141–157.

LEBEDEV, M. A. AND NELSON, R. J. The activity of vibratory-responsive monkey primary somatosensory cortical neurons is modulated prior to hand movements. *Soc. Neurosci. Abstr.* 18: 503, 1992.

LEBEDEV, M. A. AND POLYAKOV, A. V. The surface EMG of human soleus muscle under vibratory stimulation studied by spectral analysis. *Neirofiziologiya* 23: 57–65, 1991.

LEBEDEV, M. A. AND POLYAKOV, A. V. Analysis of surface EMG signals of human soleus muscle subjected to vibration. *J. Electromyogr. Kinesiol.* 2: 26–35, 1992.

LEMON, R. *Methods for Neuronal Recording in Conscious Animals. IBRO Handbook Series: Methods in the Neurosciences.* Chichester, UK: Wiley, 1984, vol. 4.

MATTHEWS, P. B. C. Proprioceptors and their contribution to somatosensory mapping: complex messages require complex processing. *Can. J. Physiol. Pharmacol.* 66: 430–438, 1988.

MILES, F. A. AND EVARTS, E. V. Concept of motor organization. *Annu. Rev. Psychol.* 30: 327–362, 1979.

MORLEY, J. W. AND GOODWIN, A. W. Sinusoidal movement of a grating across the monkey's fingerpad: temporal patterns of afferent fibers responses. *J. Neurosci.* 7: 2181–2191, 1987.

MOUNTCASTLE, V. B. Central nervous mechanisms in mechanoreceptive sensibility. In: *Handbook of Physiology. The Nervous System. Sensory Processes.* Washington, DC: Am. Physiol. Soc., 1984, sect. 1, vol. III, p. 789–878.

MOUNTCASTLE, V. B., STEINMETZ, M. A., AND ROMO, R. Frequency discrimination in the sense of flutter: psychophysical measurements correlated with postcentral events in behaving monkeys. *J. Neurosci.* 10: 3032–3044, 1990.

MOUNTCASTLE, V. B., TALBOT, W. H., SAKATA, H., AND HYVÄRINEN, J. Cortical neuronal mechanisms in flutter-vibration studies in unanesthetized monkeys: neuronal periodicity and frequency discrimination. *J. Neurophysiol.* 32: 452–484, 1969.

NELSON, R. J. Responsiveness of monkey primary somatosensory cortical neurons to peripheral stimulation depends on "motor set." *Brain Res.* 304: 143–148, 1984.

NELSON, R. J. Activity of monkey primary somatosensory cortical neurons changes prior to active movement. *Brain Res.* 406: 402–407, 1987.

NELSON, R. J. Set related and premovement related activity of primate somatosensory cortical neurons depends upon stimulus modality and subsequent movement. *Brain Res. Bull.* 21: 411–424, 1988.

NELSON, R. J. AND DOUGLAS, V. D. Changes in premovement activity in primary somatosensory cortex differ when monkeys make hand movements in response to visual vs. vibratory cues. *Brain Res.* 484: 43–56, 1989.

NELSON, R. J., SMITH, B. N., AND DOUGLAS, V. D. Relationship between sensory responsiveness and premovement activity of quickly adapting neurons in areas 3b and 1 of monkey primary somatosensory cortex. *Exp. Brain Res.* 84: 75–90, 1991.

PERSON, R. AND KOZHINA, G. Tonic vibration reflex of human limb muscles: discharge pattern of motor units. *J. Electromyogr. Kinesiol.* 2: 1–9, 1992.

PROCHAZKA, A. Sensorimotor gain control: a basic strategy of motor systems? *Prog. Neurobiol.* 33: 281–307, 1989.

RIBOT-CISCAR, E., VEDEL, J. P., AND ROLL, J. P. Vibration sensitivity of slowly and rapidly adapting cutaneous mechanoreceptors in the human foot and leg. *Neurosci. Lett.* 104: 130–135, 1989.

ROLL, J. P. AND VEDEL, J. P. Kinaesthetic role of muscle afferents in man, studied by tendon vibration and microneurography. *Exp. Brain Res.* 47: 177–190, 1982.

RUSHTON, D. N., ROTHWELL, J. C., AND GRAGGS, M. D. Gating of somatosensory evoked potentials during different kinds of movement in man. *Brain* 104: 465–491, 1981.

SCHMIDT, R. F., SCHADY, W. J. L., AND TOREBJORK, H. E. Gating of tactile input from the hand. I. Effect of finger movement. *Exp. Brain Res.* 79: 97–102, 1990a.

SCHMIDT, R. F., TOREBJORK, H. E., AND SCHADY, W. J. L. Gating of tactile input from the hand. II. Effect of remote movements and anaesthesia. *Exp. Brain Res.* 79: 103–108, 1990b.

SHIN, H.-C. AND CHAPIN, J. K. Movement induced modulation of afferent transmission to single neurons in the ventroposterior thalamus and somatosensory cortex in rat. *Exp. Brain Res.* 81: 515–522, 1990.

SOSO, M. J. AND FETZ, E. E. Responses of identified cells in postcentral cortex of awake monkeys during comparable active and passive joint movements. *J. Neurophysiol.* 43: 1090–1110, 1980.

TALBOT, W. H., DARIAN-SMITH, I., KORNHUBER, H. H., AND MOUNTCASTLE, V. B. The sense of flutter-vibration: comparison of the human capacity with response patterns of mechanoreceptive afferents from the monkey hand. *J. Neurophysiol.* 31: 301–334, 1968.

VAADIA, E., KURATA, K., AND WISE, S. P. Neuronal activity preceding directional and nondirectional cues in the premotor cortex of rhesus monkeys. *Somatosens. Mot. Res.* 6: 207–230, 1988.

VALLBO, Å. B. Discharge patterns in human muscle spindles during isometric voluntary contractions. *Acta Physiol. Scand.* 80: 552–566, 1970.

VOGT, B. A. AND PANDYA, D. N. Cortico-cortical connections of somatic

sensory cortex (areas 3, 1, and 2) in the rhesus monkey. *J. Comp. Neurol.* 177: 179–192, 1978.

VON HELMHOLTZ, H. *Treatise on Physiological Optics,* edited by J. P. C. Sothall. New York: Dover, 1962 (originally published 1866), vol. 3.

VON HOLST, E. Relationship between the central nervous system and peripheral organs. *Br. J. Anim. Behav.* 2: 89–94, 1954.

WALL, P. D. AND CRONLY-DILON, J. R. Pain, itch and vibration. *Am. Med. Assoc. Arch. Neurol.* 2: 365–375, 1960.

WIESENDANGER, M. AND MILES, T. S. Ascending pathway of low-threshold muscle afferents to the cerebral cortex and its possible role in motor control. *Physiol. Rev.* 62: 1234–1270, 1982.

ZAR, J. H. *Biostatic Analysis.* Englewood Cliffs, NJ: Prentice-Hall, 1974.

RHYTHMICALLY FIRING (20 - 50 HZ) NEURONS IN MONKEY PRIMARY SOMATOSENSORY CORTEX: ACTIVITY PATTERNS DURING INITIATION OF VIBRATORY-CUED HAND MOVEMENTS

Running Title: Rhythmic SI Neurons during Initiation of Vibratory-Cued Movements

Michael A. Lebedev and Randall J. Nelson

Address for correspondence:

Dr. R.J. Nelson

Department of Anatomy and Neurobiology

University of Tennessee, Memphis

875 Monroe Ave, Memphis, TN 38163, USA

Telephone (901) 448 5979

FAX (901) 448 7193

E-mail: rnelson@utmem1.utmem.edu

Abstract

The activity patterns of rhythmically firing neurons in monkey primary somatosensory cortex (SI) were studied during trained wrist movements that were performed in response to palmar vibration. Of 1222 neurons extracellularly recorded in SI, 105 cells (8.6%) discharged rhythmically (at ~30 Hz) during maintained wrist position. Some of these rhythmic neurons (28/105) exhibited interspike intervals at multiples of the modal period. Moreover, for 16/105 neurons, modal intervals were split by interrupting spikes. Activity suppressions or, less often, activations occurred during task execution. During suppressions, the pattern of the rhythmic activity often was disrupted rather than modulated. During activations, transitions to periods of nonrhythmic firing occurred. If the rhythmic frequency was modulated, then it was modulated only slightly (± 20%). Suppressions that consisted of transient and sustained epochs commonly occurred at ~25 ms after vibratory go-cue onset. In some cases, although the firing was partially suppressed, it was entrained to the vibratory stimulus, particularly when the stimulus frequency was close to the neuron's rhythmic frequency. Prior to movements, neuronal activity underwent an additional suppression, whereas both suppressions and activations occurred during movements. Premovement changes may have been related to peripheral reafference, since they often occurred in conjunction with the average EMG onset (~60 ms prior to movement onset). The activity of rhythmic neurons resembled a mirror image of that of quickly adapting SI neurons recorded during the performance of this task.

Features of the firing patterns of these neurons suggest several things. First, the type of rhythmic activity observed could occur due to extrinsically induced or intrinsic oscillations of membrane potential but would be unlikely to reflect integrate-and-fire neurons receiving a stable input. Second, premovement changes in activity probably were not strictly replications of the sensory input, because usually they were the same for both flexions and extensions. When comparing the activity patterns of rhythmically firing neurons with those of quickly adapting SI

neurons, the observed features suggest that these two types of neurons may gate SI activity in reciprocal ways. Finally, since disruptions of rhythmic activity of individual SI neurons were similar to those reported previously for local field potential oscillations in sensorimotor cortex during trained movements, the activity of rhythmic SI neurons and cortical population oscillations may be related.

Introduction

Rhythmic activity has been suggested to be a functionally important mode of neuronal firing that may serve to switch between behavioral modes and to establish dynamic coupling between cortical areas (for review, see Gray, 1994; Llinas, 1990; Lopes da Silva, 1991; Sheer, 1989; Singer, 1993). However, the activity patterns of rhythmically firing neurons in monkey primary somatosensory cortex (SI) exhibited during the performance of trained motor tasks are still not completely understood. Rhythmic activity in the form of population oscillations of cortical neurons at ~40 Hz has been studied most extensively in cat visual cortex (Eckhorn et al., 1988; Gray and Singer, 1989; for review, see Engel et al., 1992; Gray et al., 1991; Gray, 1994; Singer, 1993). Similar oscillations have been demonstrated in sensorimotor cortex in cat (Bouyer et al., 1981; 1987) and in monkey (Murthy and Fetz, 1992; Rougeul et al., 1979; Sanes and Donoghue, 1993). Oscillations in motor and sensory cortical areas have been suggested to play a role in sensorimotor integration (Murthy and Fetz, 1992; Sanes and Donoghue, 1993) and focal attention (Bouyer et al., 1981; 1987; Gray, 1994; Rougeul et al., 1979).

Some forms of cortical oscillations may be initiated by individual neurons having intrinsic oscillatory properties, whereas thalamocortical and corticocortical interactions are important in maintaining and propagating the oscillations (Llinas, 1990). Using *in vivo* patch clamp recording techniques, Jagadeesh et al. (1992) demonstrated rhythmic synaptic inputs to visual cortical neurons. Single morphologically identified neurons with a 40-Hz rhythmicity and that were probably inhibitory interneurons have been recorded in cortical slice preparations (Llinas et al.,

1991). The presence of rhythmic IPSPs has been demonstrated for pyramidal cortical neurons *in vivo* in urethane-anesthetized rats (Cowan and Wilson, 1994). These rhythmic IPSPs may have been evoked by cortical interneurons. Also, depolarization-induced 20- to 40-Hz oscillations have been reported for a subset of pyramidal cortical neurons recorded *in vivo* in urethane-anesthetized cats (Nuñez et al., 1992). Therefore, intrinsic properties, as well as extrinsic influences, may be involved in generating rhythmic activity.

While the majority of data on the oscillations in sensorimotor cortical areas during behavior have been obtained while recording local field potentials (LFPs) (Bouyer et al., 1981; 1987; Murthy and Fetz, 1992; Rougeul et al., 1979; Sanes and Donoghue, 1993), some studies have examined rhythmic activity of single neurons in relationship to behavior. In one such study in which the activity of second somatosensory cortical (SII) neurons of awake monkeys was recorded, Ahissar and Vaadia (1990) suggested that oscillatory activity of somatosensory cortical neurons may be important in texture analysis. Rhythmic activity of these SII neurons was often reduced by tactile stimulation or during voluntary movements. However, tactile stimulation, in this case, was performed outside of the motor task and, therefore, may not have been behaviorally significant to the monkeys.

To answer the question of what happens to the activity of rhythmically firing SI neurons when detection of tactile stimuli is a crucial facet of the behavioral task, we conducted experiments in which monkeys performed voluntary wrist flexions and extensions in response to vibrotactile go-cues. We sought to determine whether any SI neurons exhibit rhythmic activity during this behavior and, if they did, to describe the characteristics of their spike trains and how these spike trains changed in association with the presentation of vibrotactile go-cues and movement initiation. Also, we sought to relate the activity of rhythmic neurons with that of other SI neurons recorded during the same experimental paradigm (Nelson, 1988; Nelson et al., 1991; Lebedev and Nelson, 1993; Lebedev et al., 1994).

Methods

Experimental Set-Up and Behavioral Paradigm

Six adult male rhesus monkeys (*Macaca mulatta*; monkeys C, F, G, H, M, and N) were trained to perform sensory-triggered wrist movements. The monkeys were cared for in accordance with the *NIH Guide for Care and Use of Laboratory Animals,* revised 1985. Each animal sat in an acrylic monkey chair with its right forearm on an armrest and its right palm on a moveable plate (Fig. 1A). One end of the plate was attached to the axle of a brushless DC torque motor (Colburn and Evarts, 1978). A load of 0.07 Nm was applied to the plate, which assisted wrist extensions and opposed flexions. To maintain a centered wrist position, the monkeys had to exert an active pressure upon the plate. Visual feedback of wrist position was provided by a display located 35 cm in front of the animals. This display consisted of 31 light-emitting diodes (LED) (Fig. 1B). Wrist position was indicated by illuminating one of the LEDs. The middle red LED corresponded to a centered wrist position. Yellow LEDs above and below the middle LED indicated successive angular deviations of 1°. An instructional red LED was located in the upper left corner of the visual display (Fig. 1B).

Figure 1 About Here

The monkeys were trained to make wrist flexions or extensions in response to vibrotactile stimulation of their palms (Nelson, 1988; Nelson et al., 1991). The experimental paradigm is illustrated in Fig. 1C. To begin a trial, the monkey first had to center the plate. Then, a movement direction request was given. Illumination of the instructional LED informed the monkey that extension was the appropriate movement. Otherwise, the appropriate movement was flexion. The monkey was required to hold the plate in the centered position until the vibratory go-cue was presented. Movements of more than 0.5° from the center during the hold period cancelled the trial.

If the center position was held for the required time (0.5, 1.0, 1.5, or 2.0 s; pseudorandomized), the plate was vibrated (sine wave < 0.06° angular deflection) using the torque motor. Vibratory frequencies of 27, 57, and 127 Hz were tested. The onset of vibratory stimulation served as the go-cue for movement. When a movement of at least 5° in the required direction was made, the vibration was turned off, and the animal received a fruit juice reward. A new trial began when the animal once again centered the plate.

Electrophysiological Recordings and Histology

Once an animal was trained to the point of stable performance, a stainless steel recording chamber was surgically implanted to allow for extracellular recordings of the activity of SI neurons (see Nelson et al., 1991, for details). Platinum-iridium microelectrodes were used for recordings. Transdural penetrations were made daily into the region of SI that corresponded to the contralateral hand representation. The activity of single units was amplified, discriminated, and stored in a computer as pulse data by conventional means (Evarts, 1966; Lemon, 1984; Nelson, 1988; Nelson et al., 1991). Neuronal receptive fields (RFs) were examined by lightly touching skin surfaces, manipulating joints, and palpating muscles. An RF was classified as "cutaneous" if the neuron preferentially responded to light touch and "deep" if the neuron responded to bending a joint or to muscle palpation. For some neurons, no clear RF could be found.

At regular intervals, the EMG activity of forearm muscles acting across the wrist was recorded (Nelson, 1987). Intramuscular EMG wires (stranded stainless steel, TEFLON® insulated; Bergen Wire Rope Co.) were temporarily implanted in muscles by using sterile 25-gauge needles as guides. EMG activity was converted into pulse data with a window discriminator (Vaadia et al., 1988; Lebedev et al., 1994) and stored in the same form as the neuronal data.

On the last recording day, electrolytic lesions (10 μA of current for 10-20 s) were made in the cortex to mark the locations of interest. The animals were then deeply anesthetized with sodium pentobarbital and transcardially perfused with 10% buffered formol-saline. Histological

sagittal sections of the cortex were prepared, and recording sites were reconstructed based upon the depth of each electrode penetration and its location with respect to the marking lesions (Fig. 2) (Nelson, 1988; Nelson et al., 1991).

Figure 2 About Here

Analyses of Rhythmic Spike Trains

Rhythmic SI neurons were selected by examining spike trains for a 500-ms epoch immediately preceding vibration onset. This corresponded to the shortest duration of the hold period during which animals actively maintained a stable wrist position. Expectation density (ED) histograms (Mountcastle et al., 1969; 1990) were calculated for this epoch. ED, also termed the "autocorrelation function" (Zadeh, 1957), represents the probability of a neuronal discharge at a certain time after a given discharge. For rhythmic spike trains, ED histograms contain peaks at the multiples of the rhythmic period (Fig. 3) (Perkel et al., 1967; Poggio and Viernstein, 1964; Segundo et al., 1968). From the interval between peaks in ED histograms, we derived the rhythmic frequency:

$$f = 1 / T \qquad (1)$$

where f is rhythmic frequency and T is the average interval for the first three peaks.

The average height of subsequent bins in the ED histogram gradually flattened to a level that approximated the mean discharge rate (Fig. 3). We quantified the degree of rhythmicity as the ratio of the height of the first ED peak to the mean discharge rate:

$$E'_1 = E_1 / R \qquad (2)$$

where E'_1 is the normalized height of the first peak, E_1 is the height of the first peak, and R is the mean discharge rate. For the present study, only the neurons with E'_1 more than 1.5 were selected. According to estimations derived by modeling, this selection criterion is approximately

equivalent to the criterion used by Ahissar and Vaadia (1990) who classified SII neurons as rhythmic if the second peak in an ED histogram exceeded 20% of the mean firing rate.

Figure 3 About Here

Serial dependencies of the ISIs were analyzed using joint interval scattergrams that displayed each ISI as a function of its immediately preceding ISI (Fig. 4B) (Rodieck et al., 1962; Surmeier and Towe, 1987a; 1987b; Siebler et al., 1991). Rhythmic spike trains also were tested for orderliness by comparing ED and renewal density (RD) histograms (Fig. 4D&E) (Mountcastle et al., 1969; 1990; Perkel et al., 1967; Poggio and Viernstein, 1964). RD is the ED calculated for randomly shuffled ISI sequences. To estimate the difference between ED and RD histograms, we compared the magnitudes of the first, second, and third peaks in ED histograms with those of corresponding peaks in RD histograms.

Figure 4 About Here

Analyses of Changes in Neuronal Activity and EMG

Changes in neuronal activity associated with go-cues and movements were analyzed using conventional discharge histograms (Fig. 5B) and raster displays (Fig. 5C). In addition, ISI rasters were plotted that displayed the time of occurrence of each spike on the x-axis and the succeeding ISI on the y-axis (Fig. 5A). To analyze vibration-related changes in activity, the occurrences of discharges were expressed as times with respect to vibration onset (Fig. 5A-E, left panels). When analyzing movement-related changes, spike occurrences were expressed with respect to movement onset (Fig. 5A-E, right panels).

Figure 5 About Here

The onsets of changes in neuronal firing rate and of changes in EMG were determined using the cumulative sum methods (CUSUM) (Ellaway, 1977; Jiang et al., 1991). The CUSUM at a given time is the total number of discharges accumulated for all trials from some starting time. The average CUSUM was calculated by rescaling this count by dividing it by the number of trials (Fig. 3D). The CUSUM for an impulse train for which the probability of discharge is constant over time is a linearly rising curve with a slope equal to the mean firing rate. To calculate the onset of deviations from the stationary level of activity, the largest epoch of linear rise in the average CUSUM prior to a behaviorally significant event was labeled by visual inspection. A linear least-squares interpolation curve was calculated for this period. This curve was then extrapolated through the epoch containing the event. The standard deviation of the CUSUM from the fitted curve was calculated. The computer program searched forward in time to find the first change in the CUSUM from the curve of more than three standard deviations for at least 40 ms. This time was designated as the onset of a significant change in activity.

The correlation between the periodic vibratory stimulus and neuronal discharges was analyzed using a phase representation method (for details, see Lebedev et al., 1994). The phase of each poststimulus spike with respect to the stimulus cycle was calculated and plotted in a scattergram as a function of time (see, e.g., Fig. 8B). In addition, the phase was automatically calculated by the computer for the epoch preceding vibration onset. For this epoch, phase was randomly scattered. Following vibration onset, if the activity was entrained to the stimulus, a band was present in the phase scattergram that corresponded to the phase of preferential response. Cycle distribution histograms also were calculated (see, e.g., Fig. 8G).

Statistical Analyses

The characteristics of neuronal activity for several groups of neurons (having specific RF types, located in given cortical areas, etc.) were statistically compared using a multifactorial ANOVA (with the Scheffé post hoc test). The parametric *t*-test and the more robust nonparametric Mann-Whitney *U*-test were used for two group comparisons. Below, we present the most rigorous estimates of the *p*-values from all statistical tests done.

Results

Cortical Locations and Receptive Fields

Of the total recorded 1222 SI neurons, 105 neurons (8.6%) having rhythmic activity patterns were selected. The distribution of surface locations of the recording sites and their location in representative sagittal sections are shown in Fig. 2C. Rhythmic neurons were observed in all regions of SI (areas 3a, 3b, 1, and 2). No clear distribution patterns were evident, either within or across cortical areas. Seventy-seven neurons were tested for RFs. This sample contained more neurons with deep RFs than those with cutaneous RFs or no clear RF (Fig. 2B).

Characteristics of Rhythmic Activity

The activity of rhythmic neurons was analyzed for the relatively stable firing that occurred during the hold period (-500 to 0 ms prior to vibration onset). We sought to determine the frequency characteristics of the rhythmic activity as well as any serial dependencies of the ISIs. An example of spike train analysis for the hold period is presented in Fig. 4. The activity of **[6]** same neuron during task execution is illustrated in Fig. 5. This neuron was located in area 1 (Fig. 5F). It had a noncutaneous RF deeply located in the hand (Fig. 5G). In Fig. 4A, a scattergram of ISIs during a 500-ms epoch preceding vibration onset is plotted for 40 consecutive trials. This scattergram shows that the ISI distribution remained virtually unchanged from trial to trial. In Fig. 4B, a joint-interval scattergram is presented. Fig. 4C, D, and E display, respectively, ISI

distribution, ED, and RD histograms. During the hold period, this neuron was rhythmically active at ~39 Hz. The majority of ISIs were distributed within the range of ± 5 ms around the rhythmic period (~25.6 ms). Note, however, that a small number of outlying short and long ISIs were present. ED and RD histograms were not substantially different.

Statistical analyses of the rhythmic frequency (f ; equation 1) and the first normalized ED peak (E'_1, equation 2) for the sample of rhythmic neurons did not show any significant differences depending on cortical location of the neurons or on their RF type. The means and the standard deviations for f and E'_1 were 33.5 ± 5.8 Hz and 2.59 ± 0.70 Hz, respectively. The distribution of f is presented in a histogram in Fig. 6.

Figure 6 About Here

The analyses of joint interval scattergrams and of ISI distributions showed that, in some cases, rhythmic spike trains had features that are not evident in the typical example shown in Fig. 4. One feature was the multimodality of ISIs. An example of a neuron with multimodal ISI distribution is presented in Fig. 7A-D. This area 1 neuron (Fig. 7D) was rhythmically active at ~43 Hz. It had a cutaneous RF located on the second digit (Fig. 7C). The ISI distribution of this neuron contained two pronounced peaks at the modal interval (T) and at twice that interval ($2T$; Fig. 7B). The joint interval scattergram for this neuron had four clusters of ISI pairs around points (T, T), (T, $2T$), ($2T$, T), and ($2T$, $2T$). ED and RD histograms were approximately the same for this neuron. (Other examples of neurons with multimodal ISI distributions are presented in Figs. 11 and 13.) Multimodal ISI distributions of this type were observed for 28/105 cells (~27%).

Figure 7 About Here

Another characteristic of rhythmic spike trains was the occurrence, in some instances, of interrupting spikes that split the modal interval. Such spike trains previously have been reported and analyzed using joint interval methods (Surmeier and Towe, 1987a; 1987b; Siebler et al., 1991). Joint interval scattergrams for spike trains with interrupting spikes contain diagonal bands that connect points (0, T) and (T, 0). Records for a neuron that had interrupting spikes are presented in Fig. 7E-H. This neuron was located in area 3b (Fig. 7H) and was rhythmically active at ~30 Hz. No clear RF was detected for this cell. In addition to a cluster of ISIs around T, shorter ISIs were present that were approximately uniformly distributed within the range from ~2 ms to T (Fig. 7F). In the joint interval scattergram, the presence of short intervals resulted in a diagonal band. Peaks in the RD histogram were less pronounced than those in the ED histogram. Spike trains with interrupting spikes were observed for 16/105 neurons (~15%). Five neurons (~5%) exhibited both interrupting spikes and multimodal ISIs.

Joint interval scattergrams with diagonal bands are routinely observed for vibration-entrained spike trains (unpublished observations). An example of a neuron entrained to vibration at 27 Hz is presented in Fig. 8. This area 3a neuron (Fig. 8D) was activated by passive wrist extensions (Fig. 8C). Illustrated are the records from a paradigm in which, after vibration onset, the monkey was required to hold the handle still for 1 s (Nelson, 1984; 1988). Prior to vibration onset, the neuron fired nonrhythmically (Fig. 8E). For the epoch of vibratory stimulation, stimulus-entrained activity resulted in peaks in the histogram of discharges (Fig. 8A). Entrainment also was clearly seen in phase raster (Fig. 8B) and in cycle distribution (Fig. 8G). The joint interval histogram for the epoch of vibratory stimulation contained a diagonal band (Fig. 8F). ED and RD histograms were dramatically different.

Figure 8 About Here

The comparison of ED and RD histograms for the total sample of rhythmic cells showed a tendency for peaks in RD histograms to be less pronounced than those in ED histograms. The results of factorial ANOVA indicated that, for the neurons having interrupting spikes, the differences between ED and RD peaks were significantly greater compared with the rest of the total sample. For these neurons, the means and standard deviations of the differences between the first three ED and RD peaks were, respectively, 12.0 ± 6.1% ($p < 0.0002$; paired t-test), 13.5 ± 7.2% ($p < 0.0002$), and 9.7 ± 12.5% ($p < 0.005$). When the neurons with interrupting spikes were excluded from the total sample, only the difference between the first peaks in the remaining population was statistically significant (1.4 ± 3.9%; $p < 0.001$).

Vibration-Related Activity

Changes in the activity of SI neurons in this experimental paradigm commonly occur at vibratory go-cue onset and often precede movement onset (Nelson, 1988). We analyzed the changes in activity of rhythmic neurons that occurred in association with these behaviorally significant events. For 49/105 rhythmic neurons (~47%), their firing rate changed with vibration onset. An example of a typical response to vibration is presented in Fig. 9A, in which the records for an area 1 neuron are shown. This neuron was activated by passive metacarpophalangeal extension of the fourth digit (Fig. 9B). This neuron's rhythmic frequency was ~30 Hz. During task execution, the neuron's firing was suppressed following palmar vibration at ~28 ms after vibration onset. The vibratory-related suppression consisted of both transient and sustained changes in activity (schematic illustration, Fig. 9E). Suppression was the most common response to vibrations (44/49 cases, ~90%; e.g., see Figs. 5, 7, 10, 12, and 13). For only 5/49 neurons (~10%), vibration-induced activity increased. The analyses of the latency of vibratory responses are presented in Fig. 6F. This latency (~25 ms at 57 Hz) did not differ significantly between cases of activation and suppression. Also, it was not significantly different as a function of cortical location or RF type.

Figure 9 About Here

In some cases, neuronal activity during ongoing vibration, though partially suppressed, was stimulus-entrained. An example of an area 3a neuron with activity entrained to the vibratory stimulus at 27 Hz is presented in Fig. 10. This neuron was activated by passive wrist extensions (Fig. 10B). During the hold period, the neuron was rhythmically active at ~30 Hz. A transient suppression of activity occurred at ~27 ms after vibration onset and lasted for ~50 ms (Fig. 7A). Then, the activity recovered, although it was at a lower level than that during the hold period. Moreover, neuronal discharges were entrained to the ongoing 27-Hz vibration. The entrainment is clearly seen in phase raster (Fig. 10B) and in the cycle distribution histogram (Fig. 10G). The ISI distribution for the epoch of vibratory stimulation contained peaks at the vibratory period and at twice that period (Fig. 10F). ISI clusters corresponding to single and double periods were present in joint interval scattergrams. Generally, the entrainment was observed more often when stimulating at 27 Hz, which was close to the average rhythmic frequency of the studied neurons. However, the sample of neurons recorded at this frequency was relatively small (28 neurons). Eight neurons from this sample (~29%) exhibited vibration-entrained activity. The majority of the data were collected while stimulating at 57 Hz. Only 5/105 neurons (~5%) exhibited vibratory entrainment at 57 Hz. At the higher stimulus frequency (127 Hz) vibratory entrainment was never observed.

Figure 10 About Here

Premovement Activity

Changes in activity associated with movement onset may reflect peripheral reafferent

signals as well as centrally generated inputs that presumably come to SI from motor areas (Lebedev et al., 1994; Nelson, 1987; Nelson et al., 1991; Soso and Fetz, 1980). The activity of all studied rhythmic neurons changed prior to movement onset at least for one-movement direction. The earliest change of firing rate from the stabilized level of activity during vibratory stimulation was designated as premovement activity (PMA) (Nelson, 1988). PMA was detected in 101/105 instances for flexion movements and in 97/105 instances for extension movements. Figure 11A illustrates the activity pattern of an area 2 neuron that had no clear RF detected. Rhythmic frequency was ~44 Hz. The firing rate of this neuron did not change after vibration onset. However, its activity was dramatically suppressed at ~40 ms prior to the onset of extension movements. Activity suppression also was observed prior to flexions (not shown). Suppression was the most frequent PMA type (~77% of PMA cases; Fig. 11F; also see examples of premovement suppression in Figs. 5, 7, 9, 10, 12, and 13). The PMA onset of these neurons with respect to movement onset was not statistically different as a function of cortical location or RF type. Moreover, it did not differ between instances of activation and suppression.

Figure 11 About Here

To estimate the temporal relationship between PMA and the earliest movement-related peripheral signals, the PMA onsets were compared with EMG onsets. The EMG onsets were analyzed for several forearm and arm muscles (Lebedev et al., 1994; Nelson, 1987; Nelson et al., 1991). Changes in EMG occurred not earlier than 100 ms prior to movement onset (average EMG onset was ~60 ms before movement onset) (Fig. 11F). A substantial number of PMA onsets for rhythmic neurons were later than the earliest EMG onset (154/198; ~78%). PMA onsets were later than the average EMG onset in 108/198 instances (~55%).

Figure 12 About Here

During activity suppressions, rhythmic firing often was disrupted rather than modulated (e.g., Fig 11A). In the cases when the rhythmic pattern of discharges was preserved, rhythmic frequency decreased slightly (by ~20%; e.g., sustained vibratory response in Fig. 5A). Activity increases usually occurred during movements and were characterized by transitions from rhythmic to nonrhythmic firing. In Fig. 12, records for an area 1 neuron are presented that show an activation during voluntary extensions. This neuron also was activated by passive extensions of the second digit at the metacarpophalangeal joint (Fig. 12B). This neuron's rhythmic frequency was ~28 Hz. Firing was slightly suppressed at ~27 ms following vibration onset. An additional suppression occurred at ~34 ms prior to extension movement onset. Then, a pronounced activation followed at ~45 ms after movement onset. The activation was characterized by a qualitative change in the ISI distribution (Fig. 12D and E). The ISIs became shorter and the ISI distribution became Poisson-like (compare with Fig. 8E). In some instances, transitions to irregular ISI patterns occurred without substantial changes in the mean firing rate (e.g., ~200 ms after movement onset in Fig. 7E and 13A).

Activity patterns were analyzed to determine if there was any dependency of PMA types upon the direction of subsequent movement. If the sign of the activity change was opposite for flexions and extensions or if PMA occurred only for one movement direction, this instance of PMA was classified as directional. If the activity change was of the same sign for both movement directions, the PMA was classified as nondirectional. Nondirectional PMA occurred most frequently (70/105 neurons, ~67%); directional PMA was observed for 35/105 neurons (~33%). An example of an area 3a neuron with a nondirectional PMA pattern is presented in Fig. 13. The rhythmic frequency of this neuron was ~38 Hz. For both flexions (Fig. 13A) and extensions (Fig. 13D), premovement suppression of activity occurred at ~70 ms prior to movement onset.

Figure 13 About Here

Comparison with Quickly Adapting SI Neurons

We compared the activity pattern exhibited by rhythmic neurons with the types of activity of SI neurons that have been documented previously for this experimental paradigm (Nelson, 1988; Nelson et al., 1991). Classification of SI neurons according to their activity patterns may provide clues as to their functional role and interactions during behavior. The typical activity pattern of rhythmic neurons (see a schematic illustration, Fig. 9E) resembled a mirror image of the activity of quickly adapting (QA) neurons recorded during similar behaviors (Nelson et al., 1991). An example of activity of a QA neuron is presented in Fig. 14. This neuron was located in area 1 (Fig. 14D). It had a cutaneous RF on the palm near the base of the third digit (Fig. 14C). This neuron produced a short burst of spikes at ~30 ms after vibration onset. Then a pause in firing occurred. The activity of this neuron was reactivated at ~84 ms prior to movement onset. Moreover, this movement-related activity appeared to contain a sensory component because it was loosely vibration-entrained (Fig. 14B and G). Thus, this QA neuron was activated at about the same time following vibratory cue onset and prior to movement as the studied SI rhythmic neurons showed suppressions in their previously consistent firing patterns.

Figure 14 About Here

Discussion

Major Findings

We examined the activity of rhythmic neurons in monkey SI during trained motor tasks. The neurons that were selected were rhythmically active (at ~30 Hz) during active holding against a

load prior to vibrotactile go-cue onset. Rhythmic cells were found in all SI regions (areas 3a, 3b, 1, and 2). Some neurons exhibited ISIs at multiples of the modal interval (i.e., these neurons occasionally failed to discharge at times consistent with the underlying rhythmic process; Abeles, 1982). Moreover, spike trains of a number of cells contained interrupting spikes that split the modal interval (i.e., their rhythm was not reset by spike occurrences; Surmeier and Towe, 1987a; 1987b). These features of spike trains may occur due to rhythmic synaptic input or intrinsic neuronal oscillations but are unlikely to reflect an integrate-and-fire neuron having a very stable synaptic input (Segundo et al., 1968; Softky and Koch, 1993). The firing frequency of an integrate-and-fire neuron is modulated, depending upon the intensity of synaptic input. However, we observed only slight modulations of rhythmic frequency. Instead, during activity decreases, rhythmic firing often was disrupted rather than modulated. During activity increases, neurons often began to fire nonrhythmically. We conclude, therefore, that the studied neurons either received rhythmic synaptic input or were intrinsically oscillatory but were unlikely to be integrate-and-fire neurons with stable synaptic inputs.

The activity patterns of most of rhythmic SI neurons had common features during task execution. After vibration onset, the activity typically decreased. Vibratory suppressions consisted of transient and sustained changes. In some cases, although the activity was partially suppressed, it was entrained to the frequency of the ongoing vibration. The best vibratory frequency for entrainment of these neurons was close to the average frequency of rhythmic activity (~30 Hz). This observation is consistent with a prediction made by Ahissar and Vaadia (1990). The neuronal activity often was suppressed further prior to movement onset. Premovement changes most often occurred after the earliest EMG onset and therefore probably were related to changes in peripheral afferent input. However, a small proportion of changes, specifically those that preceded the earliest EMG onset (~20%), may have been of central origin (Lebedev et al., 1994; Nelson, 1987; Nelson et al., 1991; Soso and Fetz, 1980). Most premovement changes were similar for both flexions and extension movement trials. However, peripheral reafferent signals

commonly are thought to be directional (Cohen et al., 1994). Thus, premovement changes may not strictly replicate peripheral inputs. The activity patterns of rhythmic neurons resembled mirror images of those of quickly adapting neurons. It is reasonable to suggest, therefore, that rhythmic and quickly adapting neurons may participate in gating of SI activity in reciprocal ways (Nelson et al., 1991). The activity of individual rhythmic neurons has similar features to LFP oscillations in sensorimotor cortex during trained behaviors (Sanes and Donoghue, 1993). Both the firing of individual neurons and patterns of LFP oscillations are disrupted prior to movements. Thus, rhythmic activity of individual neurons and cortical population oscillations may be related. This relationship, however, still requires additional experimental demonstration.

Activity of Rhythmic Neurons during Behavior

Rhythmic SI neurons typically were suppressed at ~25 ms after vibration onset during our behavioral task. An additional decrease of activity at ~60 ms prior to movement onset also often occurred. Thus, rhythmic neurons are probably a subset of the VIB^- neurons we have previously described (Nelson, 1988) that have premovement suppression. SI neurons respond to peripheral stimuli in this behavioral task differently depending on motor set (Nelson, 1984; 1988). Many of the presently studied rhythmic neurons were activated by stimulating their receptive fields when tested outside of the behavioral task. However, during task execution, these same neurons were suppressed by peripheral vibration. Therefore, the vibration-associated activity of these neurons may represent a context-dependent response to somatosensory signals as go-cues rather than merely replicating the peripheral input.

The activity of rhythmic neurons resembles a mirror image of the pattern previously reported for quickly adapting SI neurons recorded during the performance of this behavioral task (Nelson et al., 1991). Quickly adapting neurons generate a short duration burst of spikes after vibration onset. Then, their activity decreases and is reactivated again prior to movement onset. Nelson et al. (1991) suggested that quickly adapting neurons may be involved in gating of SI

sensory responsiveness at behaviorally significant times. The function of gating may be to enhance sensory inputs that are more important for the current behavioral task while suppressing other inputs (Chapin and Woodward, 1982; Chapman et al., 1988; Coquery, 1978; Dyhre-Poulsen, 1978; Nelson, 1988; Rushton et al., 1981). It is reasonable to assume that rhythmic and quickly adapting neurons participate in gating SI activity in reciprocal ways. Thus, these rhythmic neurons may correspond to the task phase element of the SI model that was previously proposed to account for patterns of activity of quickly adapting neurons which may involve suppressing peripheral and motor inputs to them (Fig. 14F; Nelson et al., 1991).

The origin of inputs that result in premovement activity changes remains unclear. The comparison of the onsets of premovement changes of activity with the EMG onset showed that most premovement changes occurred after the earliest EMG onset. The post-EMG changes may have been related to peripheral reafference that occurred during movements. A small proportion of the pre-EMG changes may have been of central origin (Lebedev et al., 1994; Nelson, 1987; Nelson et al., 1991; Soso and Fetz, 1980). Most premovement activity changes were of the same sign for both flexion and extension trials (i.e., they were nondirectional). Recent studies further the contention that peripheral reafferent signals are likely directional. Cohen et al. (1994) recorded the activity of monkey SI neurons during arm movements in different directions and found that this activity, probably of peripheral origin, varied with the direction of movements. Neurons with deep RFs exhibited larger variations of activity with movement direction than those with cutaneous RFs (also see Soso and Fetz, 1980). Many of the rhythmic SI neurons from our sample had deep RFs. Nevertheless, they usually exhibited nondirectional activity patterns. Therefore, the premovement changes in activity of rhythmic SI neurons probably are not just replicas of peripheral reafferent signals but rather reflect intracortical processing of peripheral information.

Comparison of our observations with recently published studies of Prud'Homme et al. (1994) indirectly suggests that rhythmic SI neurons may have a specific cortical laminar distribution. Prud'Homme et al. (1994) studied movement-related activity patterns of SI neurons

as a function of their location with respect to cortical layers. Neurons with increases in activity for all movement directions were located in middle and superficial layers. Cells with reciprocal activity patterns were found in layers 3 and 5. Neurons with only decreases in activity were observed in layer 5. Rhythmic SI cells considered in the present study usually were suppressed irrespective of movement direction. Thus, their movement-associated activity is similar to that reported for layer 5 cells.

Functional Significance of Rhythmicity

The functional significance of rhythmic firing of individual SI neurons remains unclear. It is possible that the activity of individual rhythmic neurons is related to some form of cortical population oscillations. The mean rhythmic frequency of the studied SI neurons was close to the frequency reported for LFP oscillations in sensorimotor cortex (Bouyer et al., 1981; 1987; Murthy and Fetz, 1992; Rougeul et al., 1979; Sanes and Donoqhue, 1993). Similar to LFP oscillations, rhythmic activity of single SI neurons was disrupted during movement executions. LFP oscillations occur in sensorimotor cortex in cat (Bouyer et al., 1981; 1987) and monkey (Rougeul et al., 1979) during focused attention and immobility but usually disappear during movements. Disruptions of LFP oscillations in monkey motor cortex also occur prior to movements performed during trained motor tasks (Sanes and Donoqhue, 1993). In addition, Murthy and Fetz (1992) observed that LFP oscillations in monkey motor and somatosensory cortices occurred during movements. These oscillations became larger with increasing task complexity. Thus, LFP oscillations may vary as a function of attentive behavior and task requirements (for review, see Gray, 1994).

Some characteristics of rhythmic activity of individual neurons, however, differ from those reported for LFP oscillations. LFP oscillations usually occur as occasional rhythmic bursts, 100 - 200 ms in duration and often with a variable frequency from one burst to another (Eckhorn et al., 1988; Gray and Singer, 1989; Murthy and Fetz, 1992; Sanes and Donoghue, 1993; Singer, 1993). The activity patterns of the studied rhythmic SI neurons were consistent from trial to trial and were

only briefly interrupted during vibratory stimulation and movements. Thus, while individual rhythmic SI neurons may maintain relatively independent activity, when population oscillations occur, these rhythmic neurons may contribute to them (possibly, as pacemakers; Llinas, 1990; Llinas et al., 1991).

Our data provide some support to predictions made regarding the functional role of oscillatory cortical elements. Ahissar and Vaadia (1990) proposed a model in which somatosensory cortical oscillators are key elements in neuronal circuits that analyze the temporal properties of somatosensory discharge sequences. In this model, the temporal characteristics of somatosensory signals are determined by comparing their frequency with the frequency of local oscillators (phased-locked loop algorithm; Horowitz and Hill, 1980). According to this model, cortical oscillatory neurons receive thalamic input via inhibitory interneurons. Therefore, these oscillators may be inhibited by somatosensory inputs. We observed that rhythmic SI neurons were suppressed during vibrotactile stimulation. Moreover, in some cases, neuronal activity was entrained to the frequency of peripheral vibration, as might be predicted by the model. The entrainment occurred while the average activity level decreased. It is possible that the entrainment observed was caused by IPSPs triggering rebound potentials rather than by EPSPs (Cowan and Wilson, 1994; Lytton and Sejnowski, 1991).

Origin of Rhythmic Activity

Several mechanisms have been suggested that may underlie the rhythmic activity of individual SI neurons. One possibility is that rhythmic cells are integrate-and-fire neurons, and their regular spike trains occur because of a stable synaptic input (Segundo et al., 1968). Cortical pyramidal neurons of the regular firing class discharge very rhythmically, provided they receive a steady excitatory input (McCormick et al., 1985; Softky and Koch, 1993). However, the integrate-and-fire model of rhythmic activity can explain neither the multimodal ISIs nor the interrupting spikes that were observed in a number of cases. Moreover, integrate-and-fire neurons follow the intensity of synaptic input by changing their firing frequency, whereas the firing

frequency of rhythmic SI neurons was modulated only slightly. Rhythmic activity was often disrupted or replaced by nonrhythmic firing rather than modulated. Similar transitions to nonrhythmic firing previously have been reported for SII neurons (Ahissar and Vaadia, 1990). Thus, the integrate-and-fire neuronal model provides an unlikely explanation for our data.

Another possible source of rhythmic firing is an extrinsic oscillatory drive. Such a driving source can explain both the occurrence of multimodal ISIs and the interrupting spikes. ISIs at multiples of the modal interval occur if neurons occasionally fail to respond to the driving input (Abeles, 1982). These interrupting spikes may be the responses to synaptic inputs that are uncorrelated with the rhythmic drive (synaptic noise; Surmeier and Towe, 1987a; 1987b). Rhythmic drive to cortical neurons previously has been proposed. Ghose and Freeman (1992) suggested that visual cortical neurons may be driven by rhythmic cells located in lateral geniculate nucleus. As well, intracortical excitatory connections may provide a source of rhythmic drive. Singer (1993), however, suggested that because single cortical neurons make a few synapses with their target cells (Abeles, 1991), a cell may be driven only if many other neurons having contacts with this cell are active in synchrony. Jagadeesh et al. (1992) demonstrated massive rhythmic inputs to visual cortical neurons using *in vivo* patch clamp recording techniques. An interesting possibility is that the source of rhythmic drive may be rhythmic inhibitory interneurons rather than excitatory cells (Cowan and Wilson, 1994; Llinas, 1990; Llinas et al., 1991).

We compared the discharge patterns of rhythmic neurons with those undoubtedly driven by peripheral vibration (unpublished observations). The responsiveness of SI neurons to vibrotactile stimulation previously was analyzed using ED and RD methods (Mountcastle et al., 1969; 1990). In addition, we performed joint interval analyses. For most rhythmic neurons (with the exception of those having interrupting spikes), ED and RD histograms were similar. However, ED and RD histograms for vibration-driven spike trains were dramatically different (Fig. 8E and F) (Mountcastle et al. 1969; 1990). Joint interval scattergrams for vibration-driven neurons usually

had diagonal bands that indicated the presence of interrupting spikes (Fig. 8F) (Surmeier and Towe, 1987a; 1987b). Interrupting spikes result in the differences between ED and RD histograms. During random shuffling of ISIs as in the construction of RD histograms, the sequence of near-modal intervals that is split by interrupting spikes is replaced by a situation in which adjacent ISIs rarely constitute near-modal intervals. In joint interval scattergrams for vibration-driven spike trains, the center ISI cluster located at approximately the vibratory period usually was in parallel to the diagonal band (i.e., the ISIs in this cluster were negatively serially correlated; Fig. 8F). Negative serial correlation of near-modal ISIs may occur when the responses to rhythmic driving fluctuate in time because of noise (Surmeier and Towe, 1987b). For rhythmic spike trains with negative serial correlations, peaks in the ED histograms are greater than those in the RD histograms (Perkel et al., 1967). We did not observe negative serial correlations of near-modal ISIs for the studied rhythmic SI neurons. However, negative correlation may not occur if the driving frequency fluctuates in time rather than being constant (as during vibratory stimulation). We suggest, therefore, that if rhythmic neurons are externally driven, that drive is of a different nature than peripherally driven activity.

It is possible that some portion of the studied rhythmic neurons were intrinsically oscillatory cells. Two types of cortical neurons have been demonstrated to intrinsically oscillate at 10-50 Hz within layer 4 in slice preparations of guinea pig frontal cortex (Llinas et al., 1991). Neurons of the first type, broad-frequency oscillators, increased their frequency at 10-45 Hz with membrane depolarization. Cells of the second type, narrow-frequency oscillators, whose frequency was 35-50 Hz, changed their frequency depending only slightly upon the level of depolarization. The basis for rhythmicity in both types of neurons is a voltage-gated persistent sodium current. The narrow-frequency oscillatory neurons were identified morphologically to be sparsely spinous interneurons having axon collaterals in layers 3 and 4 and are probably inhibitory cells. Pyramidal cortical neurons typically do not intrinsically generate fast (20-50 Hz) oscillations (Cowan and Wilson, 1994; Silva et al., 1991). Nuñez et al. (1992), however, reported fast

oscillations in a subset of pyramidal neurons recorded *in vivo* in urethane-anesthetized cats. Intrinsic oscillations of cortical neurons may be subthreshold (Llinas et al., 1991; Nuñez et al., 1992; Wang, 1993). Therefore, during these oscillations, ISIs at multiples of the rhythmic period may occur. It is unclear whether fast oscillations are reset by spikes, or whether they are of a nonresetting type. We observed that the firing frequency of rhythmic SI neurons was modulated only slightly. Therefore, if their activity was related to intrinsic oscillations (of these same neurons or of their drivers), then these oscillations would likely be of the narrow-frequency type.

Finally, it is possible that rhythmic activity of SI neurons occurs because of local circuit interactions. Neuronal circuits may be constructed of nonoscillatory elements which then oscillate due to the manner in which they are connected (Gray et al., 1991; Gray, 1994; Selverston, 1985; Singer, 1993). Thus, the classification of neurons as pacemakers and/or driven neurons may not be appropriate in this latter case, since the oscillatory mechanisms are in the networks themselves and not in the individual elements.

Conclusions

A subset of monkey SI neurons (~8.6%) exhibited rhythmic firing (~30 Hz) during trained behaviors. Spike trains of some of these neurons contained ISIs at multiples of modal intervals and/or interrupting spikes that split modal intervals. These spike train features, as well as the rarity with which the rhythmic frequency was modulated, suggest that rhythmic cells may receive extrinsic oscillatory inputs or may be intrinsically oscillatory but are unlikely to be integrate-and-fire neurons having stable inputs. Rhythmic activity usually was suppressed by vibrotactile go-cues and prior to movements. Observed activity patterns resembled a mirror image of those of quickly adapting SI neurons. Rhythmic and quickly adapting neurons may function to gate SI activity in reciprocal ways. The changes in rhythmic activity of individual cells were similar to those reported for LFP oscillations in sensorimotor cortex during motor behavior. Thus, rhythmic neurons may be related to cortical population oscillations.

Acknowledgments

We thank John M. Denton for technical assistance during the data collection and analysis, and D. L. Armbruster, D. J. Surmeier, and C. J. Wilson for detailed comments on versions of this manuscript.

This work was supported by United States Air Force Grant AFOSR 91-0333 to R. J. Nelson.

References

Abeles M (1982) Local Cortical Circuits; Studies of Brain Functions. Vol. 6. Springer, Berlin.

Abeles M, ed. (1991) Corticonics. Cambridge University Press, Cambridge.

Ahissar E, Vaadia E (1990) Oscillatory activity of single units in a somatosensory cortex of an awake monkey and their possible role in texture analysis. Proc Natl Acad Sci USA 87: 8935-8939.

Bouyer JJ, Montaron MF, Rougeul A (1981) Fast fronto-parietal rhythms during combined focused attentive behavior and immobility in cat: Cortical and thalamic localizations. Electroenceph Clin Neurophysiol 51: 244-252.

Bouyer JJ, Montaron MF, Vahnee JM, Albert MP, Rougeul A (1987) Anatomical localization of cortical beta rhythms in cat. Neuroscience 22: 863-869.

Chapin JK, Woodward DJ (1982) Somatic sensory transmission to the cortex during movement: gating of single cell responses to touch. Exp Neurol 78: 654-669.

Chapman CE, Jiang W, Lamarre Y (1988) Modulation of lemniscal input during conditioned arm movements in the monkey. Exp Brain Res 72: 316-334.

Cohen DAD, Prud'Homme MJL, Kalaska JF (1994) Tactile activity in primate primary somatosensory cortex during active arm movements: Correlation with receptive field properties. J. Neurophysiol. 71: 161-172.

Colburn TR, Evarts EV (1978) Long-loop adjustments during intended movements: Use of brushless DC torque motors in studies of neuromuscular function. In: Desmedt JE (ed) Progress in Clinical Neurophysiology, Vol 4. Karger, New York, pp 153-166.

Coquery J-M (1978) Role of active movements in control of afferent input from skin in cat and man. In: Gordon G, (ed) Active touch: The mechanisms of object manipulation: A multidisciplinary approach. Pergamon, Oxford, pp. 161-169.

Cowan RL, Wilson CJ (1994) Spontaneous firing patterns and axonal projections of single corticostriatal neurons in rat medial agranular cortex. J Neurophysiol 71: 17-31.

Dyhre-Poulsen P (1978) Perception of tactile stimuli before ballistic and during tracking movements. In: Gordon G (ed) Active Touch: The Mechanisms of Object Manipulation: A Multidisciplinary Approach. Pergamon, Oxford, pp. 171-176.

Eckhorn R, Bauer R, Jordan W, Brosch M, Kruse W, Munk M, Reitboeck HJ (1988) Coherent oscillations: A mechanism of feature linking in the visual cortex? Biol Cybern 60: 121-130.

Ellaway PH (1977) An application of cumulative sum technique (cusums) to neurophysiology. J Physiol (Lond) 265: 1-2P.

Engel AK, König P, Kreiter AK, Schillen TB, Singer W (1992) Temporal coding in the visual cortex: New vistas on integration in the nervous system. Trends in Neurosci 15: 218-226.

Evarts EV (1966) Methods for recording activity of individual neurons in moving animals. In: Rushmer RF (ed) Methods in Medical Research. Vol II. Yearbook, Chicago, pp 241-250.

Ghose GM, Freeman RD (1992) Oscillatory discharge in the visual system: Does it have a functional role? J Neurophysiol 68: 1558-1574.

Gray CM (1994) Synchronous oscillations in neuronal systems: Mechanisms and functions. J Comput Neurosci 1: 11-38.

Gray CM, Singer W (1989) Stimulus-specific neuronal oscillations in orientation columns of cat visual cortex. Proc Natl Acad Sci USA 86: 1698-1702.

Gray CM, Engel AK, König P, Singer W (1991) Mechanisms underlying the generation of neuronal oscillations in cat visual cortex. In: Basar E, Bullock TH (eds) Induced Rhythmicities in the Brain. Birkhauser, Boston, pp 29-45.

Horowitz P, Hill W (1980) The Art of Electronics. Cambridge Univ Press, Cambridge.

Jagadeesh B, Gray CM, Ferster D (1992) Visually evoked oscillations of membrane potential in cells of cat visual cortex. Science 257: 552-554

Jiang W, Chapman CE, Lamarre Y (1991) Modulation of the cutaneous responsiveness of neurons in the primary somatosensory cortex during conditioned arm movements in the monkey. Exp Brain Res 84: 342-354.

Lebedev MA, Nelson RJ (1993) Modulation of rhythmic firing of monkey primary somatosensory cortical (SI) and neostriatal (NS) neurons during active hand movements. (319.8). Society for Neuroscience Abstracts 19: 781.

Lebedev MA, Denton JM, Nelson RJ (1994) Vibration-entrained and premovement activity in monkey primary somatosensory cortex. J Neurophysiol 72:

Lemon R (1984) Methods for Neuronal Recording in Conscious Animals. IBRO Handbook Series: Methods in the Neurosciences. Vol 4. John Wiley & Sons, Chichester, UK.

Llinas RR (1990) Intrinsic electrical properties of nerve cells and their role in network oscillation. Cold Spring Harb Symp on Quant Biol 55: 933-938.

Llinas RR, Grace AA, Yarom Y (1991) In vitro neurons in mammalian cortical layer 4 exhibit intrinsic oscillatory activity in the 10- to 50-Hz frequency range. Proc Natl Acad Sci USA 88: 897-901.

Lopes da Silva F (1991) Neural mechanisms underlying brain waves: From neural membranes to networks. Electroenceph clin Neurophysiol 79: 81-93.

Lytton WW, Sejnowski TJ (1991) Simulations of cortical pyramidal neurons synchronized by inhibitory interneurons. J Neurophysiol 66: 1059-1079

McCormick DA, Connors BW, Lighthall JW, Prince DA (1985) Comparative electrophysiology of pyramidal and sparsely spiny stellate neurons of the neocortex. J Neurophysiol 54: 782-806.

Mountcastle VB, Talbot WH, Sakata H, Hyvärinen J (1969) Cortical neuronal mechanisms in flutter-vibration studies in unanesthetized monkeys: Neuronal periodicity and frequency discrimination. J Neurophysiol 32: 452-484.

Mountcastle VB, Steinmetz, MA, Romo R (1990) Frequency discrimination in the sense of flutter: Psychophysical measurements correlated with postcentral events in behaving monkeys. J Neurosci 10: 3032-3044.

Murthy VN, Fetz EE (1992) Coherent 25- to 35-Hz oscillations in the sensorimotor cortex of awake behaving monkeys. Proc Natl Acad Sci USA 89: 5670-5674.

Nelson RJ (1984) Responsiveness of monkey primary somatosensory neurons to peripheral stimulation depends on "motor-set". Brain Res 304: 143-148.

Nelson RJ (1987) Activity of monkey primary somatosensory cortical neurons changes prior to active movement. Brain Res 406: 402-407.

Nelson RJ (1988) Set related and premovement related activity of primate somatosensory cortical neurons depends upon stimulus modality and subsequent movement. Brain Res Bull 21:411-424.

Nelson RJ, Smith BN, Douglas VD (1991) Relationship between sensory responsiveness and premovement activity of quickly adapting neurons in areas 3b and 1 of monkey primary somatosensory cortex. Exp Brain Res 84: 75-90.

Nuñez A, Amzica F, Steriade M (1992) Voltage-dependent fast (20-40 Hz) oscillations in long-axoned neocortical neurons. Neuroscience 51: 7-10.

Perkel DH, Gerstein G, Moore G (1967) Neuronal spike trains and stochastic point processes. I. The single spike train. Biophys J 7: 391-418.

Poggio T, Viernstein L (1964) Time series analysis of impulse sequences of thalamic somatic sensory neurons. J Neurophysiol 27: 517-545.

Prud'Homme MJL, Cohen DAD, Kalaska JF (1994) Tactile activity in primate primary somatosensory cortex during active arm movements: Cytoarchitectonic distribution. J Neurophysiol 71: 173-181.

Rodieck RW, Kiang NY-S, Gerstein GL (1962) Some quantitative methods for the study of spontaneous activity of single neurons. Biophys. J. 2: 351-368.

Rougeul A, Bouer JJ, Dedet L, Debray O (1979) Fast somato-parietal rhythms during combined focal attention in baboon and squirrel monkey. Electroenceph Clin Neurophysiol 46: 310-319.

Rushton DN, Rothwell JC, Graggs MD (1981) Gating of somatosensory evoked potentials during different kinds of movement in man. Brain 104: 465-491.

Sanes JN, Donoghue JP (1993) Oscillations in local field potentials of the primate motor cortex during voluntary movements. Proc Natl Acad Sci USA 90: 4470-4474.

Segundo JP, Perkel DH, Wyman H, Hegstad H, Moore GP (1968) Input-output relations in computer-simulated nerve cells. Influence of the statistical properties, strength, number and inter-dependence of excitatory pre-synaptic terminals. Kibernetic 4: 157-171.

Selverston AI (1985) Oscillatory neural networks. Ann Rev Physiol 47: 29-48.

Sheer DE (1989) Sensory and cognitive 40-Hz event-related potentials: Behavioral correlates, brain function, and clinical applications. In: Basar E, Bullock TH (eds) Springer Series in Brain Dynamics 2. Springer-Verlag, Berlin, Heidelberg, pp. 339-374.

Siebler M, Köller H, Rose G, Müller HW (1991) An improved graphical method for pattern recognition from spike trains of spontaneously active neurons. Exp Brain Res 90: 141-146.

Silva LR, Amitai Y, Connors BW (1991) Intrinsic oscillations of neocortex generated by layer 5 pyramidal neurons. Science 251: 432-435.

Singer W (1993) Synchronization of cortical activity and its putative role in information processing and learning. Annu Rev Physiol 55: 349-374.

Softky WR, Koch C (1993) The highly irregular firing of cortical cells is inconsistent with temporal integration of random EPSPs. J Neurosci 13: 334-350.

Soso MJ, Fetz EE (1980) Responses of identified cells in postcentral cortex of awake monkeys during comparable active and passive joint movements. J Neurophysiol 43: 1090-1110.

Surmeier DJ, Towe AL (1987a) Properties of proprioceptive neurons in the cuneate nucleus of the cat. J Neurophysiol 57: 938-961.

Surmeier DJ, Towe AL (1987b) Intrinsic features contributing to spike train patterning in proprioceptive cuneate neurons. J Neurophysiol 57: 962-976.

Vaadia E, Kurata K, Wise, SP (1988) Neuronal activity preceding directional and nondirectional cues in the premotor cortex of rhesus monkeys. Somatosensory and Motor Research 6: 207-230.

Wang X-J (1993) Ionic basis for intrinsic neuronal oscillations. NeuroReport 5: 221-224.

Zadeh LA (1957) Signal-flow graphs and random signals. Proc IRE 45:1413-1414.

Figure Legends

Figure 1. Schematics of manipulandum, feedback display, and task. A: Apparatus for studying wrist movements. Monkey's hand was placed on a moveable plate. The plate was attached to the axle of the torque motor. A load of 0.07 Nm was applied to the plate that assisted extensions and opposed flexions. B: Visual display of wrist position that consisted of light-emitting diodes (LEDs). The center LED was red; the LEDs above and below it were yellow. Each LED indicated an angular deviation of 1°. A red instruction LED was located in the upper left corner of the visual display. C: Experimental paradigm. To begin a trial, the monkey centered the plate. The instruction LED was illuminated if extension was the appropriate movement. After a delay of 0.5, 1.0, 1.5, or 2.0 s (pseudorandomized), the plate was vibrated by passing a sinusoidal current (27, 57, or 127 Hz) through the torque motor. Vibration remained on until the monkey made a movement of at least 5°. Then the vibration was turned off, and the monkey received a fruit juice reward if the movement was in the required direction.

Figure 2. Cortical locations of rhythmic neurons. A: A drawing of a dorsolateral view of the brain. Central sulcus (CS) and intraparietal sulcus (IPS) are indicated. B: A table showing the number of rhythmic neurons by receptive field (RF) type recorded in each SI region (areas 3a, 3b, 1, and 2). C: Location of recording sites for six monkeys. The illustration for each monkey consists of 4 panels. The top panel presents a surface map of electrode penetrations with respect to CS and IPS. The penetrations where rhythmic neurons were recorded are indicated by larger marks. The lower panels illustrate three sagittal sections through the cortex (lateral, intermediate, and medial). Locations of the neurons are shown as projections to the nearest of the three sections. RF types are marked according to the convention of panel B.

Figure 3. An example of expectation density histogram for a rhythmic spike train. The spike train was computer-simulated for a normal distribution of the interspike intervals with a coefficient of variation of 0.15. Peaks at multiples of the rhythmic interval are present. The height of

subsequent peaks gradually decreases, such that the stabilized level approximates the mean discharge rate. T is rhythmic interval, R is mean discharge rate, E_1, E_2, and E_3 are the heights of the initial three peaks.

Figure 4. Analyses of rhythmic activity (~39 Hz; same records as in Fig. 5). Spike trains for the hold period (500 ms epoch preceding vibration onset) were analyzed. A: Interspike interval (ISI) scattergram that shows ISIs for 40 consecutive trials. Each column corresponds to an individual trial. B: Joint interval scattergram showing the relationship between immediately adjacent ISIs. C: ISI distribution. D: Expectation density histogram. E: Renewal density histogram. In panels C - E, bin width is 1 ms.

Figure 5. Example of changes in neuronal activity associated with go-cue presentation and movement. Records in the left parts of panels A-E are centered on vibration onset, whereas those in the right parts are centered on movement onset. The activity pattern of a rhythmic (~39 Hz) area 1 neuron exhibited during flexion trials (40 trials) is illustrated. A: Raster displays of interspike intervals (ISIs). For each spike, these displays show the time of its occurrence on the x-axis and plot the next ISI on the y-axis. A very regular ISI pattern can be seen, modulated after vibration onset and disrupted prior to movement onset. B: Histograms of discharge activity (bin width = 5 ms). C: Raster displays of discharges. Each horizontal line corresponds to one trial, and each dot represents the time of a spike's occurrence. Bold marks indicate movement onsets (on the left) and vibration onsets (on the right). The trials were rearranged in the order of increasing reaction time from top to bottom. D: Plots of the average cumulative sum (CUSUM). The CUSUM was interpolated by linear curves for the epochs of stationary activity. The time of statistically significant deviations of the CUSUM trace from the interpolation curve are shown. The firing level (i.e., CUSUM slope) decreased at 25.7 ms after vibration onset (vibratory frequency was 57 Hz) and at 45.2 prior to movement onset. E: Average wrist position traces. F: A schematic illustration of the neuron's receptive field (RF). This neuron had a noncutaneous RF deeply located in the hand. G: Cortical location of the neuron.

Figure 6. Histogram of the distribution of the firing frequency for the total sample of rhythmic SI neurons.

Figure 7. Examples of unusual characteristics of rhythmic spike trains. A-D: Records for a rhythmic (~43 Hz) area 1 neuron with a multimodal ISI distribution. A: Activity during task execution (conventions as in Fig. 5). Suppression of activity occurred at 19.9 ms after vibration onset (vibratory frequency was 57 Hz) and at 63.7 ms prior to movement onset. B: Analyses of rhythmic activity during the hold period (conventions as in Fig. 4). ISIs at multiples of the modal interval are present. C: Receptive field (RF) schematic. This neuron had a cutaneous RF located on the second digit. D: Cortical location of the neuron. E-H: Records for a rhythmic (~30 Hz) area 3b neuron with interrupting spikes. E: Activity during task execution (conventions as in Fig. 5). Suppression occurred at 21.5 ms after vibration onset (vibratory frequency was 57 Hz) and at 39.5 ms prior to movement onset. F: Analyses of rhythmic activity during the hold period (conventions as in Fig. 4). ISIs that are shorter than the modal interval are present. These ISIs form a diagonal band in the joint interval plot. G: No clear RF was detected for this neuron. H: Cortical location of the neuron.

Figure 8. An example of a neuron with activity entrained to vibration at 27 Hz. After vibration onset, monkey was required to maintain centered wrist position for 1 s. A: Neuronal activity during task execution (conventions as in Fig.5, left panels). Periodic peaks are present in the discharge histogram corresponding to the epoch of vibrotactile stimulation. B: Phase raster. A phase band is present that indicates entrainment. C: Receptive field (RF) schematic. This neuron was activated by passive wrist extension. D: The neuron's cortical location. This was an area 3a neuron. E: Analyses of activity during the hold period (conventions as in Fig. 4). The neuron exhibited a nonrhythmic pattern of activity. F: Analyses of activity during vibratory stimulation (conventions as in Fig. 4). Expectation and renewal density histograms are dramatically different. A diagonal band is present in joint interval scattergram. The center cluster of the interspike intervals at about the vibratory period is oriented in parallel with the diagonal band. G: Cycle

distribution histogram for the epoch of vibratory stimulation.

Figure 9. Analyses of the changes in activity after presentation of the vibratory go-cues. A: A typical example of vibration-related changes in activity (conventions as in Fig. 5). The discharge of this rhythmic (~30 Hz) area 1 neuron was phasically suppressed at 27.7 ms after vibration onset. The frequency of vibration was 57 Hz. The vibratory related suppression consisted of the transient and sustained changes in activity. An additional suppression occurred at 60.3 ms prior to movement onset. B: A schematic illustration of the neuron's receptive field (RF). This neuron was activated by passive extension of the fourth digit at the metacarpophalangeal joint. C: The neuron's cortical location. D: Analyses of the rhythmic activity during the hold period (conventions as in Fig. 4). E: A schematic illustration of the typical pattern of activity modulation by vibration. F. Frequency distribution histogram of the latency of response to 57 Hz vibratory stimulation (the most extensively studied vibratory frequency). The average latency was ~25 ms. Cases of vibration-induced suppression were more frequent than the cases of activation.

Figure 10. An example of entrainment of neuronal activity to the frequency of the vibratory stimulus. A: Records for an area 3a neuron (conventions as in Fig. 5). Rhythmic activity (~30 Hz) was transiently suppressed at 26.8 ms after vibration onset. The frequency of vibration was 27 Hz. For the epoch of sustained suppression (100-400 ms following vibration onset), periodic peaks can be seen in the stimulus-centered histogram of discharges. The neuron's firing was suppressed at 60.4 ms prior to movement onset. B: Phase raster (conventions as in Fig. 8B). A band at the phase of preferential response is present. C: Receptive field schematic. The neuron was activated by passive wrist extension. D: The neuron's cortical location. E: Analyses of rhythmic activity during the hold period (conventions as in Fig. 4). The neuron's firing frequency was 30 Hz. F: Analyses of activity for the epoch of sustained vibratory response (100-400 ms after vibration onset; conventions as in Fig. 4; expectation and renewal density histograms were not calculated). Interspike intervals at the vibratory period and at twice that period can be seen. G: Distribution of discharges over the vibratory cycle.

Figure 11. An example of a premovement activity (PMA) pattern. A: Records for a rhythmic (~44 Hz) area 2 neuron (conventions as in Fig. 5). The activity of this neuron did not change after vibration onset (vibratory frequency was 57 Hz). Suppression of activity occurred at 39.4 ms prior to voluntary extensions (a similar suppression occurred for flexion trials; not shown). B: No clear receptive field was found for this neuron. C: The neuron's cortical location. D: Analyses of rhythmic activity during the hold period (conventions as in Fig. 4). E: A schematic illustration of the typical PMA pattern, i.e., suppression. F: The frequency distribution histogram of PMA onsets with respect to movement onset. Instances of premovement suppression were more frequent than instances of activation. The earliest and average EMG onset are indicated (100 ms and 60 ms prior to movement onset, respectively). Most PMA changes (~80%) occurred after the earliest EMG onset.

Figure 12. Transition of neuronal activity from a rhythmic to a nonrhythmic pattern during activation. A: Records for a rhythmic (~28 Hz) area 1 neuron (conventions as in Fig. 3). Rhythmic activity was suppressed at 26.6 ms after vibration onset (vibratory frequency was 57 Hz) and, additionally, at 33.6 ms prior to extension movement onset. Moreover, a pronounced activation occurred at 44.5 ms after movement onset. B: Receptive field schematic. This neuron was activated by passive extension of the second digit at the metacarpophalangeal joint. C: The neuron's cortical location. D: Analyses of rhythmic activity during the hold period (conventions as in Fig. 4). Interspike interval (ISI) distribution is bell-shaped. F: Analyses of activity for the epoch of activation (50-150 ms with respect to movement onset; conventions as in Fig. 4; expectation and renewal density histograms were not calculated). ISI distribution histogram is Poisson-like.

Figure 13. Comparison of the activity patterns during flexion and extension trials. A rhythmic (~38 Hz) area 3a neuron (receptive field was not tested) was suppressed prior to both flexions and extensions. A: Records for flexion trials (conventions as in Fig. 5). Activity suppression occurred

at 34.3 ms after vibration onset (vibratory frequency was 57 Hz) and at 72.1 ms prior to movement onset. B: Analyses of rhythmic activity for the hold period during flexion trials (conventions as in Fig. 4). C: Schematic illustration of the neuron's cortical location. D: Records for extension trials. Suppression occurred at 32.6 ms after vibration onset, followed by an additional suppression at 69.8 ms prior to movement onset. E: Analyses of rhythmic activity for the hold period during extension trials (conventions as in Fig. 4).

Figure 14. Illustration of the activity of a quickly adapting neuron during execution of the behavioral task. A: Records are for an area 1 neuron (conventions as in Fig. 5). Vibratory frequency was 57 Hz. The neuron discharged with a burst of spikes at 29.6 ms after vibration onset. Then, its activity decreased and was reactivated at 83.6 ms prior to movement onset. B: Phase raster (conventions as in Fig. 8B). It can be seen that the premovement activity was vibration-entrained. C: Receptive field (RF) schematic. The neuron had a cutaneous RF near the base of the third digit. D: Cortical location of the neuron. E: Schematic illustration of the typical activity pattern of quickly adapting neurons. F: A model describing the activity of quickly adapting neurons in this task (Nelson et al., 1991). The model includes a sustained sensory signal associated with vibration, a motor signal associated with initiation of movement, and a task phase component which changes state at behaviorally significant times. G: Cycle distribution for the epoch of movement-associated activity (-80 to 120 ms with respect to movement onset).

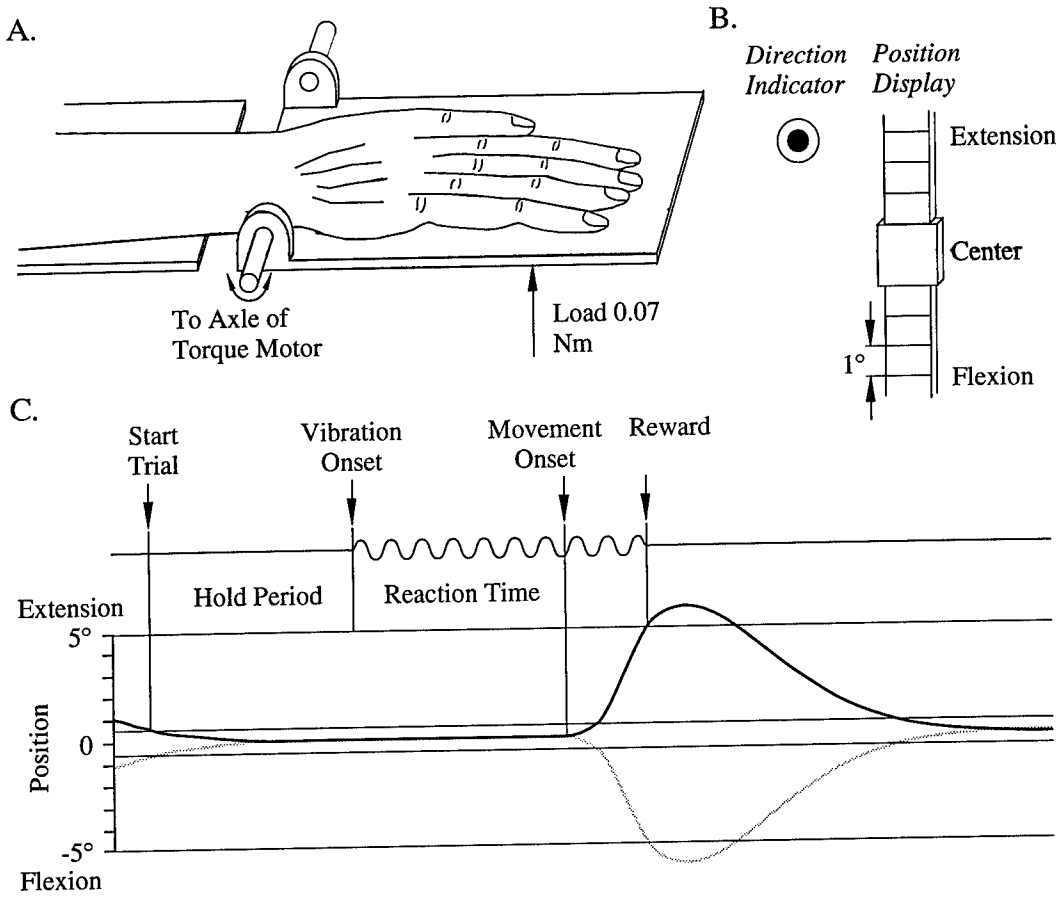
A.
To Axle of
Torque Motor
Load 0.07
Nm
B.
Direction
Indicator
Position
Display
Extension
Center
1°
Flexion
C.
Start
Trial
Vibration
Onset
Movement
Onset
Reward
Hold Period
Reaction Time
Extension
5°
Position
0
-5°
Flexion

Figure 1

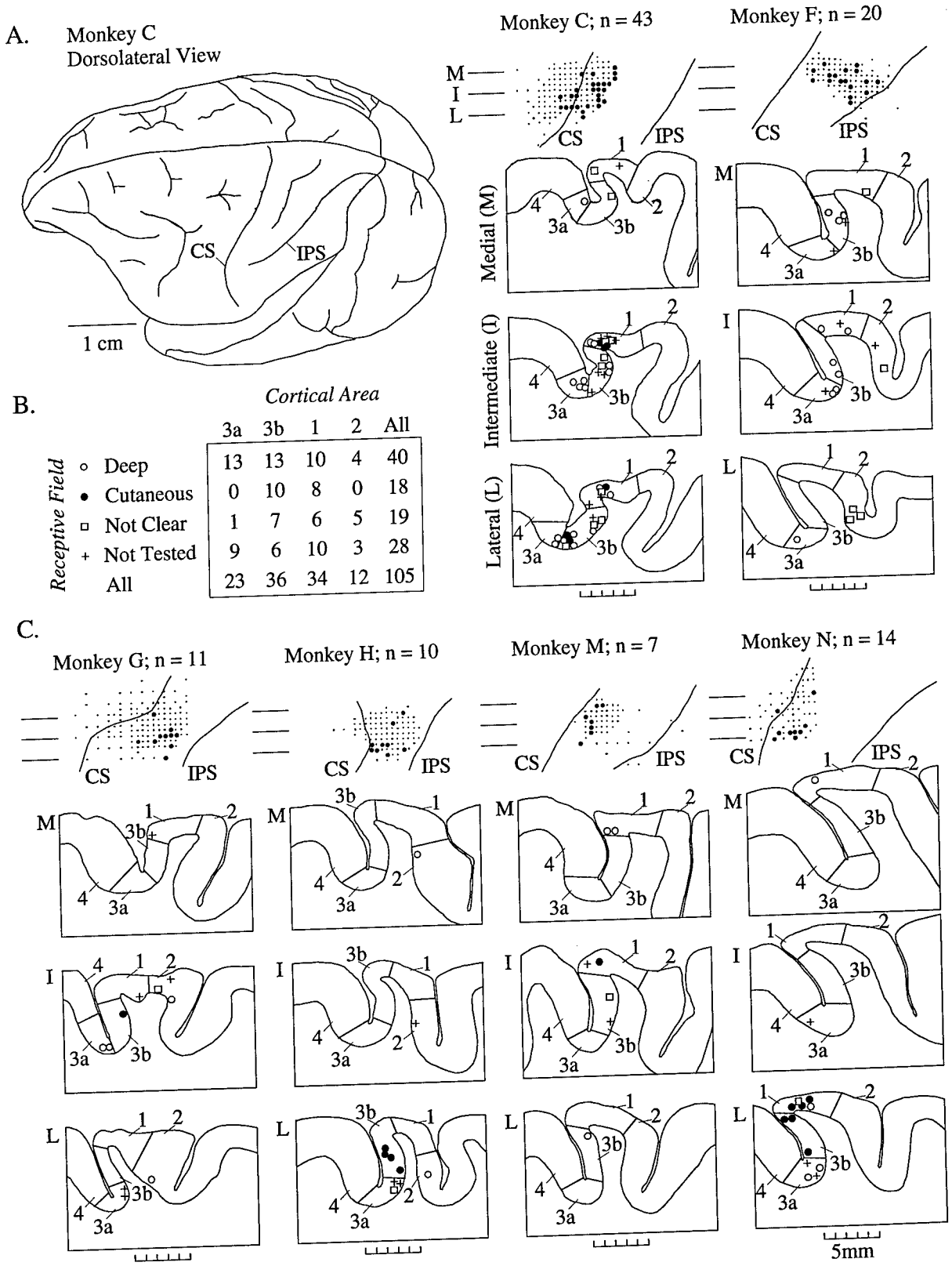

	3a	3b	1	2	All
Deep	13	13	10	4	40
Cutaneous	0	10	8	0	18
Not Clear	1	7	6	5	19
Not Tested	9	6	10	3	28
All	23	36	34	12	105

Figure 2

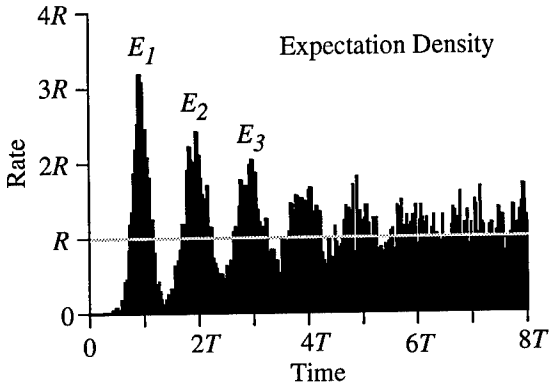

Figure 3

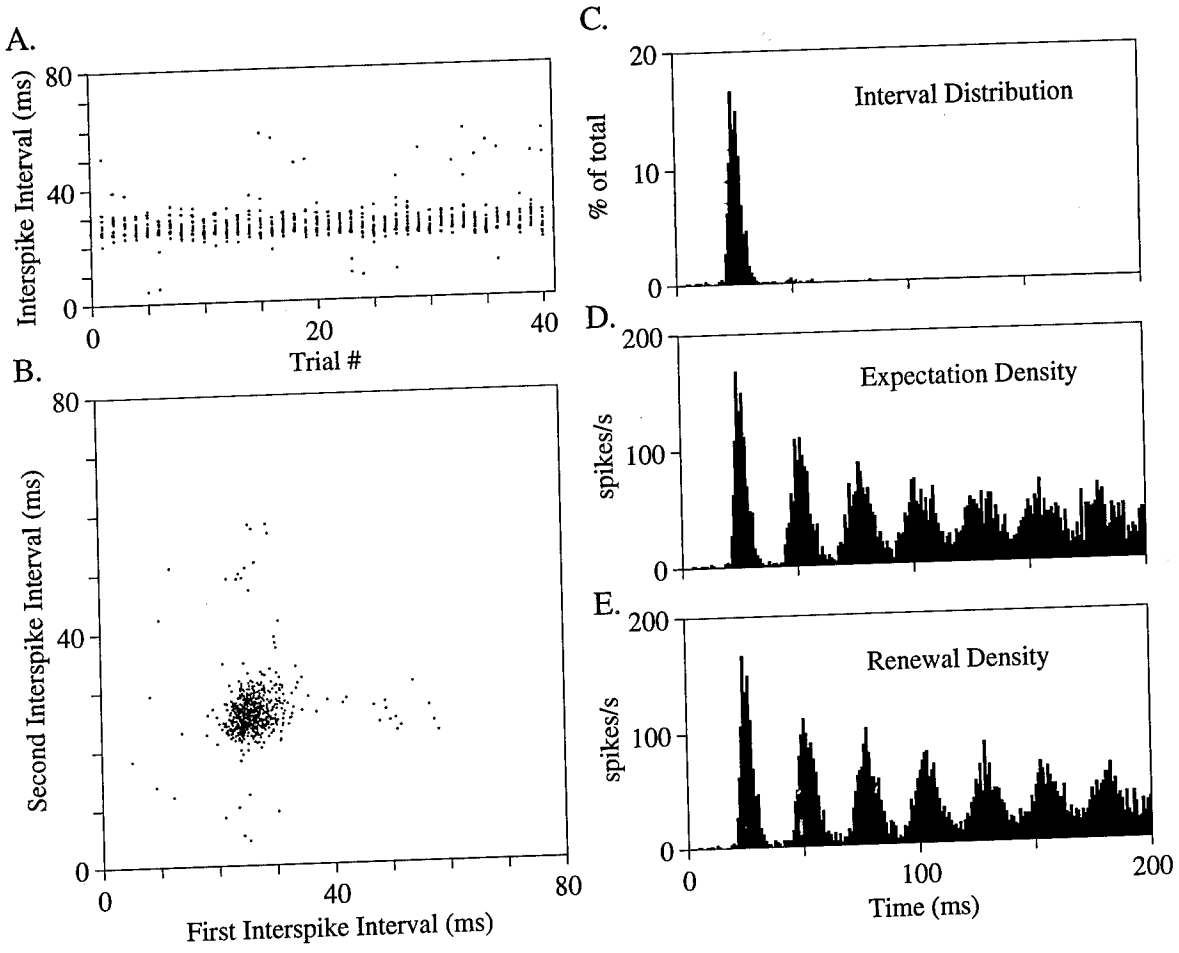
A.
Interspike Interval (ms)
80
40
0
0
20
40
Trial #
B.
Second Interspike Interval (ms)
80
40
0
0
40
80
First Interspike Interval (ms)
C.
20
10
0
% of total
Interval Distribution
D.
200
100
0
spikes/s
Expectation Density
E.
200
100
0
spikes/s
Renewal Density
0
100
200
Time (ms)

Figure 4

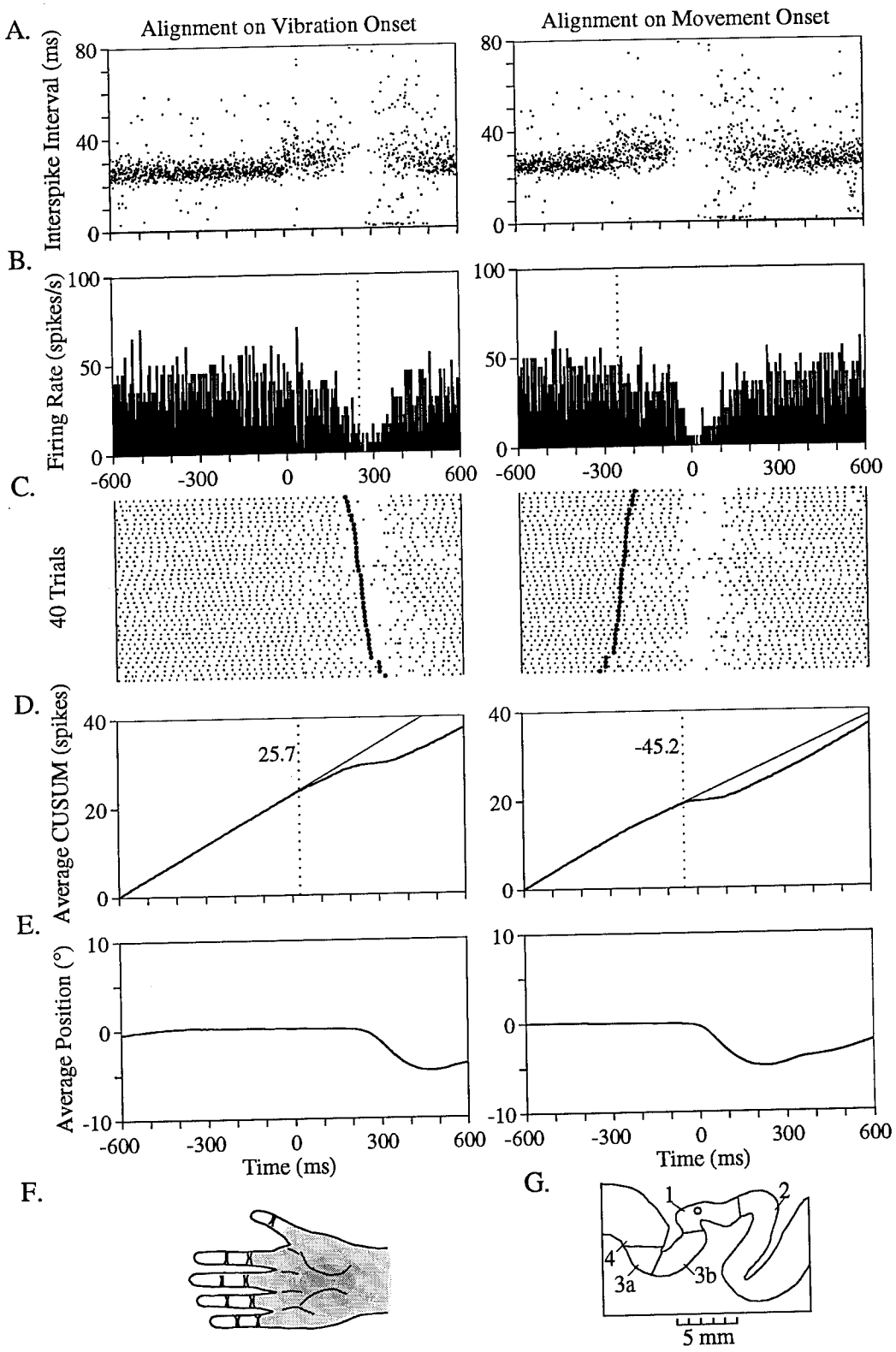
A.
Alignment on Vibration Onset
Alignment on Movement Onset
Interspike Interval (ms)
80
40
0
B.
Firing Rate (spikes/s)
100
50
0
-600
-300
0
300
600
C.
40 Trials
D.
Average CUSUM (spikes)
40
20
0
25.7
-45.2
E.
Average Position (°)
10
0
-10
Time (ms)
F.
G.
1
2
3a
3b
4
5 mm

Figure 5

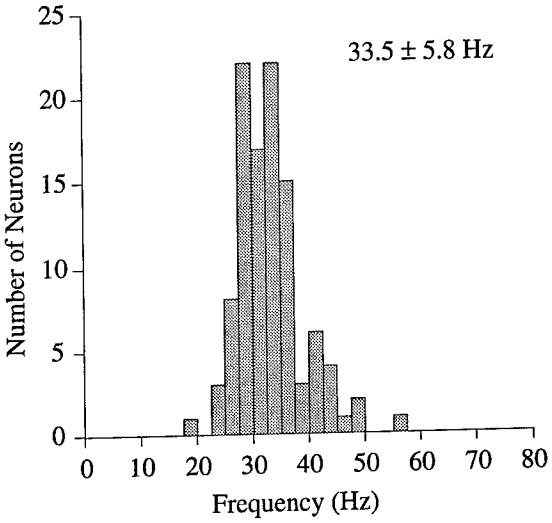
25
20
15
10
5
0
Number of Neurons
33.5 ± 5.8 Hz
0
10
20
30
40
50
60
70
80
Frequency (Hz)

Figure 6

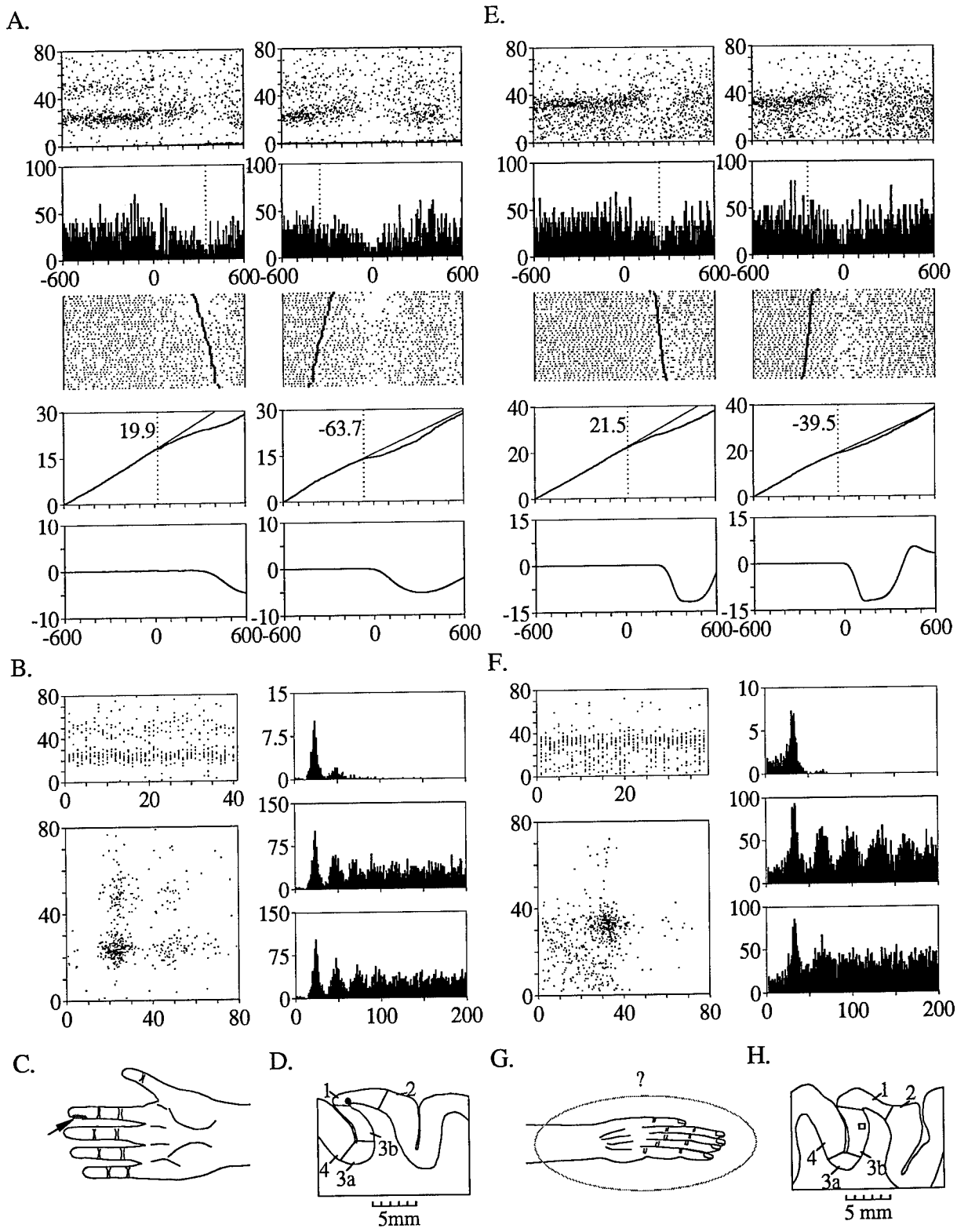

Figure 7

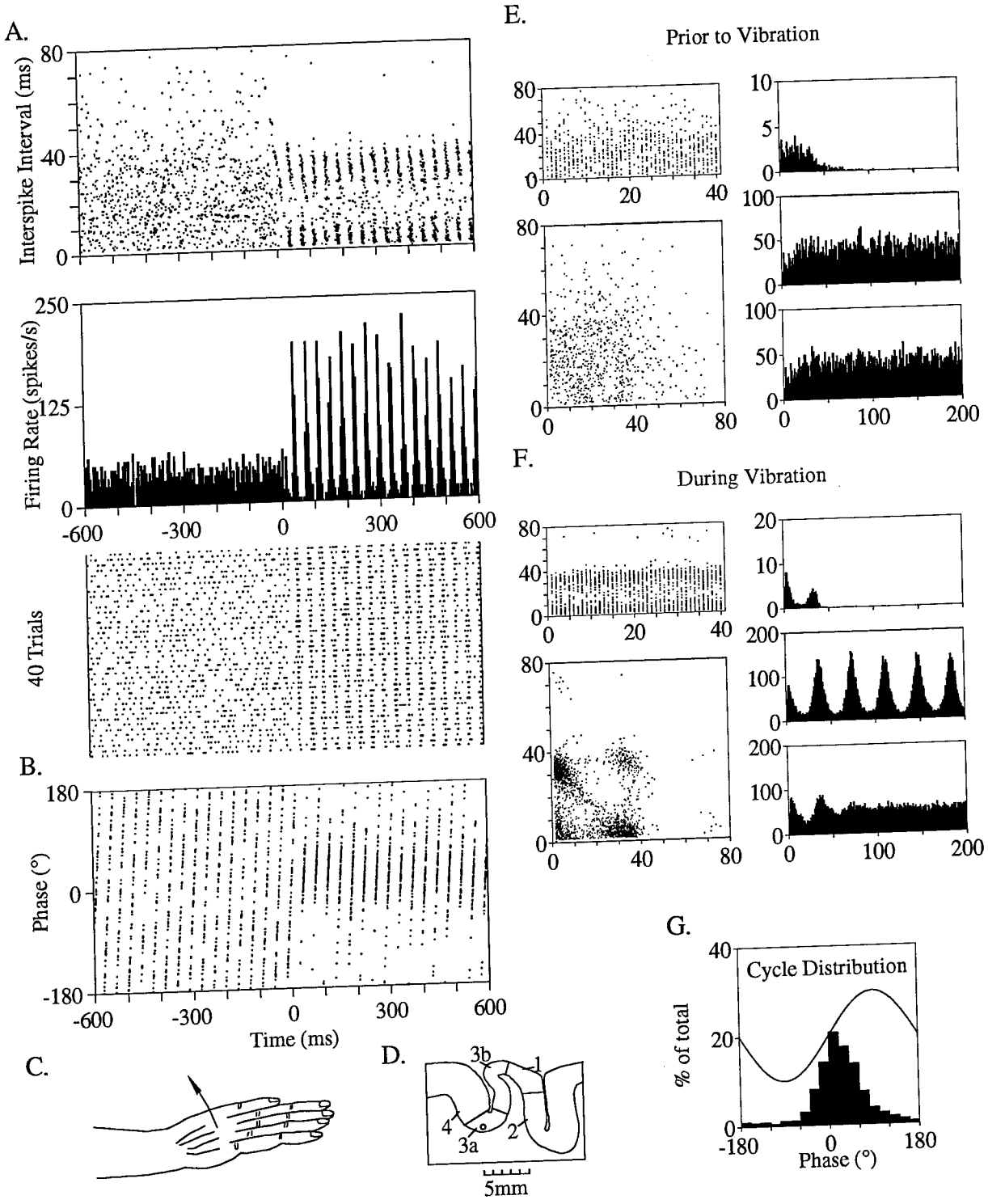
A.
Interspike Interval (ms)
80
40
0
Firing Rate (spikes/s)
250
125
0
-600
-300
0
300
600
40 Trials
B.
Phase (°)
180
0
-180
-600
-300
0
300
600
Time (ms)
C.
D.
3b
1
4
2
3a
5mm
E.
Prior to Vibration
80
40
0
0
20
40
10
5
0
100
50
0
100
50
0
0
100
200
80
40
0
0
40
80
F.
During Vibration
80
40
0
0
20
40
20
10
0
200
100
0
200
100
0
0
100
200
80
40
0
0
40
80
G.
Cycle Distribution
% of total
40
20
0
-180
0
180
Phase (°)

Figure 8

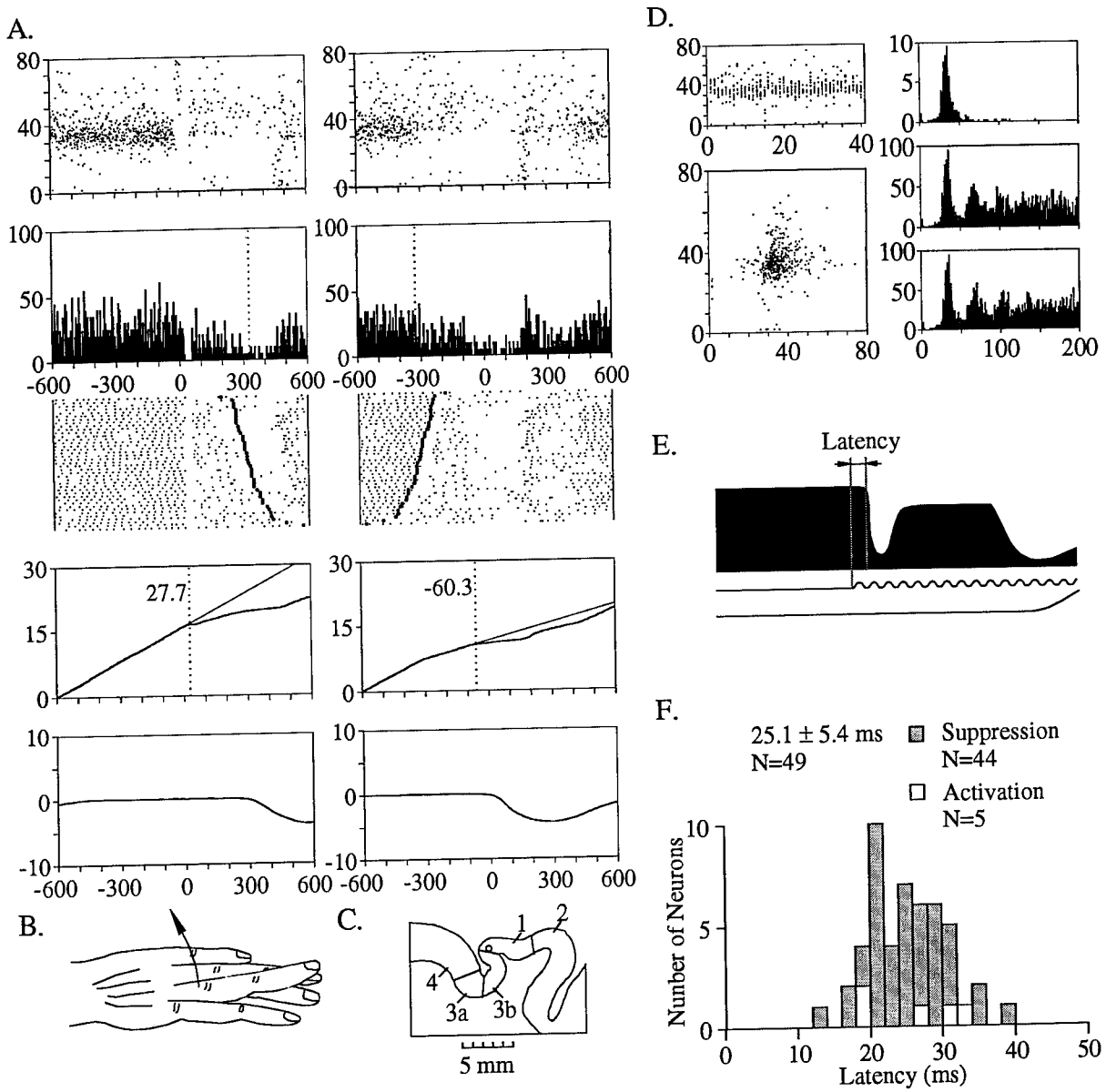
A.
80
40
0
100
50
0
-600 -300 0 300 600
30
15
0
27.7
-60.3
10
0
-10
B.
C.
1
2
4
3a
3b
5 mm
D.
0 20 40
0 40 80
10
5
100
50
0 100 200
E.
Latency
F.
25.1 ± 5.4 ms
N=49
Suppression
N=44
Activation
N=5
Number of Neurons
0 10 20 30 40 50
Latency (ms)

Figure 9

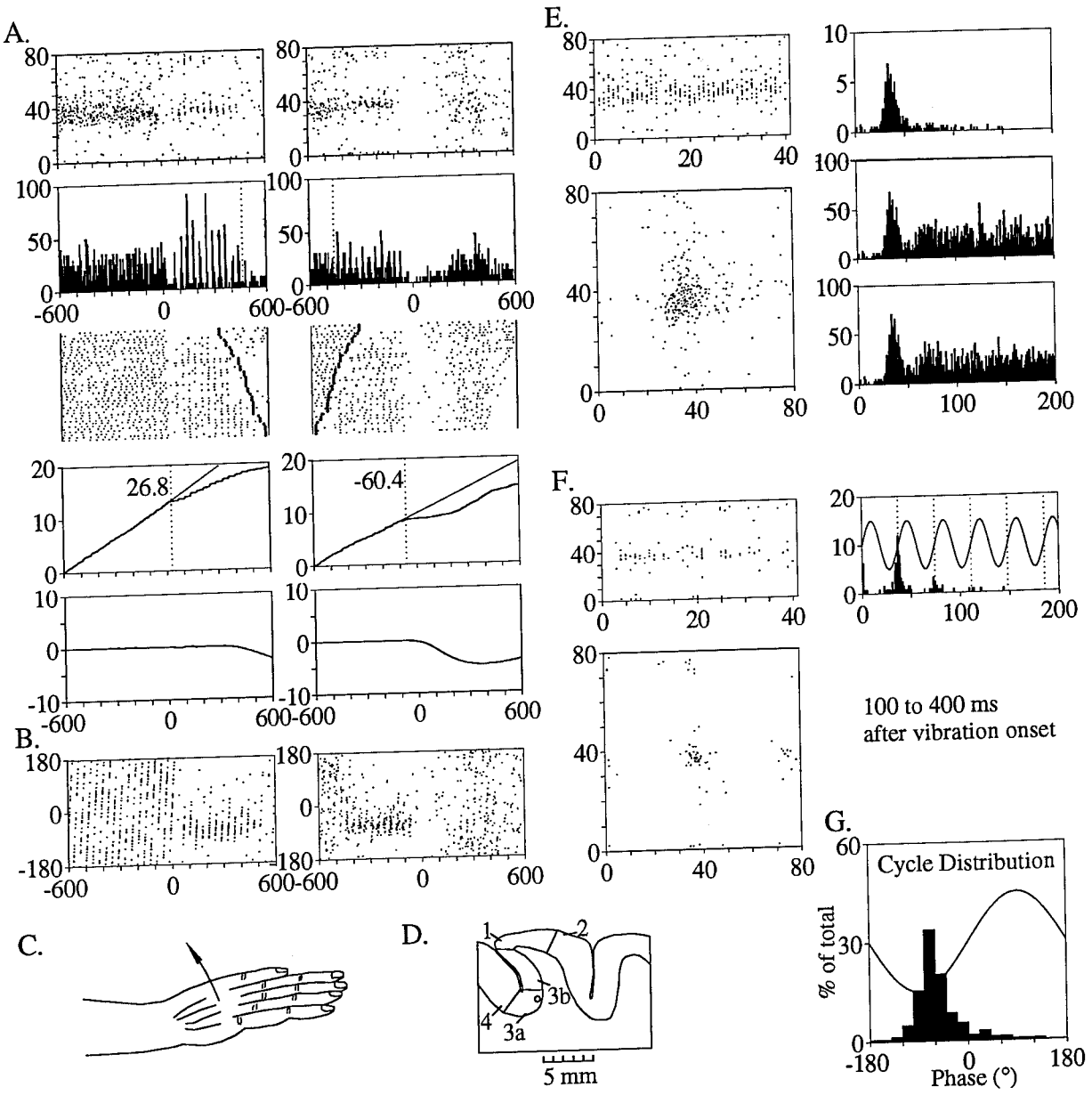
A.
B.
C.
D.
E.
F.
G.
26.8
-60.4
100 to 400 ms
after vibration onset
Cycle Distribution
% of total
Phase (°)
5 mm
1
2
3b
4
3a

Figure 10

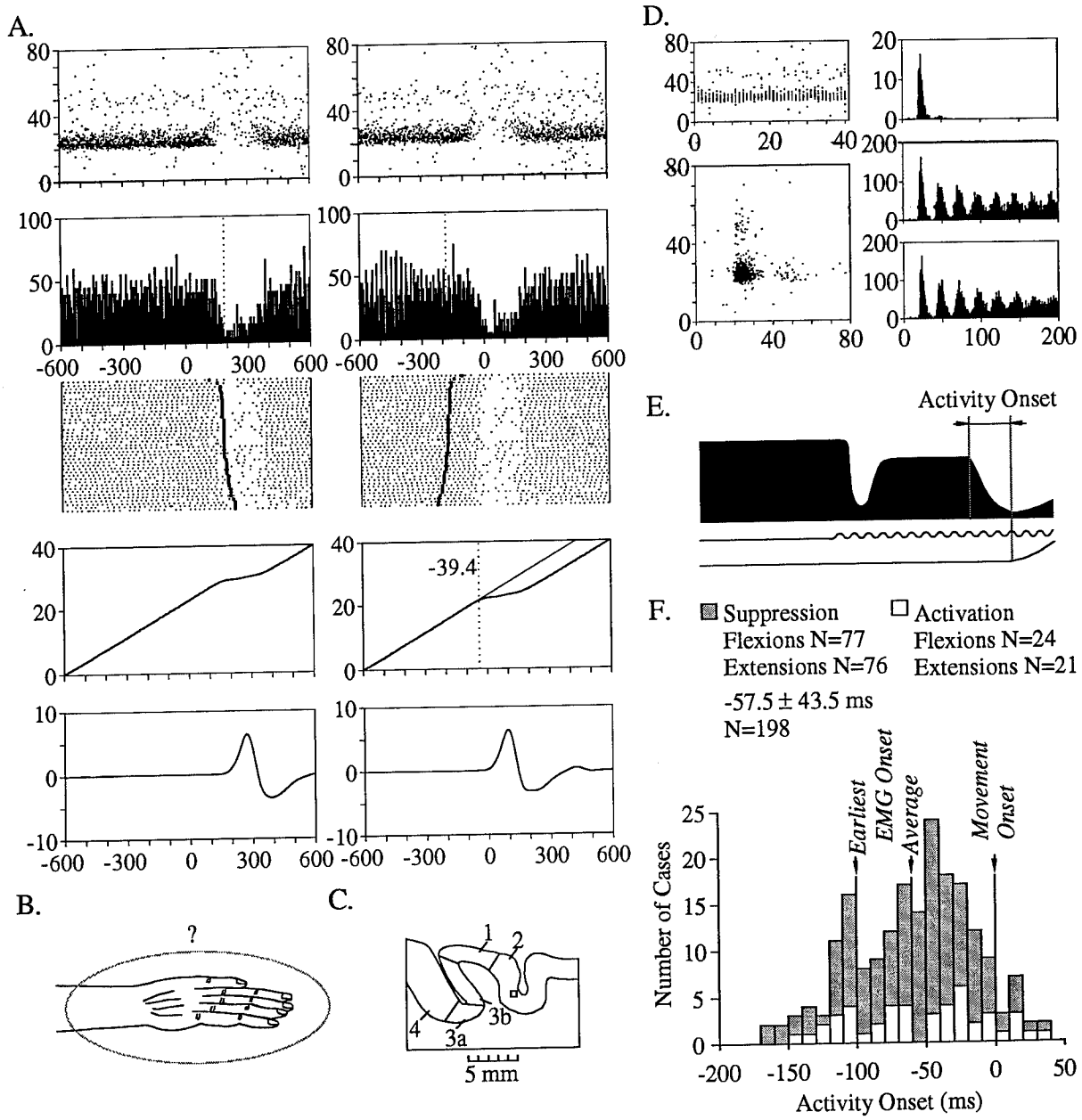
A.
80
40
0
100
50
0
-600 -300 0 300 600
40
20
0
-39.4
10
0
-10
B.
?
C.
1
2
3b
4
3a
5 mm
D.
0 20 40
0 40 80
20
10
200
100
0 100 200
E.
Activity Onset
F.
Suppression
Flexions N=77
Extensions N=76
Activation
Flexions N=24
Extensions N=21
-57.5 ± 43.5 ms
N=198
Earliest EMG Onset
Average
Movement Onset
Number of Cases
25
20
15
10
5
0
-200 -150 -100 -50 0 50
Activity Onset (ms)

Figure 11

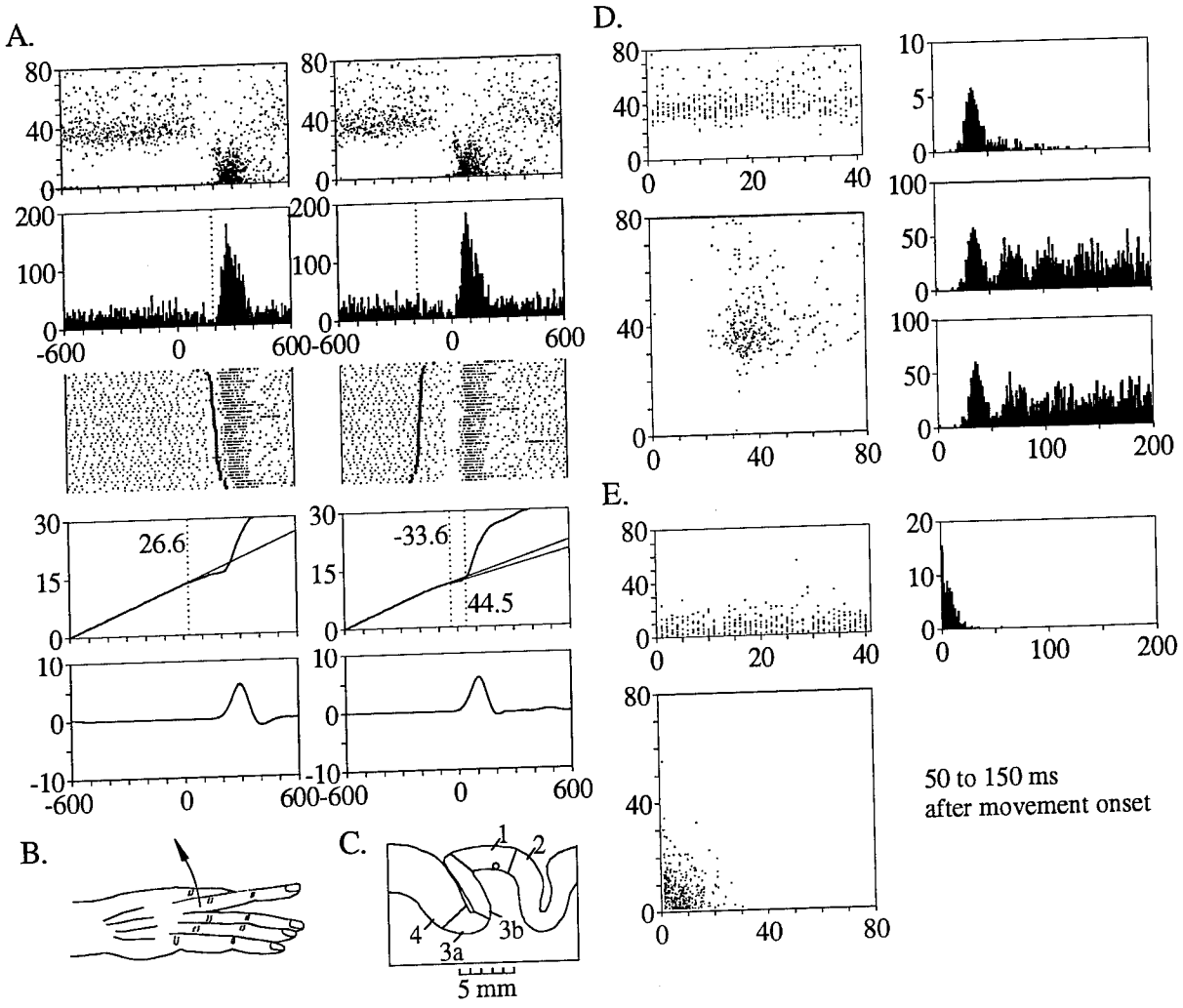
A.
80
40
0
200
100
0
-600
0
600
30
15
26.6
-33.6
44.5
10
-10
B.
C.
1
2
3b
4
3a
5 mm
D.
20
40
10
5
50
100
200
E.
50 to 150 ms
after movement onset

Figure 12

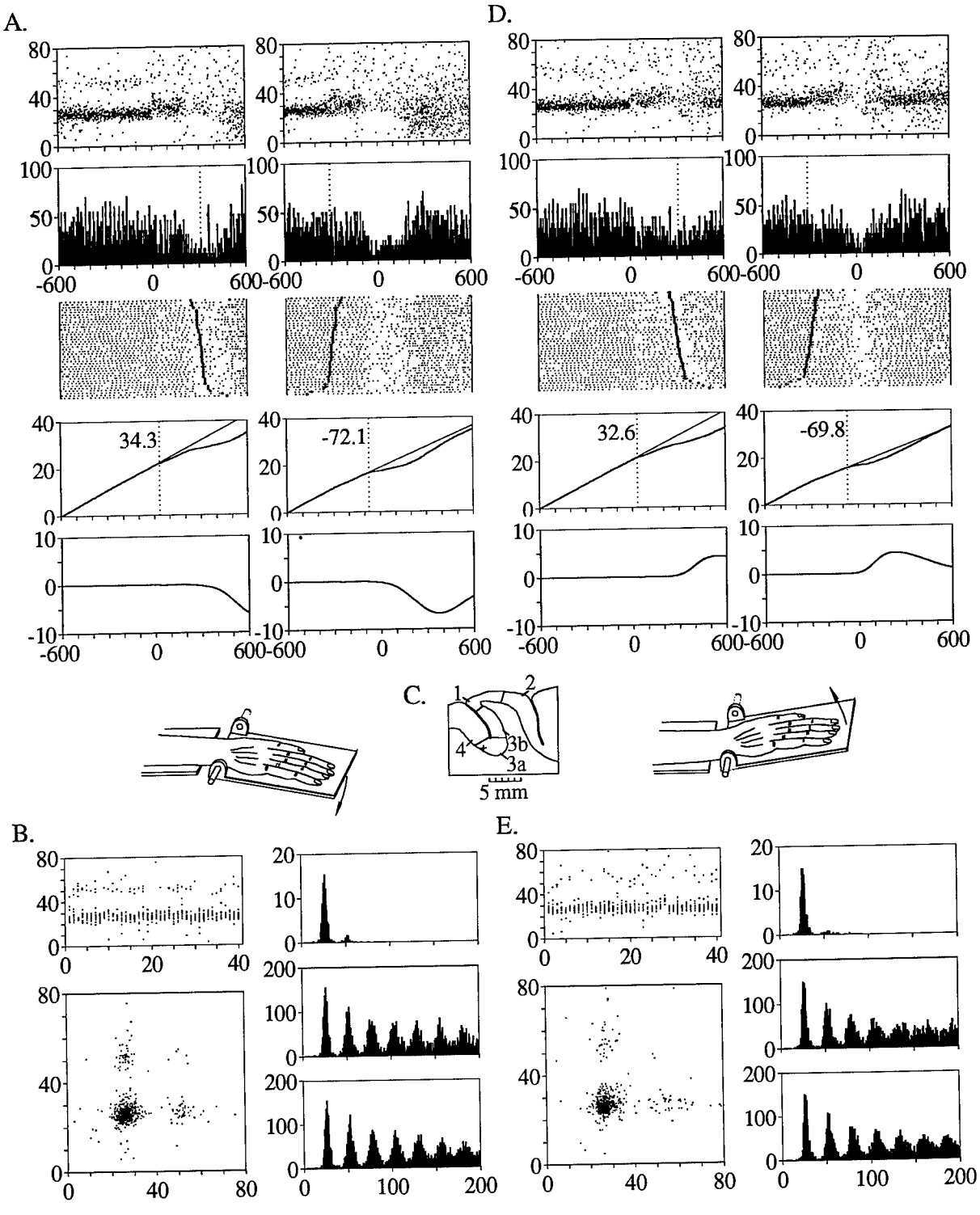

Figure 13

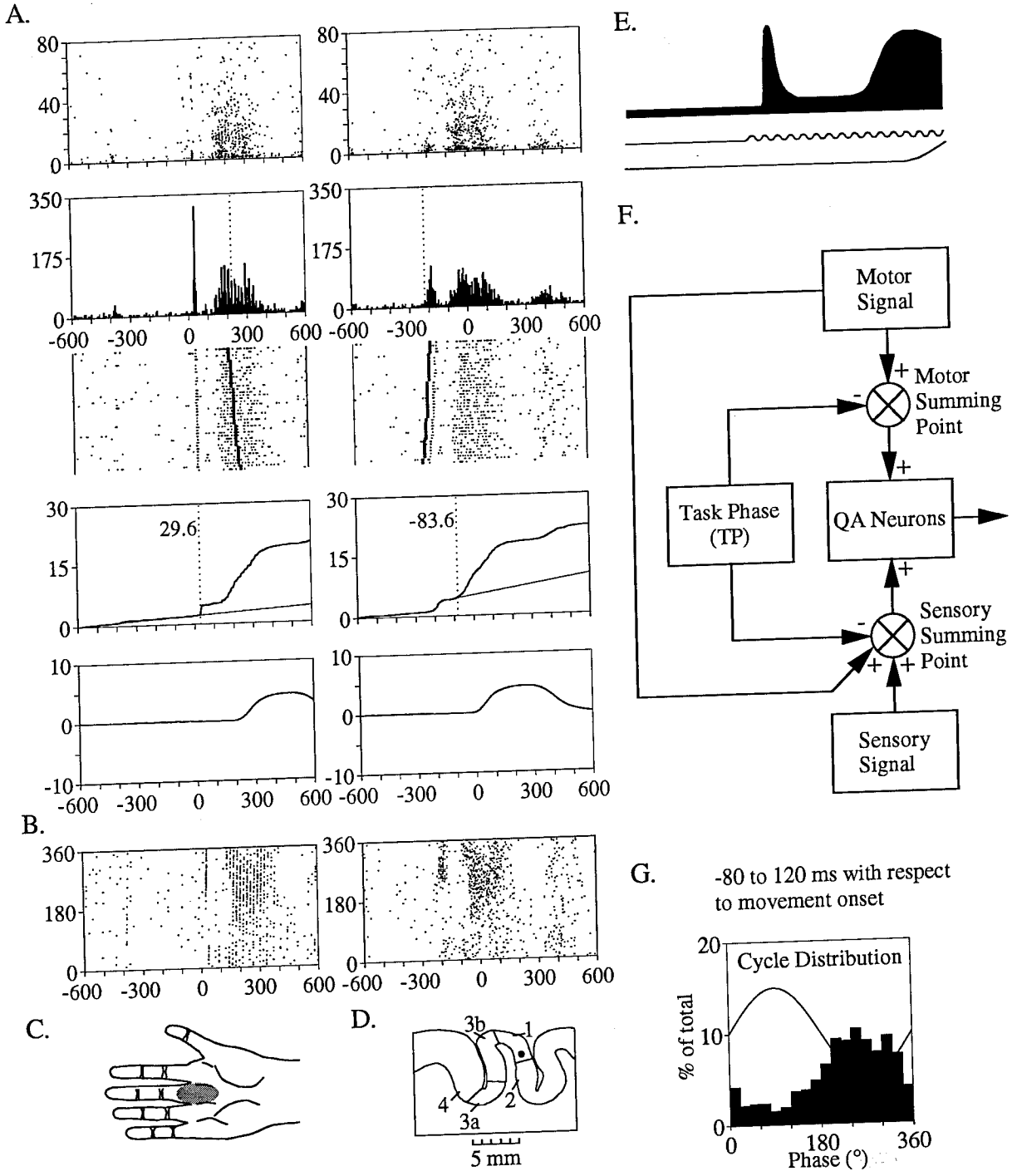

Figure 14